PREVENTING AND TREATING HEPATIC METASTASES OF COLON AND PANCREATIC CANCERS BY TARGETING CANCER CELL METABOLISM

By

AMER H. AL-ASADI

A dissertation submitted to the

School of Graduate Studies

Rutgers, The State University of New Jersey

In partial fulfillment of the requirements

For the degree of

Doctor of Philosophy

Graduate Program in Physiology and Integrative Biology

Written under the direction of

Shengkan Jin

And approved by

_____

_____

_____

_____

New Brunswick, New Jersey

May, 2018

ABSTRACT OF THE DISSERTATION

Preventing and treating hepatic metastases of colon and pancreatic cancers by targeting cancer cell metabolism

By AMER H. AL-ASADI

Dissertation Director:

Shengkan Jin

Alteration of glucose metabolism is a unique feature for a majority of cancers. Cancer cells exhibit aerobic glycolysis also known as the Warburg effect even in the presence of oxygen. During this mode of glucose metabolism, a majority of pyruvate is converted to lactate rather than entering mitochondria for complete oxidation through oxidative phosphorylation. The functional importance of aerobic glycolysis to cancer cells is becoming clear. Basically, aerobic glycolysis prevents pyruvate from complete oxidation inside mitochondria. This shunts glycolytic intermediates to pathways for synthesis of NADPH and building blocks of macromolecules, which are required for cell growth and proliferation.

Pyruvate entrance into mitochondria is enhanced via mitochondrial uncoupling, a process that permits proton influx through the mitochondrial inner membrane without generating ATP. Consequently, mitochondrial uncoupling stimulates “idle ” oxidation of acetyl-CoA, leading to complete oxidation of glucose. Thus, we hypothesize that safe

mitochondrial uncouplers could be strong anticancer agents to inhibit the anabolic role of the Warburg effect. We utilized two approaches to address this hypothesis.

First, we tested two mitochondrial uncoupler compounds, NEN (niclosamide ethanolamine) and oxyclozanide, on their metabolic effects and anti-cancer activities. We used metabolomics NMR to study the effect of mitochondrial uncoupling on glucose metabolism in colon cancer MC38 cells. We further examined the anti-cancer effect of NEN and oxyclozanide in cell models and hepatic metastasis of colon cancer in animal model. We found that mitochondrial uncoupling stimulates pyruvate influx to mitochondria and decreases various anabolic pathway activities. Moreover, mitochondrial uncouplers arrest cell cycle progression, inhibit cell proliferation and reduce clonogenicity. Furthermore, oral treatment with mitochondrial uncouplers diminishes hepatic metastasis of colon cancer cells transplanted intrasplenically in mice.

Second, we tested MB1-47, a novel mitochondrial uncoupler with good pharmacokinetic and toxicological profiles, in preventing and treating pancreatic cancer. Our study demonstrated that MB1-47 is effective in inducing mitochondrial uncoupling in pancreatic cancer cells and inhibits the proliferation of multiple murine and human pancreatic cancer cell lines. In the tumor xenograft mouse models, oral MB1-47 treatment exhibits excellent activity in preventing tumor growth and metastasis.

Our data support a unique approach for targeting cancer cell metabolism for cancer prevention and treatment and identified prototype compounds for this mechanism.

Acknowledgements

I would like to introduce my deepest thanks to my advisor, Dr. Shengkan Jin for his supervision, enthusiastic encouragement, and useful guidance during the planning and development to finish my project. My deepest thanks are further extend to my committee members, Dr. Debabrata Banerjee, Dr. Huizhou Fan, and Dr.Joseph Fondell for their valuable suggestions, insight and encouragement during my study.

I also want to extend my thanks to all of the faculty and staff of the many facilities at Rutgers-RWMS that provided their support over the time of my study specifically Dr. Janet Alder, Alexandria Bachmann, Marsha Nabors, Carolyn Ambrose and Tina Cicolella.

To my lab members, particularly Dr. Hanlin Tao, Juan Collantes, and Jingjing Guo, I would like to express my thanks for their generous help and friendship. In addition, I would like to acknowledge Iraqi Government specially (HCED, Ministry of Higher Education, and Thi-Qar University), Mito Biophrama and Graduate school of Biomedical Science for their financial support.

I would like to introduce my thanks to my family; my parents and I wish to express my sincere esteem to my wife, Noor Fadhil. I am truly grateful to her patient and support, to finish my study.

Dedication

To

(Noor, Rawaan, Fatima, and Mohammed)

Table of Contents

List of tables

List of illustrations

Chapter I

1. Introduction

1.1 Cancer cell metabolism

Cancer cell metabolism is an important area of cancer research and it is older than the oncogene and tumor suppressor discovery. This area of research is based on the observation that cancer cell metabolism is different compared to normal cell, and this difference is essential and necessary to maintain the malignancy of cancer (1,2).

Decades ago, Otto Warburg found that cancer cells use aerobic glycolysis as energy source to provide the necessary requirements for cell proliferation. This feature of cancer cells is known as the Warburg effect. In contrast, normal cells use oxidative phosphorylation to support growth and proliferation (1-5). Warburg's finding was approved and validated in many human cancers with the radioactive glucose analogue by fluorodeoxyglucose positron emission tomography to monitor glucose uptake in cancer and normal tissue (6,7). Recently, Warburg effect has been considered one of the hallmarks of cancer along with other traits such as sustaining proliferative signaling, resisting cell death, evading growth suppression, activating invasion and metastasis, enabling replicative immortality and angiogenesis (8-10). Moreover, genomic instability and mutation, avoiding immune system, and tumor enhancing inflammation are emerging hallmarks that are involved in the cancer pathogenesis (11-14).

1.2 Roles of glucose in cancer cell metabolism

Altered glucose metabolism through aerobic glycolysis is an inefficient way to produce energy because and it gives 2 adenosine triphosphates (ATPs) per glucose

molecule, whereas oxidative phosphorylation gives 36 ATPs from glucose oxidation via the Krebs cycle (2,15-17). Several studies have demonstrated that most cancer cells rewire glucose oxidation to aerobic glycolysis instead of oxidative phosphorylation even in the presence of oxygen. Cancer cells redirect glucose intermediates to macromolecules biosynthetic pathways for biomass accumulation. This process will maintain tumor progression by providing materials to replenish tumor cells as well as generating reducing agents such as nicotinamide adenine dinucleotide phosphate (NADPH) for metabolic processes (2,17-19).

Glucose is the primary and crucial energy source for all mammalian cells. Glucose is metabolized in cytosol to pyruvate through a precise metabolic pathway called glycolysis (20). One glucose molecule (comprised of 6 carbon atoms, or 6C) is metabolized into two pyruvate molecules (3C) and 2 molecules of ATP are generated in this process (21). Pyruvate can have two fates through glycolysis: (i) it can be completely oxidized inside mitochondria via oxidative phosphorylation (OXPHOS), or (ii) it can be converted into lactic acid (fermentation) inside cytosol in the absence of oxygen (22). In normal cells, glucose oxidizes to CO2 inside mitochondria through OXPHOS in presence enough levels of the oxygen, while in hypoxic condition glucose is fermented to lactic acid. Glucose oxidation via OXPHOS efficiently produces 36 ATPs, however the rate of ATP generation becomes greater if the respiration process happens through aerobic glycolysis and with an unlimited source of glucose (23,24).

In differentiated cells, glucose metabolism is dependent on oxygen availability, either through OXPHOS (in presence of oxygen) or fermentation (in absence of oxygen) (25-27). In proliferative cells, particularly in cancer cells, pyruvate from glucose is converted

to lactic acid through an aerobic glycolysis, also know as Warburg effect, regardless of oxygen availability. In addition to ATP production from glucose metabolism through glycolysis, glucose supplies the substrates for Pentose Phosphate Pathway (PPP) to produce ribose -5-phosphate that is necessary for nucleotides biosynthesis, and NADPH to maintain the redox hemostasis of cells (2,28).

Moreover, glycolytic intermediates are necessary for biosynthesis of some amino acids such as 3-phosphoglycerate, a precursor to the serine biosynthetic pathway, which in turn provides the essential elements for the synthesis of many nonessential amino acids. Also, pyruvate converts to alanine through transamination, and citrate shunts out mitochondria into cytosol for fatty acid biogenesis (19,29-31). This shows that cancer cells effectively take advantage of dysregulated metabolism to support survival.

1.3 Tumor cells utilize glutamine for glucose-independent TCA

Cancer cells not only utilize glucose as their only energy source. Glutamine is a free amino acid in human blood, and has been classified as conditionally essential. This means its synthesis can be reduced under certain pathophysiological conditions and catabolic problems (32). Glutamine synthetase (GS) catalyzes the assembling reaction between glutamate and ammonia to form glutamine (33,34).

Glutamine has roles in protein and lipid biosynthesis, specifically in cancer cells, as wells as energy hemostasis besides glucose. It is a source for carbon, citric acid and glutamate biosynthesis (35). Glutamine is the main precursor for Tricarboxylic Acid (TCA) cycle fuel in the culture medium of cancer cells and the majority of glutamine is converted inside mitochondria to glutamate by glutaminase (GLS), (32,33). Glutamate is

subsequently converted to α-ketoglutarate by glutamine dehydrogenase or transmission. Then, α-ketoglutarate is metabolized inside mitochondria through TCA cycle to generate oxaloacetate and 4 C unit (34,36).

Furthermore, glutamine is a nitrogen donor for pyrimidines, purines, asparagine. Importantly, it is also a source of nicotinamide adenine dinucleotide (NAD), and is a precursor of glucosamine biosynthesis (34). In addition to glucose roles to promote cancer cell proliferation, cancer cells are addict to glutamine uptake and utilization to support anabolic pathways for sustained cell survival (20).

Oncogene c-Myc stimulates the expression of glutamine transporters such as SLC1A5, SLC7A5/SLC3A2, and GLS (37). Glutamine deficiency in cancer cells expressing c-Myc induces apoptosis (38,39). In a number of tumors, GS activity and glutamine biosynthesis are enhanced to support tumor cell proliferation and growth (40,41). Data from experiments using glucose labeling have demonstrated that higher activity of GS led to integration of carbon from glucose into glutamine through α-ketoglutarate/glutamate, in contrast to a glutamine replenishment process (40,41). Furthermore, pharmacological targeting or loss of one allele in GLS or GS is an efficient way to inhibit cancer cell proliferation and tumor growth in mouse cancer models (42,43).

1.4 Oncogenes roles in cancer cell metabolism

Despite the many genetic and histological differences of tumor tissue, there are permanent signaling pathways that control the malignancy of a tumor (24,44). In normal

cells, phosphatidylinositol 3-kinase (PI3K), AKT (also known as Protein Kinase B,PKB) and mammalian Target Of Rapamycin (mTOR) are activated via growth factors, thus enhancing strong anabolic pathways including robust glycolytic flux activities, and synthesis of fatty acid (45), a process that is tightly controlled in these cells. On the other hand, tumor cells contain frequent mutations, which allow the PI3K-AKT-mTOR crosstalk to achieve the highest signaling activity with less reliance on growth factors stimulation (44,46).

Myc gain of function is another deregulated pathway in many cancers like lung, colon, and pancreatic cancers (47,48). Several studies have demonstrated that Myc oncogene has roles in upregulating the expression of several genes encoding enzymes involved in glycolysis, metabolic transporters, pyruvate and lactate dehydrogenase, fatty acids synthesis, glutamine one carbon pathway and mitochondrial metabolism (45). Moreover, Myc plays a role in upregulating the transcription of genes that are required for glutamine metabolism, such as glutaminase-1 and glutamine transporters that form glutamate from glutamine (49). Then, α-ketoglutarate can be produced from glutamate and subsequent enters to the TCA, so glutamate production provides the carbon necessary for TCA intermediates, which are essential for amino and fatty acids biosynthesis. Then, glutamate can be converted to glutathione and the latter participates in the maintenance of cellular redox homeostasis (47,50). Collectively, these anabolic pathways promote the anabolic roles of Warburg effect in many cancers.

Oncogenic Kras is highly mutated in many cancers. It enhances tumor progression through PI3K-AKT-mTOR signaling network, via upregulation many metabolic

enzymes, which are required for metabolic pathways (51,52). Mutated Kras enhances glycolytic pathway activity by activation of the Mitogen-activated protein kinase (MAPK) pathway as well as activation of transcription factors, like Myc or Hypoxia Inducible Factor -1 (HIF-1) (53). Several studies showed that Kras upregulation switches the cellular metabolism from (OXPHOS) to aerobic glycolysis in cancer cells (51,53,54).

p53 is a tumor suppressor transcription factor, which is mutated in 50% of all human cancer, and is thought to control cell metabolism in stress conditions. It exerts its suppressive action through DNA repair, senescence, cell cycle arrest and apoptosis (55-57). Nevertheless, recent work suggests that the suppressive action of p53 might be related to regulation of cell metabolism and oxidative stress (58). Loss or dysregulation of p53 activity enhance glycolytic intermediate flux to stimulate anabolism and redox hemostasis, processes necessary to promote tumor malignancy (59).

Jones & Thompson also demonstrated the role of the p53 in changing the balance between glycolysis utilization and oxidative phosphorylation via activation of cytochrome c oxidase synthesis (60). Therefore, p53 mutations diminish cytochrome c oxidase synthesis, thus conferring an advantage to cancer cells to shift toward glycolysis (61). Other study suggested that p53 regulates glycolysis dependent on the transcription activity of Nuclear Factor kB (NF-$_k$B) (62).

The highly organized induction of metabolic signaling pathways that promote tumor malignancy through combination of P13k-AKT-mTOR crosstalk deregulation, damage of tumor suppressive, and stimulation of oncogene activity that is required to amplify many metabolic enzymes every second.

It is obvious that the cancer cells display aerobic glycolysis (Warburg effect) due to oncogenes activation, damage of tumor suppressor, and PI3k upregulation. The advantages that cancer cells get from highly glycolytic metabolism are to provide anabolic molecules for biomass production and reducing agents for cell proliferation (2).

Moreover, many studies showed that the cancer cells could produce energy from glucose oxidation (glucose-carbon sources can enter TCA cycle and produce energy ATP via oxidative phosphorylation) (18,63). Nevertheless, decreasing ATP production from glycolysis by decreasing the pyruvate kinase activity fails to decrease cancer growth, clarifying that the main function of glycolysis is not provide ATP to the cancer cells but biomass and reducing agents (17,19).

1.5 Mitochondria and cancer cell metabolism

Mitochondria are critical bioenergetic organelles that control the normal production of ATP, regulate calcium balance, regulate programmed cell death and also are a major site for fatty acid and lipid oxidation (64). Mitochondria are involved in specialized cellular processes, such as respiration through Electron Transport Chain (ETC), fatty acid oxidation, TCA cycle, and to biosynthesis of amino acids, lipids, nucleotides, sulfur cluster, heme and NADPH to maintain their own antioxidant status (65-67). NADH and $FADH_2$ electron carrier molecules are generated through TCA. They control the power of ETC, which lead to generate the proton gradient cross the inner mitochondrial membrane and subsequently to generate ATP through ATP synthase system.

Beside the bioenergetics and signaling roles of mitochondria, it is also a site for

biosynthesis of the building blocks necessary to sustain cell survival and proliferation. This requires consistent supplementation of 2C and 4C units, which are provided from pyruvate carboxylation, glutamine oxidation, pyruvate, acetate and other amino acids respectively (20,68,69). Furthermore, mitochondria have a major role in one carbon (1C) metabolism, which provide the necessary metabolites for purines, pyrimidines and methionine biosynthesis (70,71).

Mitochondrial metabolism is crucial for cancer cells proliferation and differentiation. Therefore, although their huge glycolytic rate, most of cancer cells produce ATP using mitochondrial oxidative phosphorylation, with few exception of cancers having a mutations in mitochondrial respiration enzymes like succinate dehydrogenase (SDH) and fumarate hydratase (FH) (72,73). However, cancer cells with SDH and FH mutations are still depending on mitochondrial metabolism to provide TCA intermediates and reactive oxygen species that are required for cancer cell growth (73,74). Furthermore, amino acids and fatty acids also can provide intermediate substrates for TCA cycle to maintain ATP production from mitochondria in cancer cells (41).

Fatty acid oxidation occurs in mitochondria through β-oxidation to generate acetyl Co-A and the reducing agents NADH and $FADH_2$. These molecules are used in the ETC to generate ATP inside mitochondria (75,76). In addition, glutamine metabolizes to glutamate and consequently to α-ketoglutarate to supply TCA cycle through glutaminolysis (35). Thus, cancer cells can adapt to harness these metabolic routes that can supply TCA cycle with essential metabolites, that are in turn used to supply enough fuel for cell survival in the unusual environment during tumor evolution (9,20).

1.6 Biosynthetic pathways support cancer cell metabolism

Biosynthetic pathways are an essential part of cancer cell metabolism, because of their roles in generating the essential macromolecules for cell division, proliferation and growth (77). First, these pathways acquire simple nutrients (sugar, amino acid, lipid, etc) from extracellular space, and then converted through core metabolic pathways like glycolysis, PPP and TCA to biosynthetic intermediates and lastly the large molecule assembly happen via ATP dependent processes (77,78).

Alongside with glucose, lipid, protein, nucleic acid are the most macromolecules that studied on cancer research, which comprise about 80% of whole dry mass in mammalian cells. Evidence demonstrate that (lipid, protein, nucleic acids) molecules biosynthesis under the control of similar signaling pathways that control cell growth and stimulated in cancer via many carcinogenic mutations, specially PI3K-AKT-mTOR signaling (41,79).

1.6.1 Protein effects in cancer cell metabolism

Protein synthesis is precisely controlled and requires essential and non-essential amino acids. Cancer and non-cancer cells obtain these molecules under the effect of growth factor signaling by providing surface transporters, which allow them to attain these molecules from extracellular sources (37,80). In addition to raw materials that are provided for protein synthesis in cancer cells, surface transporters support them to maintain mTOR-signaling network. mTOR is activated via amino acids and stimulates the protein synthesis via its effective roles on translation and ribosome biosynthesis (37,79).

In proliferative cancer cells, glutamate pool is the precursor for nonessential amino acids and it comes via glutamine deamination and transamination reactions (81). mTOR controls glutamine uptake and glutaminase activity. Glutamate supply is necessary for transamination reactions and to maintain TCA cycle activity, which additionally supports the synthesis of amino acids (36). Moreover, high intracellular level of glutamine is used use to stimulate mTOR and protein biogenesis. Under growth conditions, mTOR activity is stimulated by the abundancy of glutamine and amino acids, thus enhancing protein synthesis (77,82).

1.6.2 Fatty acids and cancer cell metabolism

Tumor cells generate fatty acid for membrane biogenesis, lipid modifications, and signaling pathway activity (83). Fatty acid biosynthesis requires acetyl- Co A and reducing agents, specifically NADPH (cytosolic form). Active fatty acid biosynthesis therefore demands integration with other carbon metabolic pathways and oxidation-reduction processes. Glucose is the main source of acetyl-Co A for fatty acid biosynthesis in most culture medium (75,76,84).

In hypoxia and mitochondrial dysfunction, glutamine and acetate are the alternative sources for acetyl-Co A (85-88). In addition, leucine degradation is another source of acetyl-Co A in some cell lines (89). Furthermore, recent studies have indicated that glucose is the main source for fatty acyl carbon in tumor tissues (90). Metabolic labeling experiments suggested that most of cytosolic NADPH for fatty acid biosynthesis originates from the oxidative branch of the PPP (91,92).

Fatty acids biosynthesis is regulated by SREBP-1 transcription factor (93). SREBP-1 controls the enzymes that are required to convert the Acetyl-CoA into fatty acid and the enzymes of PPP that are needed to convert acetate and glutamine to Acetyl-CoA. Thus, SREBP-1 controls genes that help or catalyze the synthesis of fatty acid (94).

In cancer cells with high rate of fatty acid biosynthesis, mTOR signaling pathway through its downstream target S6Kinase (S6K) assist to maintain the transcription activity of SREBP-1 and SREBP-2. The latter proteins control the transcription of genes involved in sterol synthesis (93). Thus, SREBP-1 and SREBP-2 are necessary for mTOR to stimulate and promote cell proliferation and growth. Normal and cancer cells obtain the fatty acid and lipid from extracellular space to use them to supply cell membrane biogenesis. Under the effect of growth factors, PI3k enhances the fatty acid and lipid uptake and inhibit lipid oxidation (β-oxidation) inside mitochondria to maintain cell proliferation (95).

In cancer cells under hypoxia, mTOR-signaling pathway plays important roles to support endoplasmic reticulum activity to maintain protein synthesis through extracellular supplying of desaturated fatty acid. In addition, ATP citrate lyase the last enzymes that converts acetate to Acetyl-CoA to prevent cancer cells proliferation and growth (96).Therefore, targeting the fatty acid transport and biosynthesis could have potential effect to inhibit cancer cell proliferation.

1.6.3 Nucleotide biosynthesis and cancer cell growth

Nucleotide biosynthesis (purine and pyrimidine) is a necessary process for RNA and

DNA biosynthesis. Biosynthesis of nucleotides is a complex process, required huge cooperation from other pathways in precise fashion. Ribose -5- phosphate (intermediate of the PPP) provides the backbone (phosphoribosylamine) and glutamine uses as amide sources for nucleotide synthesis (97,98). Different nonessential amino acids and methyl-donated group from one carbon pathway are also included on the synthesis of purine and pyrimidine. Moreover, oxaloacetate from TCA cycle is transaminated to aspartate, which is also an important intermediate required for purine and pyrimidine base biosynthesis (98,99).

NADPH is also required to convert the ribonucleotides to deoxynucleotides via ribonucleotide reductase. It is well known there is feedback inhibition mechanism to prevent nucleotide accumulation and any mutation disturb this mechanism lead to pathological condition like gout and uric acid precipitation (98). In this way, pharmacological interventions targeting nucleotide synthesis are good strategies to inhibit some cancer types. For example, drugs that interfere with nucleotide metabolism, such as nucleoside analogues and antifolates, have been used for decades as cancer treatment (27).

It is not obvious how oncogenic signaling pathways affect nucleotide biosynthesis. It is probably through the effective roles of oncogenic pathways to the metabolic core pathways (glycolysis, PPP, and TCA cycle) because their main roles to provide the precursors for nucleotides synthesis. Moreover, some studies suggested that activation of mTOR signaling supports nucleotides biosynthesis (100). mTOR's effector ribosomal K6S phosphorylates the trifunctional enzyme CAD (carbamoyl- phosphate synthetase 2, aspartate transcarbamoylase, dihydroorotase) which, promote the first steps of pyrimidine

biosynthesis. CAD S1859 phosphorylation is necessary for mTOR mediated pyrimidine synthesis (100).

1.7 AMP-activated protein kinase (AMPK)

AMP-activated protein kinase (AMPK) is a cellular sensor for energy homeostasis and is essentially expressed in all eukaryotic cells. AMPK consists of three subunits, the catalytic (α) subunit and the regulatory (β and γ) subunits. In humans, each subunit has many isoforms and each isoform is encoded by a specific gene (101).

AMPK activates via energetic stresses through a mechanism that senses increase in AMP/ATP and ADP/ATP ratios. AMPK activation restores energy hemostasis by switching on the catabolic pathways and switching off the anabolic pathways to enhance ATP generation to restore energy balance (102,103). Moreover, AMPK promotes glucose utilization through oxidative metabolism in less proliferative cells rather than rapid glucose uptake and glycolysis that are used in proliferative cells (104).

AMPK analogue in the yeast *Saccharomyces cerevisiae* is necessary to switch the yeast's metabolism from fermentation (glycolysis) to oxidative metabolism in starvation conditions. This metabolic switching is like to reversal of the aerobic glycolysis (Warburg effect) that appears in many quickly proliferating cells, including tumor cells (105). Pharmacological activation of AMPK is well known via salicylate and metformin (106,107). AMPK activation is determined by phosphorylation of conserved threonine reside (Thr172), which is located in the activation loop of a subunit kinase domain (108). The γ subunit of AMPK has three binding sites for AMP, ADP, and ATP binding in competition with AMP (109,110). AMP binding activates AMPK through three specific

mechanisms: (i) via increased Thr 172 phosphorylation by LKB1 (tumor suppressor and upstream target of AMPK), (ii) decreased dephosphorylation of Thr172 by a phosphatase and (iii) triggered allosteric activation. All these activation are because of AMP binding to AMPK it self and not due to phosphatase or upstream kinase effect (109,111).

After activation through energy stress, AMPK restores the energy hemostasis by stimulating catabolic pathways to generate ATP and inhibiting the anabolic pathways that consume ATP (111,112). In addition, most anabolic pathways are stimulated by mTOR signaling pathway, which in the end inhibit by AMPK activation (113). AMPK inhibits the biosynthesis of lipid, RAN, and protein, and then it reduces cell growth and proliferation. Moreover, it arrests the cell cycle at G0/G1 phase by stimulating p53 phosphorylation, thus stopping DNA synthesis (45,114).

Loss of one allele of AMPK-a enhances B cell lymphoma development in mice carrying c-Myc transgenic expression in B cells, while loss of two alleles induces a severe effect (115). Therefore, this indicates that AMPK may act as a tumor suppressor and mutation in any genes encode any subunits of AMPK seems to be infrequent in human cancer. This could be because of the redundancy among AMPK isoform or probably because lower levels of AMPK are needed to support viability throughout the metabolic stress that cancer cells frequently face. Therefore, reduced AMPK functions might be essential for tumor cell survival and tumor malignancy by restraining effects of AMPK on cell growth and proliferation (116).

AMPK activation is a good way to reduce cancer cell metabolism by inhibiting the anabolic pathways and activating the catabolic pathways. Histological staining of human

breast cancer samples showed that phosphorylation of AMPK-α subunits level is lower than surrounding normal tissue (117). Another study showed that AMPK-α phosphorylation frequently occurred in human hepatocellular carcinoma (118). Moreover, other study suggested that AMPK is a negative regulator of the Warburg effect in *vitro* and *vivo* models (119).

Many mechanisms have been suggested to explain the downregulation of AMPK activity. Genetic loss of LKB1 is moderately frequent in non-small cell lung and cervical cancers and it is lower in other cancers (120-123). Hyperactivation of Insulin/IGF1-regulated protein kinase Akt/PKB is another mechanism for AMPK downregulation, as gain of functions mutations of AKT and loss -functions mutations of PTEN tumor suppressor occur in many tumors (124,125). Human melanoma cells having B-Raf ^{V600E} mutation is another mechanism for AMPK downregulation activity. Mutation of B-Raf causes activation of Erk and RSK kinases, which promote the phosphorylation of the C terminal domain of LBK1, thus restrained its activity to induce AMPK activation (126). Additional mechanisms have been also proposed for AMPK downregulation, and many of them could be good target therapeutically.

Collectively, downregulation of AMPK is required for cancer cell proliferation and differentiation to defeat the bioenergetics and nutritional stresses during cancer cell development and AMPK activation might be a way to restrain cancer cell survival and growth.

1.8 Mammalian Target of Rapamycin (mTOR) roles in cancer cell metabolism

mTOR is a central component of an important signaling pathway for cell

proliferation. mTOR is an evolutionarily conserved serine/threonine kinase and play vital roles in protein synthesis. The downstream effectors of mTOR signaling include the ribosomal protein S6 kinase beta-1 (p70S6K) and eukaryotic translation initiation factor 4E binding protein 1 (eIF-4E BP1) (45,127,128).

mTOR has regulatory roles in many biological processes like cell metabolism, autophagy, survival, migration, lysosome biogenesis and growth, which are essential for normal and abnormal cell growth. Consequently, it governs balance between the anabolic and catabolic processes corresponding to environmental factors (45,82,129). mTOR is severely and allosterically inhibited by rapamycin (82,129).

In addition to its role in protein synthesis, mTOR supports de novo lipid biosynthesis via the sterol responsive element binding protein (SREBP) transcription factor that regulates expression of metabolic genes included in fatty acid and cholesterol synthesis (130-132). Moreover, new studies have showed that mTOR plays crucial roles in nucleotides biosynthesis, which are necessary for ribosome biosynthesis and DNA replication in growing and proliferating cells (37,94,100,129,133,134).

Furthermore, mTOR promotes the mitochondrial tetrahydrofolate cycle that supplies 4C units for purines biosynthesis by increasing the expression level of ATF-4 (the key component of this cycle) (100). Moreover, phosphorylation and activation of carbamoyl-phosphate synthetase (CAD) increases by S6K, and CAD is essential for pyrimidines biogenesis pathway (100,135). mTOR also stimulates cell growth and proliferation by switching glucose metabolism from oxidative phosphorylation to glycolysis that facilitate nutrients incorporation into biosynthetic pathways (94).

Furthermore, mTOR increases the translation of HIF1α transcription factor that in turn drives the expression of several glycolytic enzymes like phosphofructokinase (PFK). Nevertheless, mTOR promotes SREBP activation and this lead to enhanced the metabolites influx through the oxidative phase of PPP, which used the glycolytic intermediate generate NADPH and other essential metabolites to promote cell growth and survival (94,114,129,134).

mTOR hyperactivation has been reported in many cancers with frequent mutation in PI3K/AKT, RAF and ERK oncogenic signaling pathways because it is downstream effector for these pathways (129,136,137). Furthermore, TP53 and LKB1 the common tumor suppressors are negative regulators for mTOR activity (129,138). AMPK activation decreases the phosphorylation of P70S6K and 4E-BP1 proteins (139,140). Thus, mTOR's activity is reduced and this consequently inhibits cell proliferation and growth. Targeting cancer cell metabolism through mTOR and its effectors could be a way to reduce cell proliferation and growth.

1.9 Mitochondrial uncoupling and cancer cell metabolism

Mitochondrial uncoupling is a process that allows the proton influx into inner mitochondrial membrane without generation of ATP. It has many applications in different normal and pathological conditions. Historically, uncoupling compounds have been used to enhance oxygen utilization without increase in ATP production (141). Chemically, the uncoupling process is the dissipation the electrochemical proton gradient allowed H^+ futile cycle through mitochondrial inner membrane (11,142).

Recently, Tao et al. showed the effective role of the mitochondrial uncoupler compound niclosamide ethanolamine (NEN) in preventing diabetes mellitus type II by enhancing lipid oxidation inside the liver and insulin sensitivity to glucose throughout the body (142). Therefore, the targeting the cell metabolism using mitochondrial uncoupler compounds could be a new way to target many metabolic chronic diseases and cancers.

Mammalian cells can endure mild mitochondrial uncoupling (143). Mitochondrial uncoupling enhances the metabolic rate and consequently reduces body fat (144-147). It burns energy molecules, such as glucose and fatty acids, through oxidative phosphorylation rather than using them for biomolecules biosynthesis, leading to a reduction in NADPH generation and building blocks that are necessary for biosynthetic pathways (144,148,149). In cancer cells, this ultimately enhances cell cycle arrest and inhibits cell proliferation (140,150,151). It also has effective roles in reprogramming cancer cell metabolism (140).

One group studying colon cancer demonstrated that tumor growth is increased when a mitochondrial uncoupling protein is downregulated in mice (152). Moreover, other study reported that mitochondrial uncoupling mechanism is a way to reduce cell proliferation and tumorigenesis via Akt inhibition in skin cancer. It has also been suggested that there is a relationship between anabolic signaling pathways and mitochondrial uncoupling. Also, the study proposed that mitochondrial uncoupling might be a good way to treat malignant cancer by targeting the anabolic roles of AKT signaling pathway (153).

Chapter II

2. Effect of mitochondrial uncouplers niclosamide ethanolamine (NEN) and oxyclozanide on hepatic metastasis of colon cancer

2.1 Introduction and rationale

Cancer cell exhibits a unique glucose metabolism through an aerobic glycolysis also known as Warburg effect. During aerobic glycolysis, majority of pyruvate derived from glucose is converted to lactate rather than entering to mitochondria for oxidative phosphorylation. (3,10,154,155).

Majority of cancer cells exhibit aerobic glycolysis. Now, the aerobic glycolysis is consider as one of the cancer hallmarks (8). The functional significance of the aerobic glycolysis to cancer cells is to prevent complete oxidation of glucose and glycolytic metabolic intermediates are shunt to pentose phosphate pathway required for biomass production (28).

Colorectal cancer (CRC) is one of the most common malignancies in the Western world. While it is important to eradicate the primary tumor, it has become evident that the main problem in the treatment of CRC tumors is the formation of incurable metastases.

In more than half of all patients with colorectal carcinoma (CRC), liver metastases will develop during the course of the disease.(156,157) In 25% of the patients, these metastases are already present at the time of diagnosis of the primary tumor.(158,159) Another half of the patients will develop metachronous liver metastases within 5 years (160). Surgical resection of metastatic liver tumors, which is possible in 20–50% of

patients at first presentation, 10 to 58% is the only chance for cure with a reported 5-year survival rate.(160-164). Still, more than 90% of these patients ultimately die because recurrent disease. Mortality rate is mainly associated with the occurrence of metastases in the liver (66,159,160,164,165).

There is an important need for developing efficacious prevention or treatment ways for hepatic metastases of CRC. We propose to target this mode of cell metabolism for treating and preventing hepatic metastasis of colon cancer through mitochondrial uncoupler compounds.

Cancer cell metabolism relies on aerobic glycolysis rather than oxidative phosphorylation for ATP production (21). This altered metabolism feeds the building blocks that allow tumors to proliferate and progress. Targeting the cancer cell metabolism by mitochondrial uncoupling could be a new strategy for treating and preventing hepatic metastasis of colon cancer. Niclosamide is a mild and safe mitochondrial uncoupling compound that has been used to treat tapeworm infections. Niclosamide ethanolamine (NEN) is the ethanolamine salt of Niclosamide, our lab revealed that NEN is effective for treating diabetes type II in mice by reducing fat accumulation in liver and increase insulin sensitivity (142,166).

Niclosamide is an anthelmintic FAD approved drug used to treat tapeworm and its mechanism of action through uncouples mitochondria of the worm (167,168). Several previous studies showed that niclosamide has a robust in vitro anticancer activity against many of cancer cells like breast cancer (169,170), colon cancer (171,172), adrenocortical

carcinoma (173), hepatocellular carcinoma (174), prostate cancer (175,176) ovarian cancer (177,178), and other types of cancers (179-182). There is no specific target of niclosamide was recognized on the previous studies and many possible anticancer mechanism/pathway were suggested, including S100A4 (171), Wnt/β-catenin(170,178,183), CDC37 (174), State3 (184), NF-κB (185) and other signaling pathways (174,181).

NEN (niclosamide ethanolamine) is the ethanolamine salt of niclosamide that has a similar tremendous safety profile like niclosamide (167,186-188) and has an excellent water solubility and systemic exposure (188). Our previous study demonstrated that NEN is completely metabolized inside liver (142). Thus, we propose that mitochondrial uncoupling could increase pyruvate influx to mitochondria and antagonize the anabolic effect of the Warburg effect. It could be a new and attractive avenue for preventing and treating hepatic metastasis of colorectal cancer.

We decided to study the uncoupling and antitumor effects of NEN and as well as close family member oxyclozanide on colon cancer culture models. Oxyclozanide is veterinary anthelmintic drug; mainly it is used for treatment and control flatworms in farm animal and it has a longer half-life and it is metabolized in liver (189-191). NMR experiment was performed to study the effect of NEN on glucose metabolism on colon cancer cells.

In addition, NEN and oxyclozanide were used for preventing and treating hepatic metastases of colon cancer on mouse model. Our finding strongly suggest that the mild mitochondrial uncouplers NEN and oxyclozanide could be new and an effective way for

preventing and treating hepatic metastasis of colon cancer by targeting the glucose metabolism of colon cancer.

2.2 Results

2.2.1 NEN uncouples mitochondria and antagonists the anabolic effect of aerobic glycolysis

The main hallmark of mitochondrial uncoupling is increasing of Oxygen Consumption Rate (OCR) in the presence of ATPase synthesis inhibitor like oligomycin (**Figure 2.1a**). The chemical structure of NEN and Oxyclozanide are shown in (**Figure 2.1b and 1c**). In order to study whether NEN and oxyclozanide can increase the OCR, Seahorse OCR assay was performed, our results confirmed that NEN increases OCR and uncouples mitochondria at 2 μM as shown in (**Figure 2.1d**). Same results obtained with oxyclozanide at 20 μM (data not shown). Mitochondrial uncoupling process is often correlated with decreasing of mitochondrial membrane potential. Our lab previously reported that NEN reduces the mitochondrial membrane potential at 0.5 μM in 3T3-NIH fibroblast by using robust and accurate method using TMRE stain (142). As shown in (**Figure 2.1b)** our new data showed that NEN uncouples mitochondria and reduces the mitochondrial membrane potential starting at 0.5 μM in MC38 cells as shown in (**Figure 2.1e and 1g**). In addition, oxyclozanide also reduces the membrane potential starting at 20 μM (**Figure 2.1f and 1h**). Moreover, Similar results we obtained when used Human adenocarcinoma (HCT116) (**Figure 2.2 a and b)**.

In order to test the effect of NEN and oxyclozanide on plasma membrane potential, MC38 cell treated with same concentrations that are uncoupled and reduced the membrane potential then the plasma membrane potential was measured using DiBAC4 (3) dye. Our results showed that NEN and oxyclozanide at low concentrations had no

clear effect on plasma membrane potential and at higher concentrations decreased the plasma membrane potential of MC30 which probably because the continuous reduction of ATP concentration due to large mitochondrial uncoupling as shown in (**Figure 2.3 a-d**).

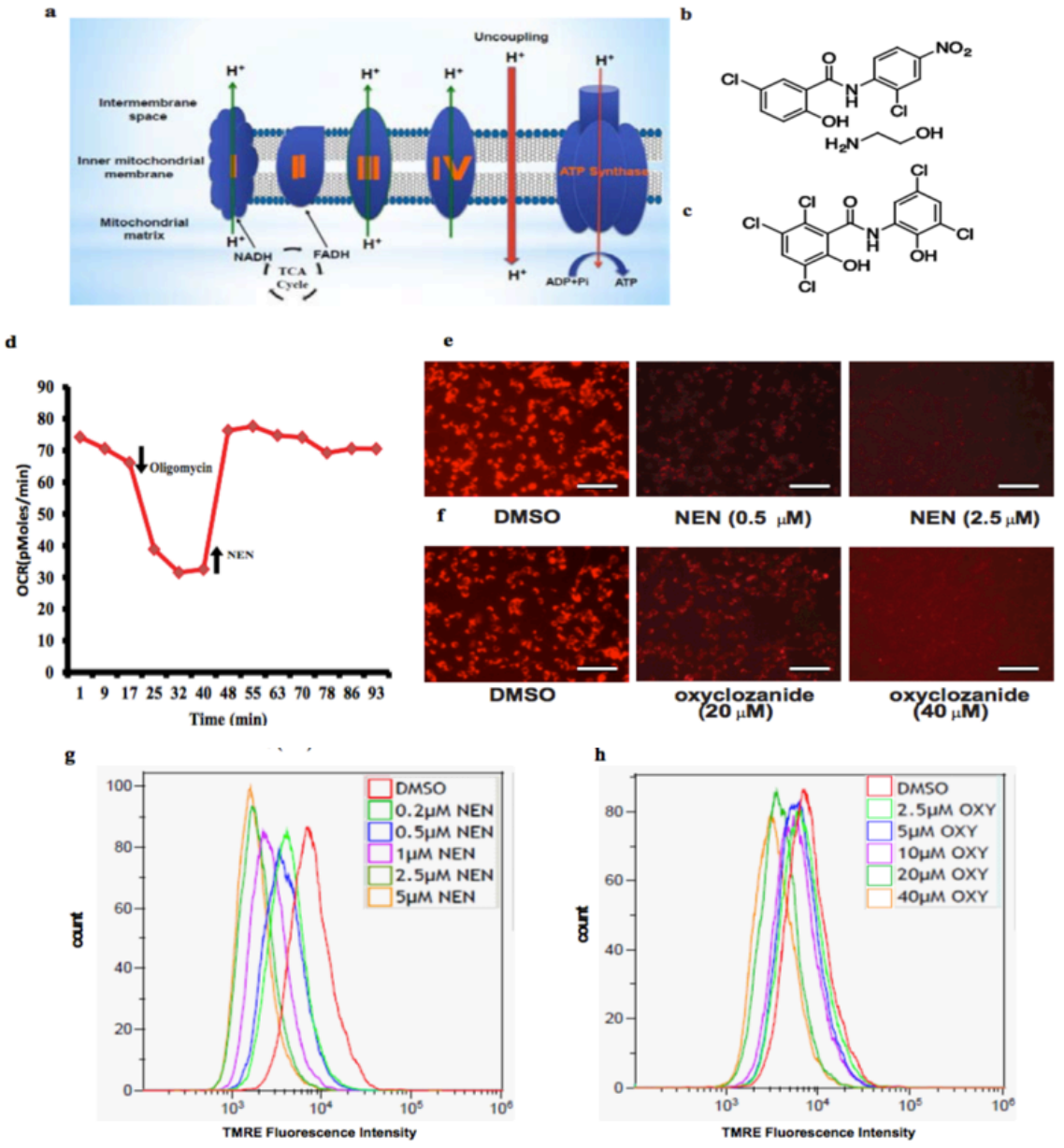

Figure 2.1 NEN and oxyclozanide uncouple mitochondria in cultured cells. (**a**) Schematic representation showing mitochondrial uncoupling process. (**b**) Chemical structure of NEN. (**c**) Chemical structure of oxyclozanide. (**d**) Oxygen Consumption Rate (OCR) of cultured cells with sequential addition of oligomycin (final concentration 2.5 μM) and NEN (final concentration 2.0 μM), as indicated. (**e-f**) Determination of minimal efficacious concentrations of NEN (**e**) and oxyclozanide (**f**) for mitochondrial uncoupling

in murine colon cancer MC38 cells, scale bars, 200 μm. MC38 cells were treated with various concentrations of NEN or oxyclozanide while the control group was treated with vehicle DMSO for 2h, followed staining with (TMRE) for 10 min. (**g-h**) Quantification of TMRE staining by flow cytometry analyses. Results are showed as means ± SD values from three independent experiments and statistical significance (*P*) was determined by student *t*- test: $^{**}P < 0.01$; ***, $P < 0.001$ vs. control.

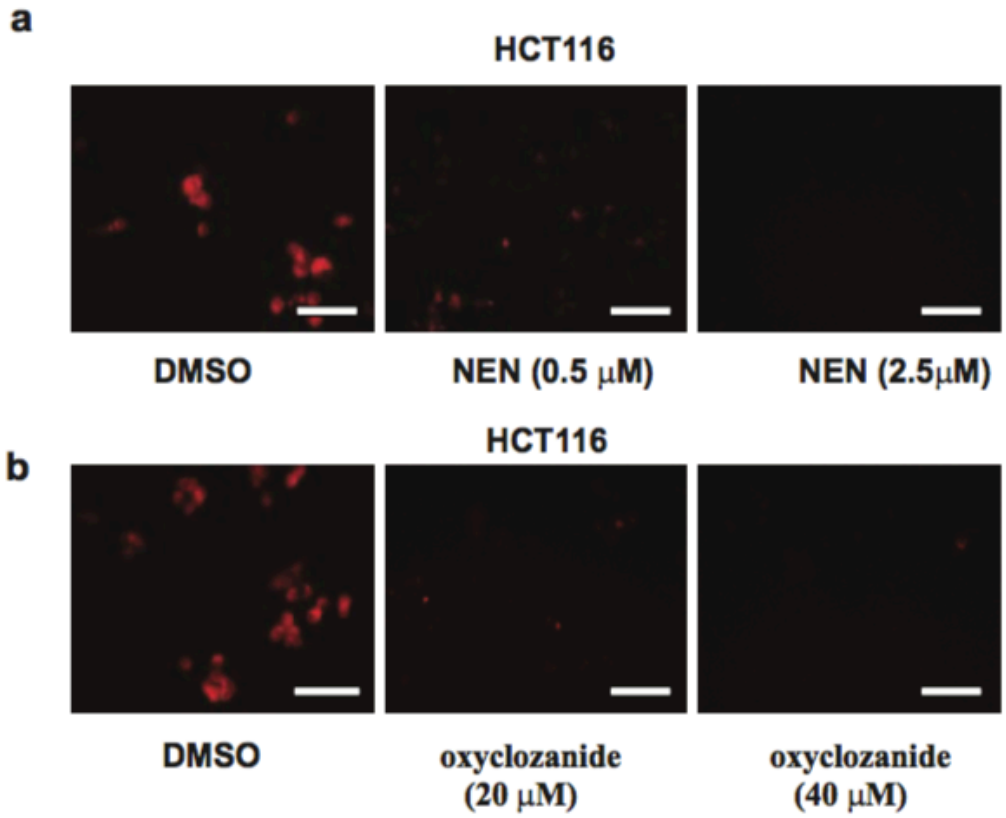

Figure 2.2 Determination of the efficacious NEN and oxyclozanide concentrations that uncouple mitochondria in HCT-116 cells. NEN (**a**) or oxyclozanide (**b**) Cells were treated with NEN or oxyclozanide at various concentrations and mitochondrial membrane

potential was measured with TMRE staining, scale bars, 200.

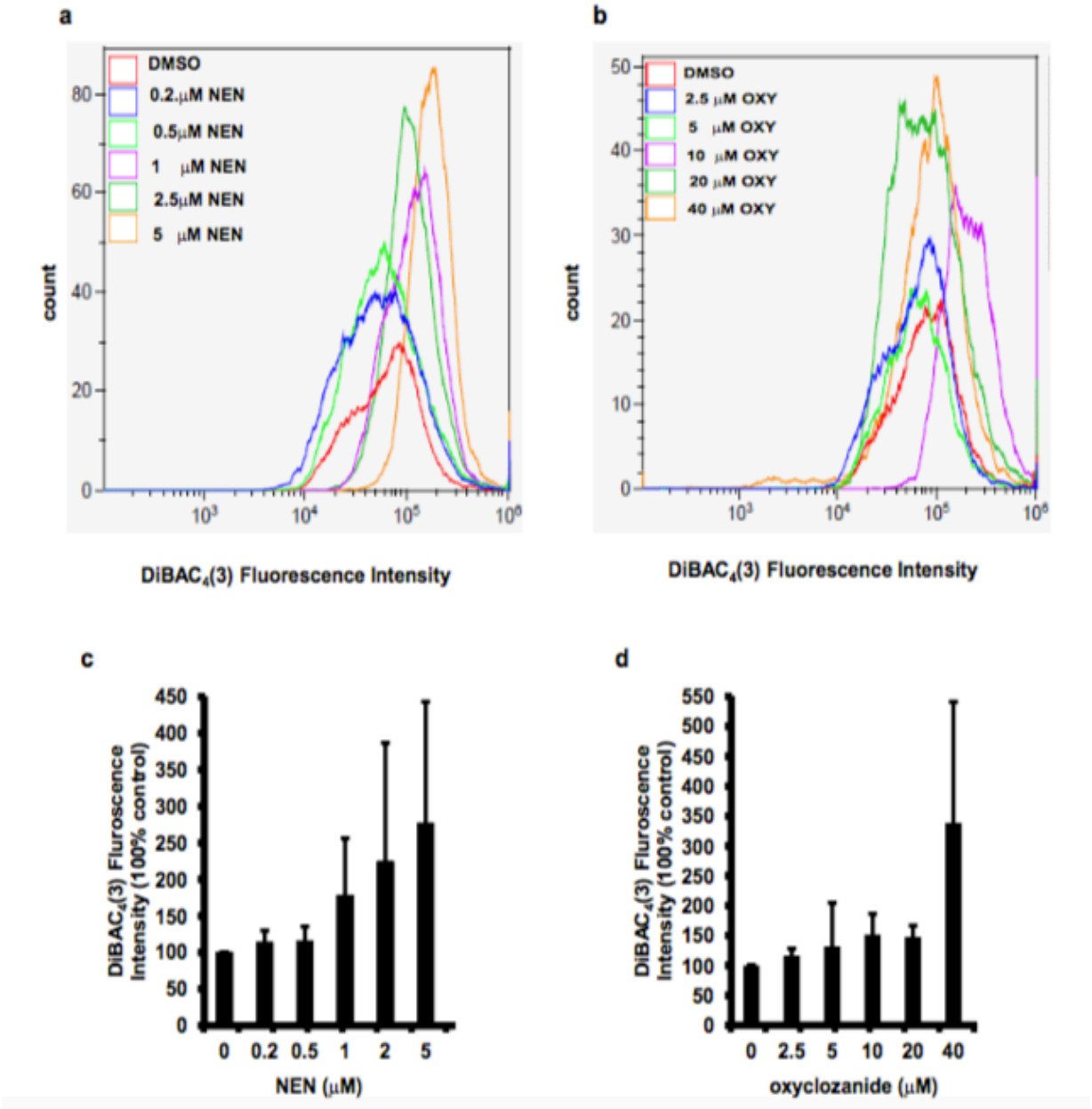

Figure 2.3 Effect of the NEN and oxyclozanide on plasma membrane potential of MC38 cells using DiBAC$_4$(3) dye staining. (a-b) Representative flow cytometry showing the results of NEN and oxyclozanide effects on the plasma membrane potential

of MC38 cells. (**c-d**) Quantification of the effect of NEN and oxyclozanide on plasma membrane potential from three independent experiments. MC38 cells were treated with NEN or oxyclozanide at various concentrations and plasma membrane potential was measured with $DiBAC_4$ (3) dye followed by flow cytometry analyses. For quantification, Mean intensity of DMSO treated cells was set as 100, the relative changes were normalized with DMSO treated cells. Increase in fluorescence intensity is indicative of reduction in plasma cell membrane potential. All results are represented means ± SD from triplicate experiments.

2.2.2 NEN enhances pyruvate influx into mitochondria and inhibits PPP

Metabolomics analysis has assisted oncologic studies to reveal novel targets for cancer therapeutics, and these efforts have ultimately helped to improve therapies and enhance clinical results (192). With that in mind, we decided to study the effect of NEN on the metabolic pathways that are related to glucose metabolism in aerobic glycolysis as shown in **(Figure 2. 4a)**. Specifically we meassured glycolysis, pentose phosphate pathway (PPP), lactate production rate, and glutamine metabolism in MC38 cells incubated with medium containing 50% labeled U-^{13}C glucose and with either NEN (2 μM) or DMSO for 6 and 12 hours. We used [U-^{13}C] glucose tracers and nuclear magnetic resonance (NMR) spectroscopy technique to track the metabolic changes in these pathways in the presence or absence of NEN in the media. All the metabolites and their representative 2D [^{13}C-^{1}H]-HSQC spectra are shown in (**Figure 2.4 and Figure 2. 5**) and Table 1 respectively.

First, we measured the pyruvate dehydrogenase (PDH) to pyruvate carboxylase

(PC) rate by analyzing the ^{13}C labeling pattern of glutamate at C-γ against C-β (**Figure 2.4b**). Our results revealed that the PDH/PC rate is dramatically increased in the NEN treated cells than in the control group, demonstrating that NEN treatment enhances pyruvate influx and oxidation inside mitochondria.

Also, lactate ($^{13}C\alpha$-^{1}H) production was measured, consistent with highly pyruvate oxidation, lactate relative rate significantly decreased in the NEN group compared to control group (**Figure 2.4c**). Furthermore, to test the effect of NEN on PPP rate, we used ^{13}C labeling pattern of ribose C2 UTP or UDP to determine the relative PPP rate. Our results suggested that the PPP rate is lower in NEN treated group compared to the control group as shown in (**Figure 2.4d**).

One carbon pathway also assessed by measuring the relative levels of the serine and glycine. NEN treated group has lower relative level of serine $^{13}C\gamma$- $^{1}H_3$ (**Figure 2.4e**) and glycine $^{13}C\alpha$- $^{1}H_3$ (**Figure 2.4f**) compared to DMSO group. Interestingly, our results also show a reduction in glutamine pool size upon NEN treatment (**Figure 2. 4g**). Taken together, these results suggest that NEN treatment induces pyruvate influx and oxidation inside mitochondria, attenuates PPP, inhibits one carbon pathway, and reduces glutamine pool size.

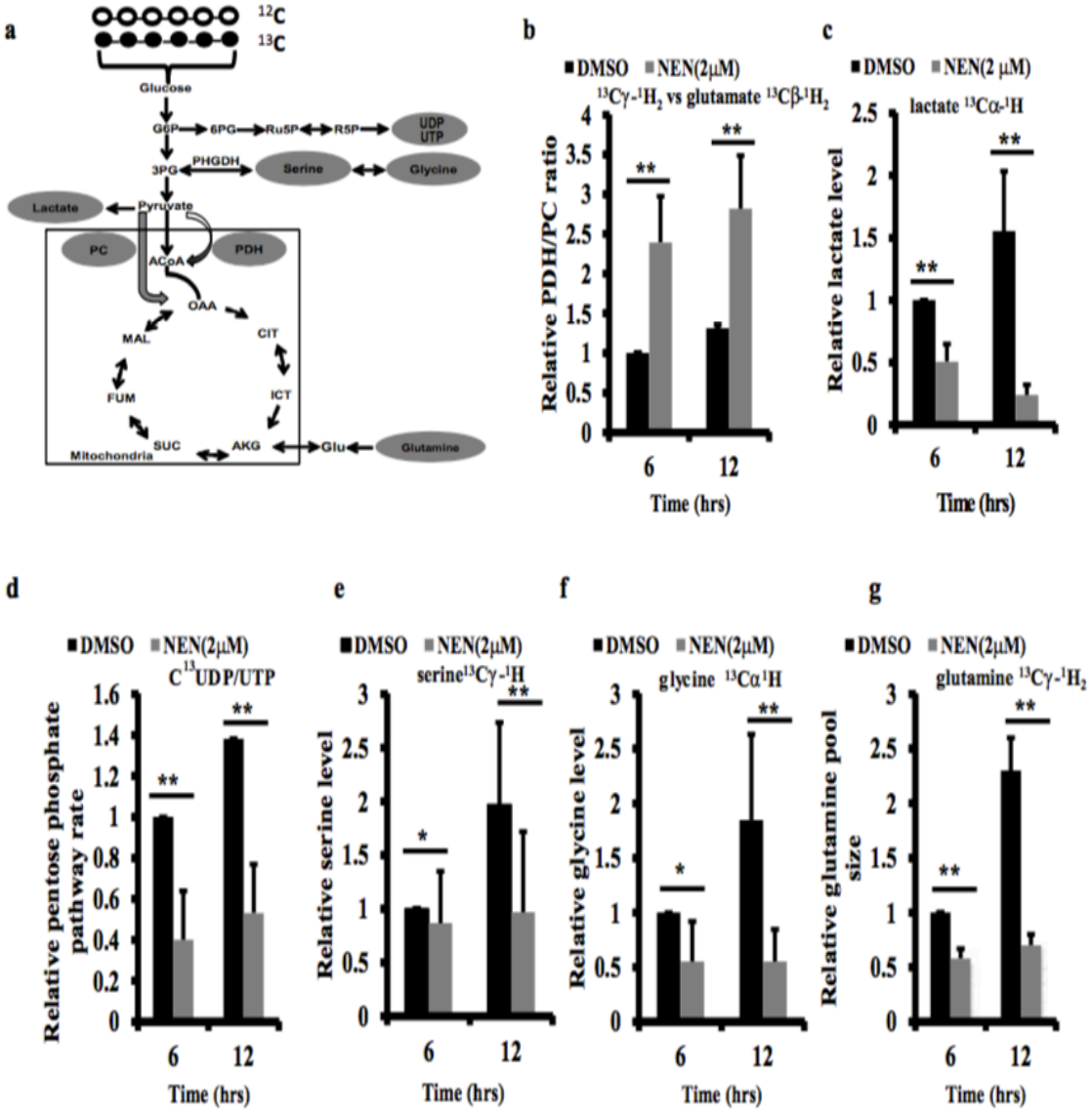

Figure 2.4 NEN inhibits the anabolic effect of aerobic glycolysis on colon cancer cell.

(**a**) Schematic of pathways and molecules measured in metabolomic NMR experiment. (**b**) Relative PDH/PC ratio determined by the ratio of glutamate $^{13}C\gamma\text{-}^{1}H_2$ vs glutamate $^{13}C\beta\text{-}\ ^{1}H_2$. (**c**) Relative lactate level determined by measuring lactate $^{13}C\alpha{-}1H3$. (**d**) Pentose phosphate pathway (PPP) rate determined by measuring UDP/UTP ^{13}C labeling at ribose C2 position. (**e**) Relative serine level determined by measuring serine $^{13}C\gamma\text{-}^{1}H_3$.

(**f**) Relative glycine level determined by measuring glycine $^{13}C\alpha$- $^{1}H_3$. (**g**) Relative glutamine level determined by measuring $^{13}C\gamma$- $^{1}H_2$. For (**b-g**) MC38 cells were grown in medium containing 50% ^{12}C + 50% U- ^{13}C glucose, treating with 2 μM NEN or vehicle DMSO for 6 or 12 hrs as indicated. The cell metabolites were extracted using cold methanol-chloroform extraction process. Abbreviations: G6P, glucose-6-phosphate; 3PG, 3- phosphoglycerate; PHGDH, phosphoglycerate dehydrogenase; 6PG, 6-phosphogluconate; Ru5P, ribulose-5-phosphate; R5P, ribose-5- phosphate; ACoA, acetyl coenzyme A; GlcNAc, N-acetyl-glucosamine; OAA, oxaloacetate; ICT, isocitrate; AKG, a-ketoglutarate; SUC, succinate; FUM, fumarate; MAL, malate. PDH, pyruvate dehydrogenase; PC, pyruvate carboxylase; Glu, glutamine. Results are showed as means ± SD values from three independent experiments and statistical significance (*P*) was determined by student t- test: **P* < 0.05; ***P* < 0.01; vs. DMSO control.

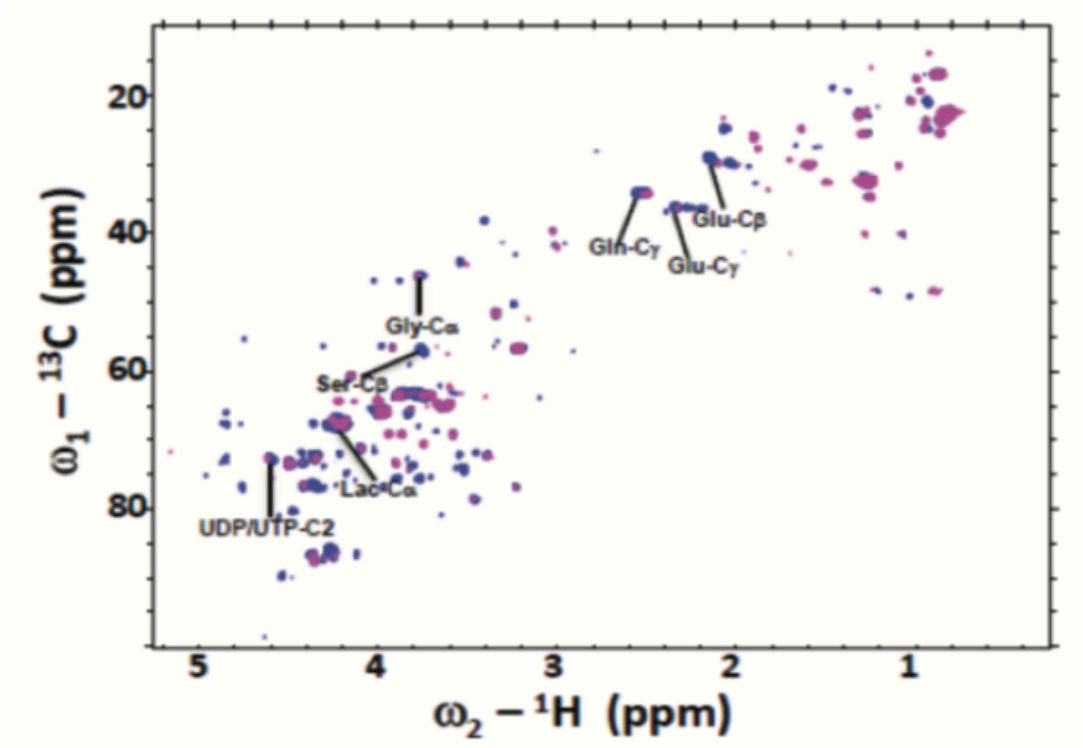

Figure 2.5 Representative 2D ^{13}C-^{1}H- HSQC spectrum of colon cancer MC38 cells untreated (blue) or NEN treated (Magenta) acquired on a 800MHz NMR spectrometer at 25^{o}C. The cross peaks analyzed in the data shown in the Figure 2 are labeled. Abbreviations: Lac, lactate; Glu, glutamate; Gln, glutamine; Gly, glycine; Ser, serine.

Table 2.1 Identification of glucose metabolites based on 2D^{13} C-^{1}H- HSQC spectrum. Colon cancer cells were fed [U-^{13}C] glucose.

Supplementary Table1. 2D ^{13}C-^{1}H-HSQC spectrum of colon cancer cell were acquired based on [U-^{13}C]glucose labeling.

Number	Metabolites	Carbon position	^{1}H chemical shift (ppm)	^{13}C chemical shift (ppm)
	Amino acids			
1	Glutamate	Cβ	2.07, 2.13	29.58
	Glutamate	Cγ	2.36	36.22
2	Glutamine	Cγ	2.46	33.56
3	Glycine	Cα	3.57	44.20
4	Serine	Cβ	3.58	57.26
	Organic acids			
5	Lactate	Cα	4.12	71.22
	Nucleotides			
6	UTP / UDP	C2	4.39	76.49

2.2.3 Mitochondrial uncoupling compounds affect colon caner growth and survival

In order to study the effect of NEN and oxyclozanide on cell cycle profile of murine (MC38) and human (HCT116) colon cancer cell, MC38 cells were treated for 24 hours with 2.5 μM while the control group was incubated with DMSO. NEN caused a significant accumulation of cells in G_0/G_1 with the concomitant reduction of cells in S phase compared to control group (**Figure 2.6 a-c**). Next, we sought to test NEN's anticancer properties in MC38 cells. To this end, cell viability and colony formation assays were performed. NEN treated group ranging from (0.5-5 μM) showed a significant reduction in cell viability and this likely due to slow down the cell growth (**Figure 2.6 a**). The anticancer property was more analyzed using colony formation assay. By Incubate the MC38 cells with low concentrations of NEN for long period. Our results indicated that NEN reduces the colony formation at dose dependent manner (**Figure 2.6 d**). In addition, we obtained the same results when we use HCT116 (**Figure 2.7 a-d**). Then, we tested the anticancer activity of oxyclozanide against (MC38 and HCT116) cells. Our result showed oxyclozanide at effective mitochondrial uncoupling concentrations arrests the cell cycle at G0-G1, reduces colony formations and inhibits the cell growth and proliferation at higher concentration as shown in (**Figure 2.8 a-d**). In summary, our results indicate that NEN or oxyclozanide has potential anticancer effects by inducing cell cycle arrest and reducing cell viability and in colon cancer cells.

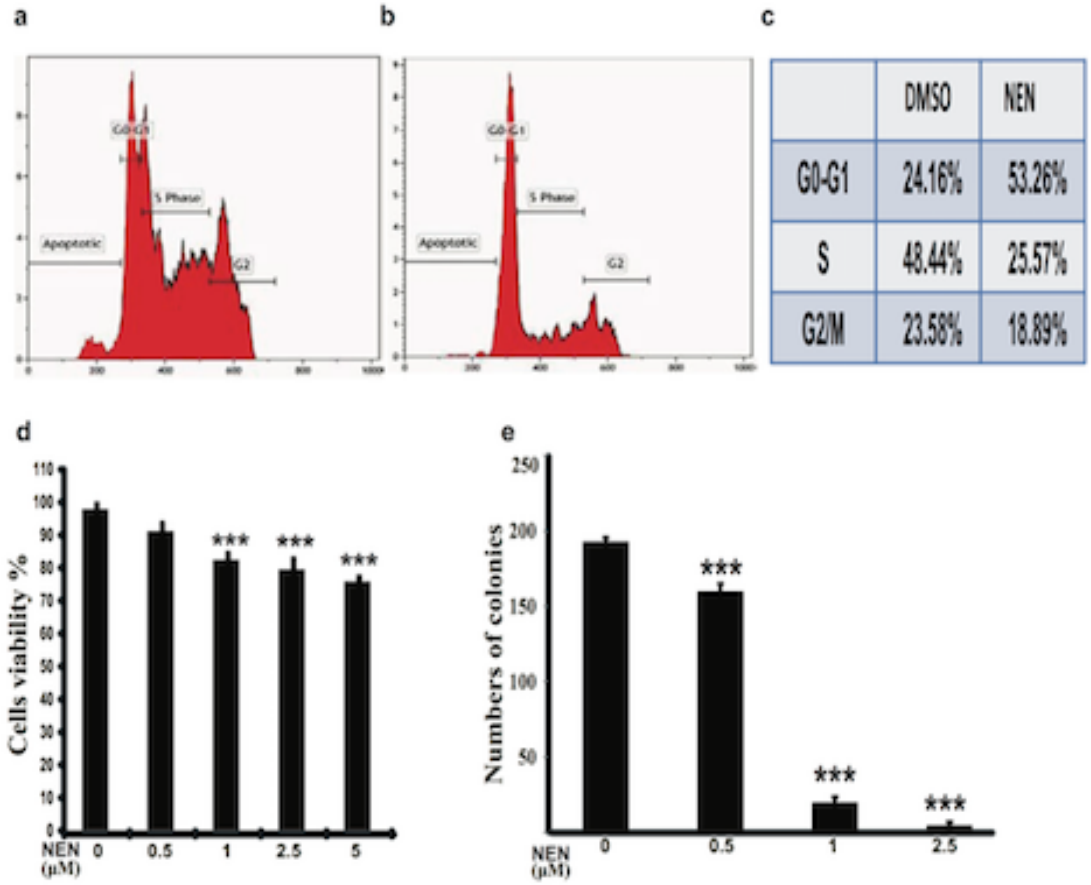

Figure 2.6 NEN affects cell cycle progression and reduces colony formation of colon cancer cells. (**a-c**) Cell cycle profile of MC38 cells treated with DMSO vehicle (**a**) or 2.0 μM NEN (**b**) for 24h, with percentage of cells in each phase summarized in (**c**). (**d**) Cell viability of MC38 cells after a 24 h treatment with NEN at various concentrations, detected by trypan blue exclusion assay. (**e**) Clonogenicity of MC38 cells, cells were grown in medium containing NEN at various concentrations, as indicated, for 2 weeks, and the colonies formed were counted. Results from D-E are shown as means ± SD from three independent experiments and statistical significance (*P*) between the control and treated cells was determined by student t-test: ***, $P < 0.001$

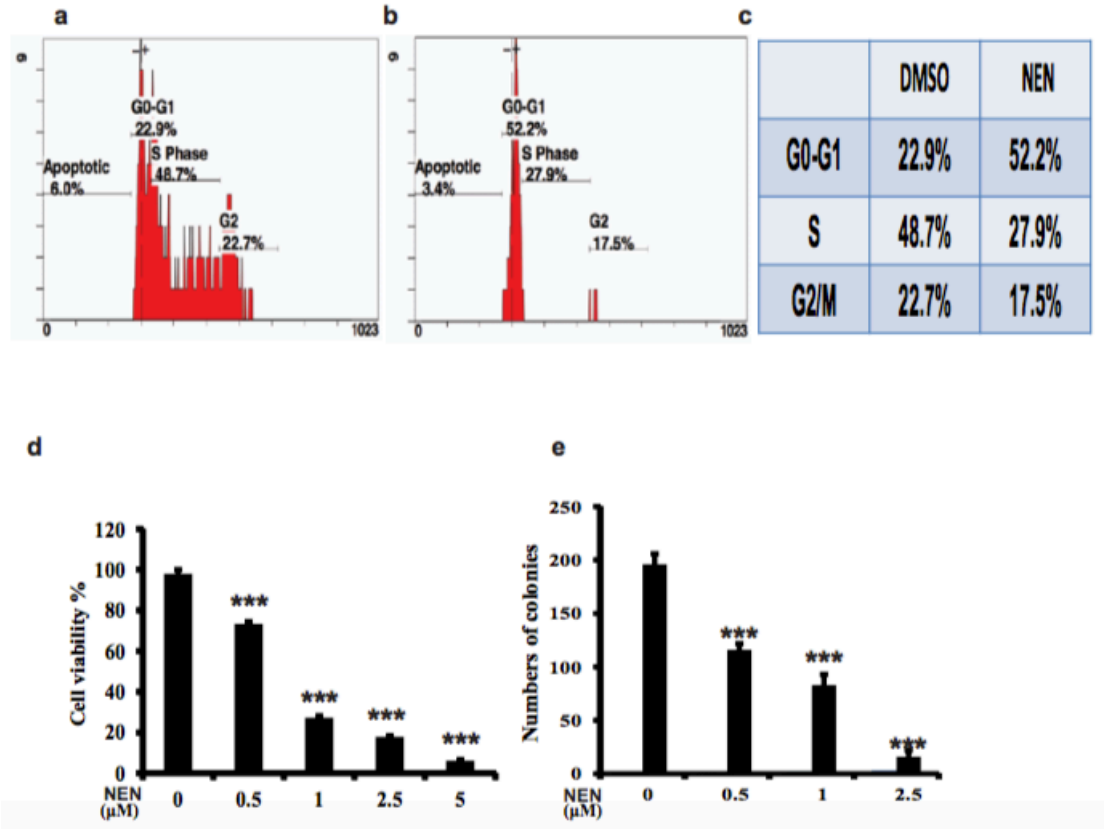

Figure 2.7 NEN affects cell cycle progression and reduces colony formation of human colon cancer HCT 116 cells. (**a- c**) cell cycle profile of HCT116 cells treated with DMSO vehicle (a) or 2.0 μM NEN (b) for 24h, with percentage of cells in each phase summarized in (c). (d) Cell viability of HCT116 cells after a 24 h treatment with NEN at various concentrations, detected by trypan blue exclusion assay. (**e**) Clonogenicity of HCT116 cells, cells were grown in medium containing NEN at various concentrations, as indicated, for 10 days, and the colonies formed were counted. Results from **(d-e**) are shown as means ± SD from three independent experiments and statistical significance (*P*) between the control and treated cells was determined by student t-test. ***, $P < 0.001$.

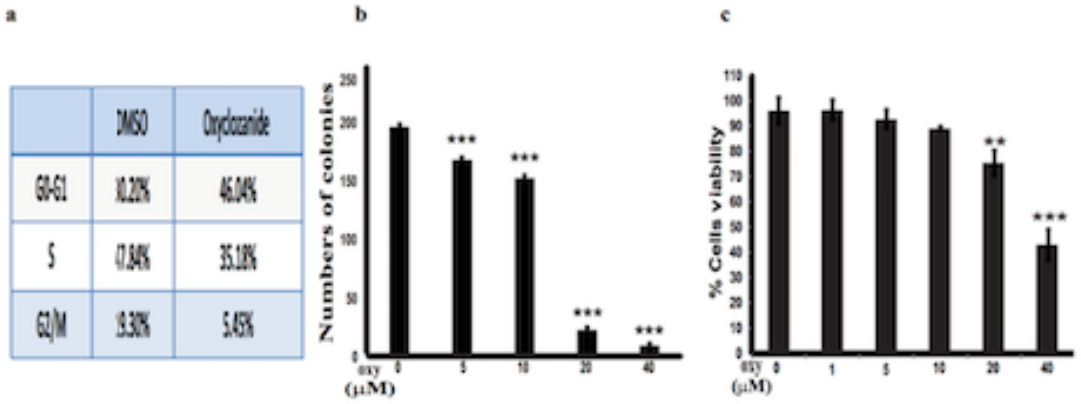

Figure 2.8 Effect of oxyclozanide on cell cycle progression and clonogenicity of MC38 cells. (**a**) Oxyclozanide causes cell cycle arrest, MC38 were treated with (40 μM) oxyclozanide for 24h and percentage of cells at each phase was determined by flow cytometry assay. (**b**) Oxyclozanide reduces cell viability, MC38 cells were treated with different concentrations oxyclozanide for 24 h, and then the cell viability was detected by trypan blue staining. Values expressed means ± SD from triplicate experiments. (**c**) The effect of oxyclozanide on colony formation in MC38 cells. All results are represented means ± SD from triplicate experiments and (*P*) value was detected by (ANOVA) (**P* < 0.05; ***P* < 0.01; ****P* < 0.001 vs. DMSO control).

2.2.4 NEN and oxyclozanide prevent cancer cells invasion and migration

To study the inhibitory effect of the uncoupling compounds on MC38 colon cancer cells, invasion and migration assays were performed. First, we tested the inhibitory effect of NEN on colon cancer cell invasion using a Boyden chamber assay. NEN treated cells showed a substantial inhibition of invasion when compared to the control group (DMSO vs 1 μM NEN mean = 91% vs 21%, *P*< 0.001) (**Figure 2.9a and b**). Next, we analyzed

the effect of NEN on colon cancer cell migration by using a wound-healing assay. MC38 cells were treated with vehicle completely closed the wound after 12h treatment while NEN treated cells showed impaired migration, preventing the wound to close even after 12h (**Figure 2.9 c and d**). Same results we obtained when we used oxycloxanide as shown in (**Figure 2.10a-d**). These results indicate that NEN and oxyclozanide treatment inhibits colon cancer cell mobility, impairing invasion and migration.

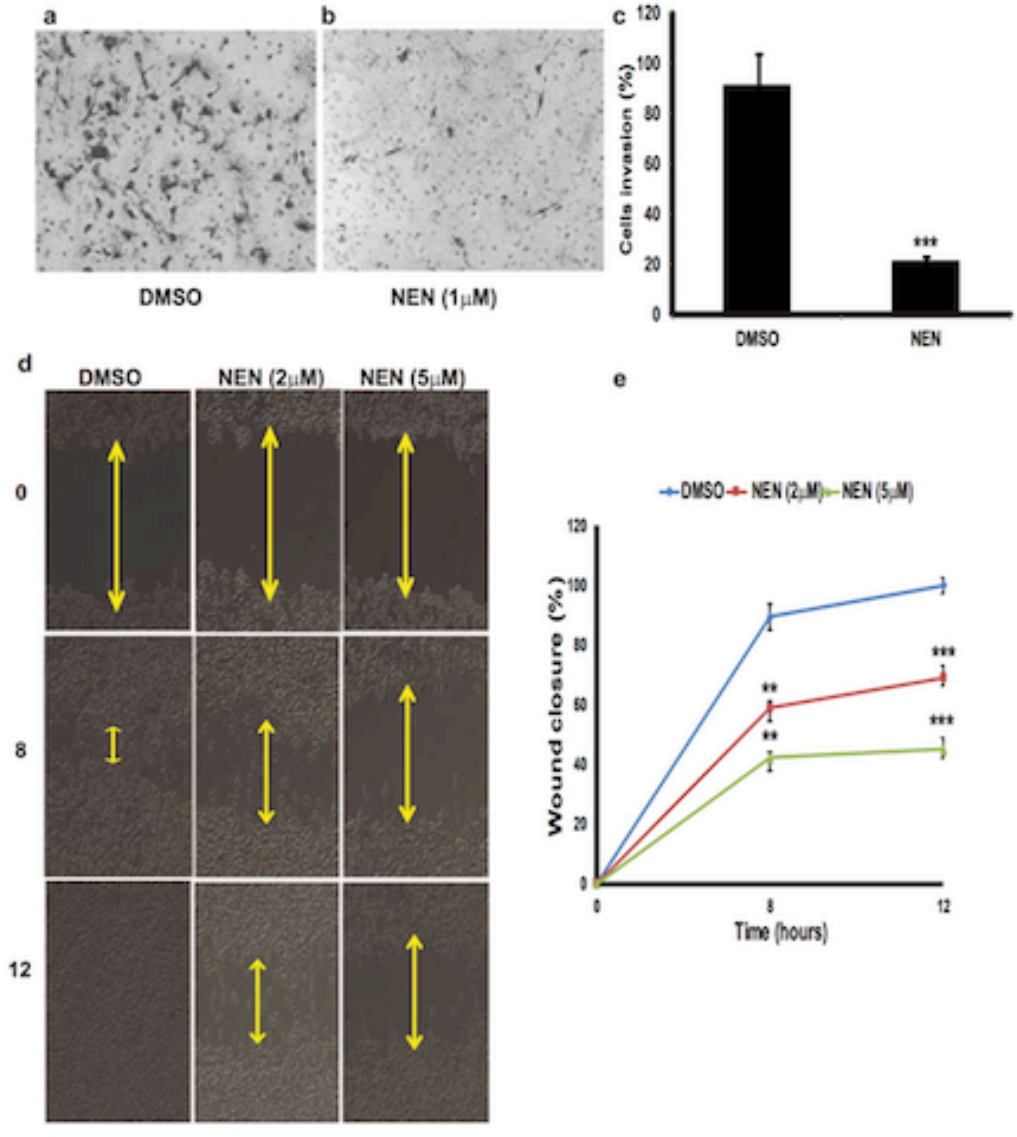

Figure 2.9 NEN reduces colon cancer cell invasion and migration. (a-b) Boyden chamber assay showing representative pictures of stained cell migrated through the trans-wells, either under control condition (a), or in the presence of 1 μM NEN. Scale bars, 50 μm. (c) Quantification of (a-b). (d) Representative pictures showing wound closure of cells treated with vehicle (DMSO) or NEN (either 2 μM or 5 μM as indicated) at 0, 8, 12 h time points. (e) Quantification of percentage of wound closure, under each condition; the gaps were measured at 5 different positions and averaged. Results shown as means ± SD. Scale bars, 20 μm. Statistical significance (*P*) was determined by student-t test between the control and drug treated cells. **, P<0.01; ***, $P < 0.001$. All data show representative results from three independent experiments.

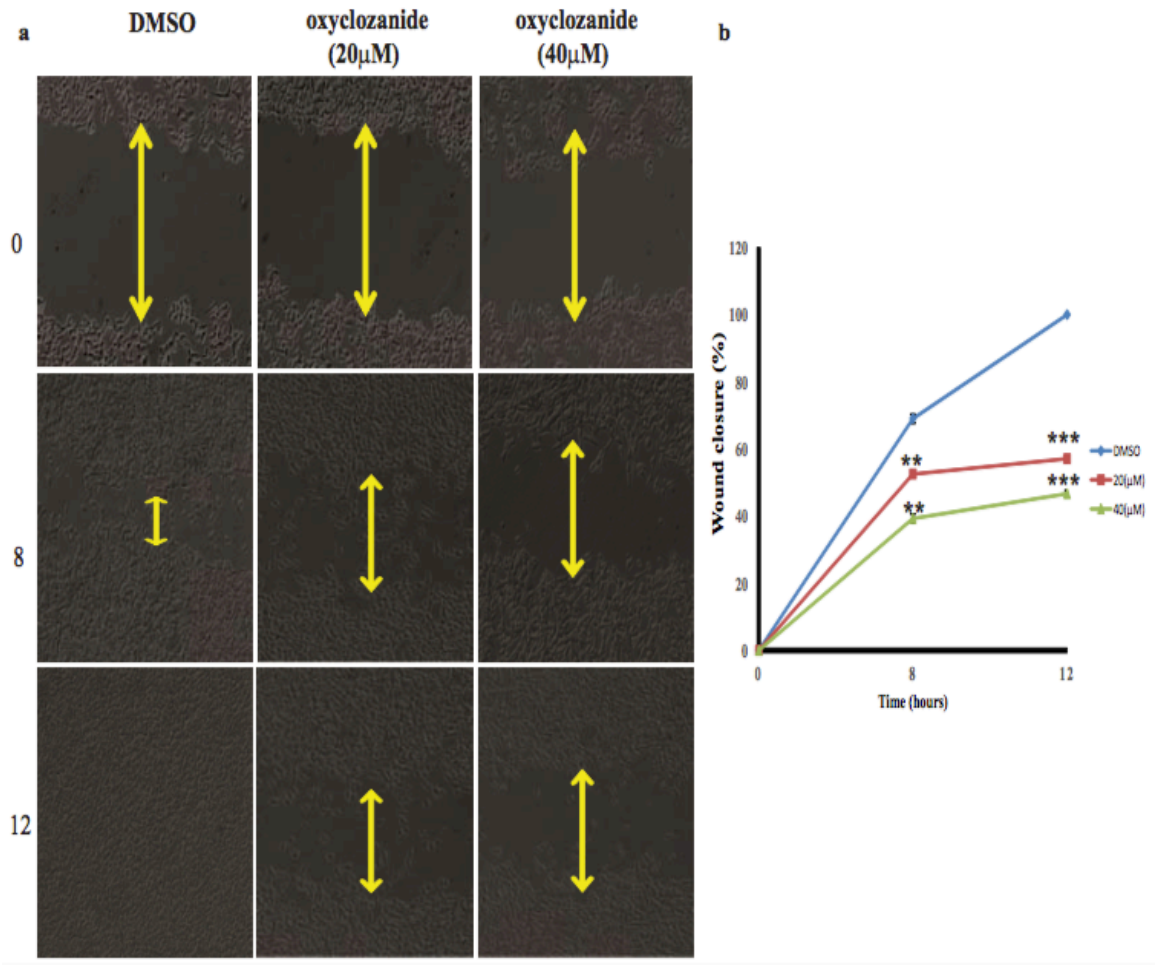

Figure 2.10 Oxyclozanide reduces colon cancer cell migration. (a) Representative pictures showing wound closure of MC38 cells treated with vehicle (DMSO) or oxyclozanide (either 20 μM or 40 μM as indicated) at 0, 8, 12 h time points, as indicated. (b) Quantification of percentage of wound closure. Under each condition, the gaps were measured at 5 different positions and averaged. Scale bars, 20 μm. Results shown as means ± SD. Statistical significance (*P*) was determined by student-t test between the control and drug treated cells. **, P<0.01; ***, $P < 0.001$. All data show representative results from three independent experiments.

3.2.5 Mitochondrial uncoupling compounds impair colon cancer growth and metastasis

In order to study the inhibitory effect of NEN or oxyclozanide on liver metastasis of colon cancer, we used a well-established model of liver metastasis in NOD mice, MC38 cells were injected intrasplenically in NOD mice. Then, the animals were randomly divided into three groups. The control group was fed with AIN-93M normal rodent diet, while the treated groups were fed with either AIN-93M diet containing NEN 2000 ppm or oxyclozanide 800 ppm or for 3 weeks. Our data revealed that tumor growth was reduced in the NEN and oxyclozanide treated groups compared to control animals as shown in (**Figure 2.11a-c**). In addition, histological sections from livers showed that the tumor cells proliferation was higher in control group than in NEN or oxyclozanide group (**Figure 2.11d-f**). Importantly, the number of tumors resulting from splenic metastasis was significantly reduced in the NEN ($P < 0.03$) and oxyclozanide ($P < 0.0004$) groups when compared to the control group. Our results indicate that oral NEN or oxyclozanide either totally prevented tumor metastasis to liver or drastically reduced metastatic tumor numbers and tumor volume.

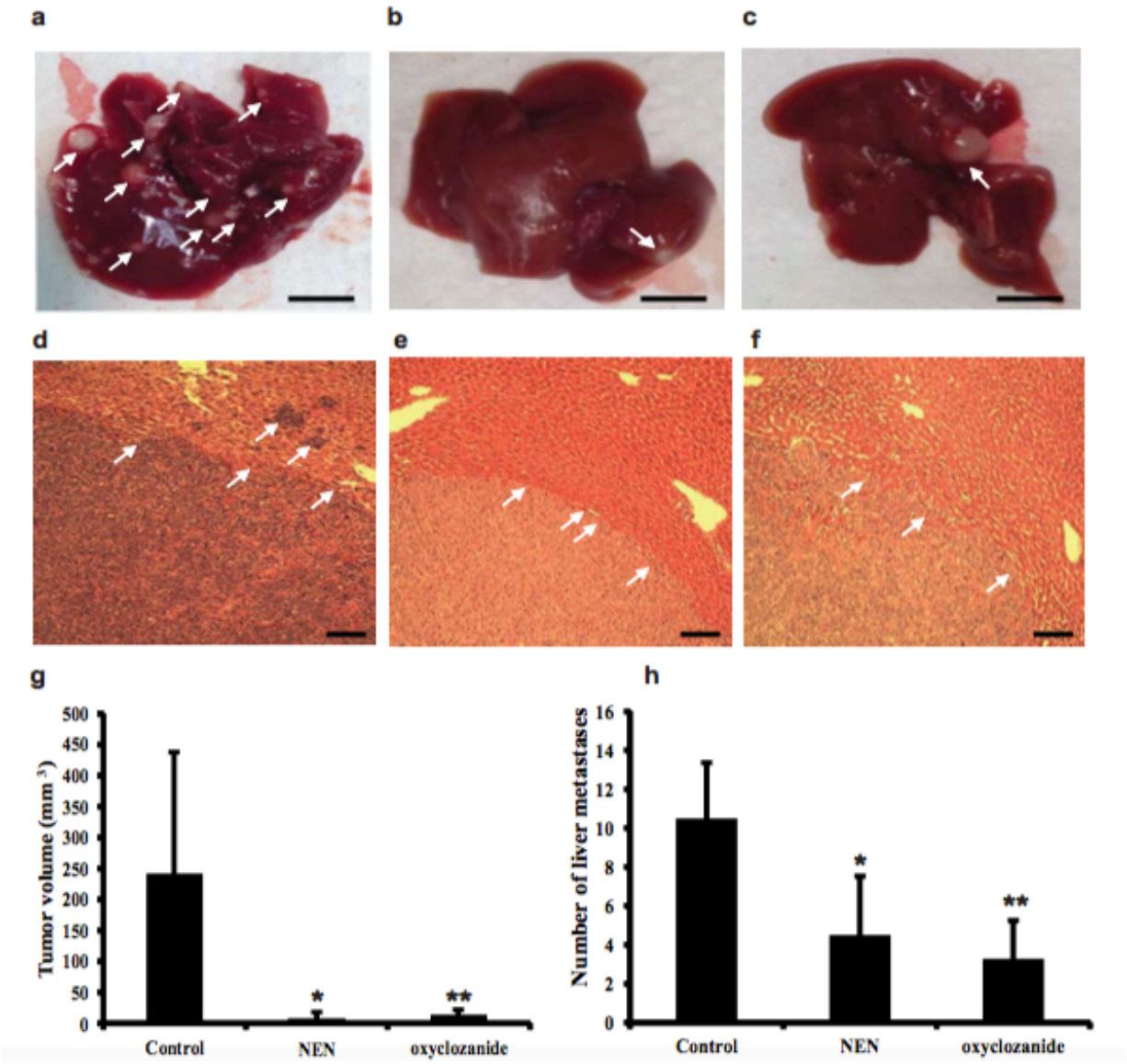

Figure 2.11 Effect of NEN and oxyclozanide on liver metastasis of colon cancer cells. (**a-c**) Representative liver pictures (scale bars, 10 mm) showing the tumor nodules from mice fed normal chow (**a**) or diet containing 2000 ppm NEN, or diet containing 800 ppm oxyclozanide. (**d-f**) Representative hematoxylin and eosin (H & E), (scale bars, 200 μm), staining of histological section of metastatic tumors mice fed normal diet (**d**), diet containing NEN (**e**), or diet containing oxyclozanide (**f**). (**g-h**), average metastatic tumor

volume (**g**) or number of node (h) per mouse in animals with indicated treatment. MC38 cells were injected into male NSG mice intrasplenically and randomized into 3 groups (n=10 per group). The mice were fed normal chow, or chow containing 2000 ppm NEN, or chow containing 800 ppm oxyclozanide for three weeks, before euthanization and characterization of metastatic hepatic cancer. Numbers are presented by means ± SD. *P* value between control and each treated group was determined by student t-test: $*P < 0.05$ and $**P < 0.01$. The data show representative results from two independent experiments.

2.2.6 Mitochondrial uncoupling compounds induce AMPK activation and downregulate mTOR activity

AMP-activated protein kinase (AMPK) is a master regulator of cellular energy homeostasis (114). In a recent study, AMPK was found to be a negative regulator for Warburg effect and cancer progression (119).Our lab previously demonstrated that NEN has the ability to activate AMPK in cultured cells (142). To test if NEN or oxyclozanide able to activate AMPK in MC38 colon cancer cells, MC38 cells treated with different concentration of NEN or oxyclozanide for 2 hours and cells lysate used for western blot analysis. Our data showed that NEN or oxyclozanide indeed activated AMPK in a dose and time that uncouples the mitochondria as shown in (**Figure 2.12a**).

Mammalian target of rapamycin (mTOR) is a conserved serine-threonine protein kinase that has a controlling role in cellular growth, proliferation, sensor for protein synthesis, cell metabolism and growth (128) .In addition, mTOR is a downstream target of AMPK signaling (114). Phosphorylation of p70SK and 4EBP1 can be used as readout for mTOR activity, since these proteins are mTOR's natural substrate (127).

In order to study the effect of AMPK activation by NEN on mTOR activity in cancer cells, MC38 cells were treated with different concentration of NEN and phosphorylation of p70S6K and 4EBP1 was monitored by western blot. As shown in (**Figure 2.12 a and b**) NEN has the ability to downregulate mTOR activity by decreased phosphorylation of p70S6K and 4EBP1.

Lastly, we wondered whether NEN or oxyclozanide could induce AMPK activation in vivo. To this end, mice were fed for 3 weeks with mature diet contain either NEN 2000 ppm, oxyclozanide 800 ppm or mature diet only. Then, liver tissue was collected and homogenized to test AMPK activation by western blot. The results demonstrated that chronic treatment with NEN or oxyclozanide activate AMPK (**Figure 2.12c**).

In order to check the activation of AMPK upon acute treatment, oxyclozanide was administered to male C57BL/6J mice via oral. Briefly, oxyclozanide was dissolved in 0.5% methylcellulose and then given to (n = 2 for each time point) by oral gavage at a dose of 80 mg per kg body weight. Mice were then euthanized after 6 hours after gavage (**Figure 3.12d**). Western blot results indicated that oxyclozanide has the ability to activate AMPK in liver tissue after 6 hours from oral administration. In addition, our data demonstrated that the chronic oral treatment with NEN or oxyclozanide also inhibit mTOR activity in hepatic tissue as shown in (**Figure 2.12e**). Together, these results suggest that mitochondrial uncoupling upregulates AMPK *in vitro* and *in vivo* and the AMPK activation led to downregulate mTOR activity.

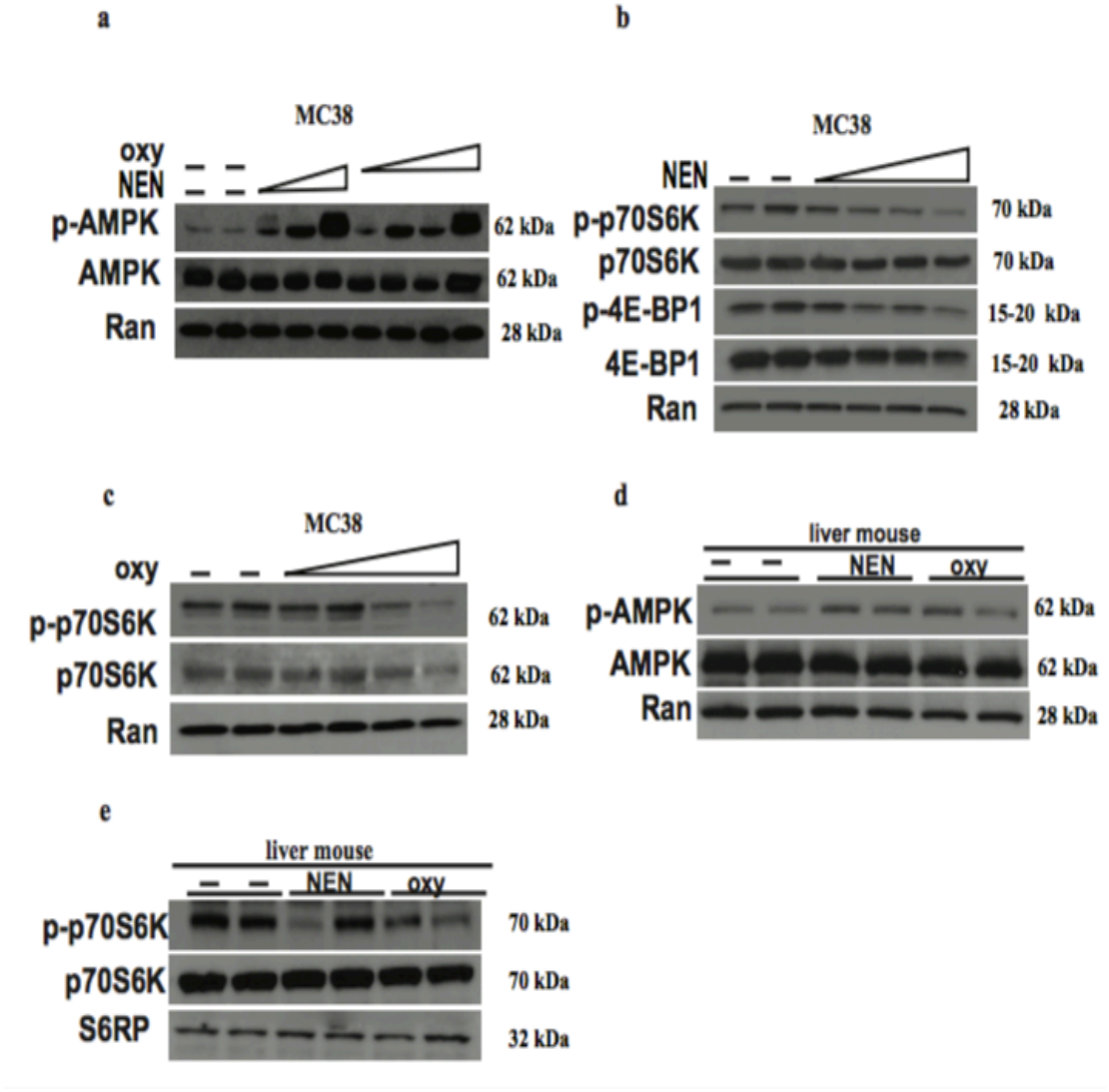

Figure 2.12 NEN and oxyclozanide activate AMPK and downregulate mTOR *in vitro* and *in vivo*. (**a-c**) Immunoblot analyses of MC38 cells without or with treatment of NEN (1,2.5 and 5μM) or oxyclozanide (5,10,20 and 40μM) for 2 hrs with indicated antibodies. (**d-e**) Immunoblot analyses of mouse liver tissues from mice fed normal chow, or chow containing 2000 ppm NEN, or chow containing 800 ppm oxyclozanide for three weeks, with indicated antibodies. The data are representative results from two independent experiments

Chapter III

3. Treating pancreatic cancer and its hepatic metastasis through targeting cancer cell metabolism by mitochondrial uncoupler

3.1 Introduction and rationale

Pancreatic Ductal Adenocarcinoma (PDA) is incurable and devastating tumor that is characterized by rapid progression, metastatic recurrence and highly resistance to therapeutic treatment (193,194). PDA is the fourth leading cause of death within five years survival rate for only 6% of all stages and less than six months as median survival rate after diagnosis (193,195). PDA cells exhibit aerobic glycolysis, or the Warburg effect (8,196,197). In the presence of oxygen, cancer cells convert a majority of pyruvate derived from glycolysis to lactate (2,24). The most important functional significance of the Warburg effect to tumorigenesis is to reduce pyruvate flux into mitochondria, preventing the complete oxidation of glucose (2,119). A significant amount of glucose is thus shunted into pathways for synthesis of the building blocks (ribose) and reducing agents (e.g. NADPH) for biosynthesis required for cell proliferation (23,198,199). In addition, PDA cells are highly addicted to glutamine for supporting new building blocks, which are necessary for PDA cells proliferation (20,38,200,201).

Mitochondrial uncoupling is a process that facilitates protons influx across the mitochondrial inner membrane without generating ATP (202,203). Consequently, mitochondrial uncouplers stimulate an “idle” cycle of acetyl- CoA oxidation. Therefore, mitochondrial energy efficiency is disputed. In order to the cells keep the cellular energy, pyruvate influx into mitochondria is likely increased that promote glucose and glutamine

oxidation completely inside mitochondria. This kind of metabolic behavior induced through mitochondrial uncoupling and could possibly reduce the anabolic role of aerobic glycolysis and glutamine metabolism on PDA cells.

Niclosamide is an anthelmintic FAD approved drug used to treat tapeworm and its mechanism of action by uncouples mitochondria of the worm (167,168). Previous studies demonstrated that niclosamide has a robust in vitro anticancer activity against many of cancer cells.

NEN (niclosamide ethanolamine) is the ethanolamine salt of niclosamide that has a similar safety profile like niclosamide (167,186-188) and has good water solubility and systemic exposure (188). Our previous study demonstrated that NEN is completely metabolized inside liver (142). In addition, our recent study demonstrated that NEN uncouples mitochondria, arrests the cell cycle, inhibits colony formation and reduces the cell viability in murine and human colon cancer. Furthermore, NEN reduces liver metastasis of colon cancer. Moreover, NEN antagonized the anabolic roles of aerobic glycolysis by increases pyruvate oxidation inside mitochondria, inhibits PPP and one-carbon pathways. Therefore, we propose that mitochondrial uncoupler compound could a new strategy for preventing and treating pancreatic cancer and its liver metastasis by targeting the cell metabolism. Here we used a new synthesized a mitochondrial uncoupler MB1-47 and NEN to study their metabolic effects and anti-cancer activity in both cultured PDA cells and mouse models. Hepatic metastasis is a major type of recurrence after pancreatectony therapy and influence survival gain significantly. Thus, our focusing on the hepatic metastasis of PDA metastasis because NEN and MB1-47 are completely metabolized inside the liver.

3.2 Results

3.2.1 MB-47 and NEN effects uncouple mitochondria in pancreatic cancer

Increasing the Oxygen Consumption Rate (OCR) of mitochondria is the hallmark of mitochondrial uncoupling in presence of ATP synthase inhibitor like oligomycin. The chemical structure MB1-47 is shown in (**Figure 3.1a**). In order to test the uncoupling activity of MB1-47 on pancreatic cancer cells, OCR was measured by Seahorse oxygen consumption rate assay in Panc02 cells upon treatment MB1-47. As shown in (**Figure 3.1 b**) our data showed that MB1-47 increases the OCR and uncouple the mitochondria at 2.5 μM.

Mitochondrial uncoupling process is regularly correlated with reducing the membrane potential of mitochondria that acts a good and accurate method to determine the lowest concentration needed to induce mitochondrial uncoupling. Previously, we showed that NEN uncouples mitochondria and reduces mitochondrial membrane potential in colon cancer cells at 0.5 μM.

Here our data showed that MB1-47 is effective to uncouples the mitochondria of murine and human pancreatic adenocarcinoma cell lines (Panc02 and Panc1) respectively starting at 0.5 μM (**Figure 3.1 c and d**). Same data we obtained when pancreatic cancer cell treated with NEN as shown in (**Figure 3.2 a-d).** Together, these data demonstrated that MB1-47 and NEN have the ability to increase the OCR, uncouple the mitochondria and reduce the membrane potential of murine and human pancreatic cancer cells.

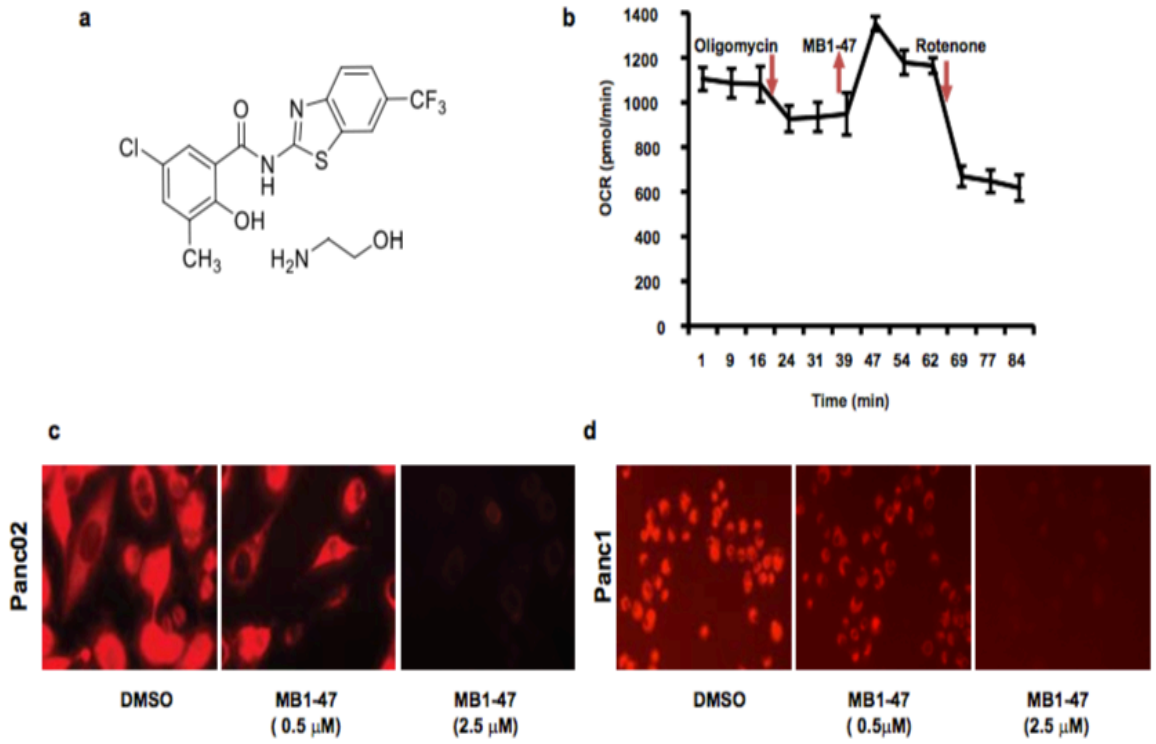

Figure 3.1 MB1-47 uncouples mitochondria in pancreatic cancer cells. (**a**) Chemical structure of MB1-47. **(b)** Oxygen Consumption Rate (OCR) of Panc02 cells with sequential addition of Oligomycin (final concentration 5 μM), Rotenone (final concentration 2.5 μM), and MB1-47 (final concentration 2.5 μM) as indicated. (**c and d)** Minimal effective concentrations of MB1-47 for mitochondrial uncoupling in murine Panc02 and human (Panc1 pancreatic cancer cells, scale bars, 200 μm. Panc02 and Panc1cells were treated with various concentrations of MB1-47 while the control group was treated with vehicle DMSO for 2h, followed staining with (TMRE) for 10 min. Results are indicated as means ± SD values from three independent experiments.

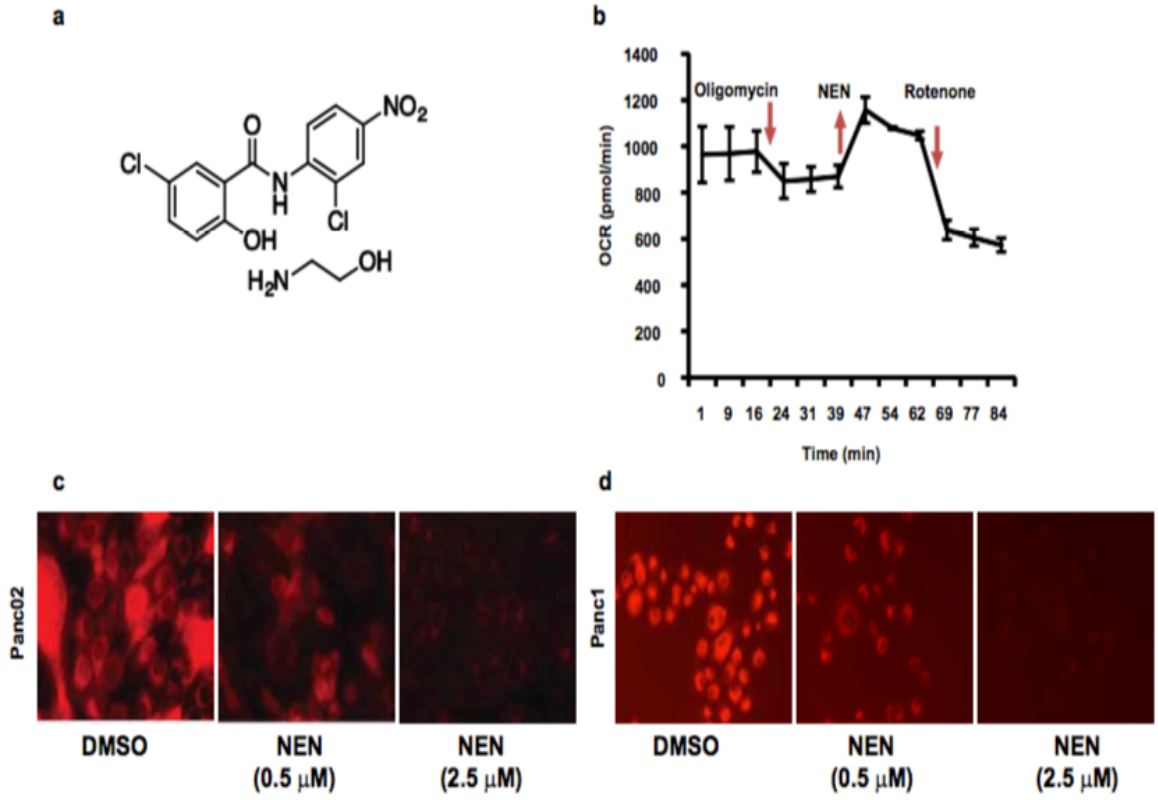

Figure 3.2 NEN uncouples mitochondria in pancreatic cancer cells. (**a**) Chemical structure of NEN. **(b)** Oxygen Consumption Rate (OCR) of Panc02 cells with sequential addition of Oligomycin (final concentration 5 μM), Rotenone (final concentration 2.5 μM), and NEN (final concentration 2.5 μM) as indicated. (**c and d)** Minimal effective concentrations of NEN for mitochondrial uncoupling in murine Panc02 and human (Panc1 pancreatic cancer cells, scale bars, 200 μm. Panc02 and Panc1cells were treated with various concentrations of NEN while the control group was treated with vehicle DMSO for 2h, followed staining with (TMRE) for 10 min. Results are indicated as means ± SD values from three independent experiments.

3.2.2 Mitochondrial uncoupler compounds inhibit cell cycle progression, reduce the colony formation and decrease the cell proliferation of pancreatic cancer cells

We next study the effect of MB1-47 compound on murine and human pancreatic cancer cell proliferation. First, we decided to study MB1-47 effect on cell cycle profile of murine and human pancreatic cancer cells. Our results indicated that MB1-47 significantly enhanced the accumulation of cells in G_0/G_1 with the simultaneous decreasing the cells number in S phase compared to control group as shown in **(Figure 3.3 a-d)**. The anti-cancer action of MB1-47 was further investigated with colony formation assay. Continuously exposure to low concentration of MB1-47 led to over 90% (1 μM) to near 100% (2.5 μM) reduction in colony formation (**Figure 3.3 e and f**). In addition, we study the antigrowth effect of MB1-47 against pancreatic cancer cells. Seven pancreatic cell lines were treated with different concentrations of MB1-47 for 48hr, and the cell proliferation percentage was evaluated by SRB assay. The results revealed that MB1-47 at low concentrations ranging from 0.2μM to 5 μM led to decrease the pancreatic cancer cell proliferation at dose dependent manner as shown in (**Figure 3.3 g)**. Furthermore, NEN also arrests the cell cycle profile, reduces colony formation and inhibits the pancreatic cells growth as shown in (**Figure 3.4 a-g**). These data showing MB1-47 and NEN have a powerful anti-cancer activity *in vitro* cell culture models. In addition, MB1-47 is more effective than NEN on the inhibiting pancreatic cancer cell proliferation and differentiation in vitro cells models.

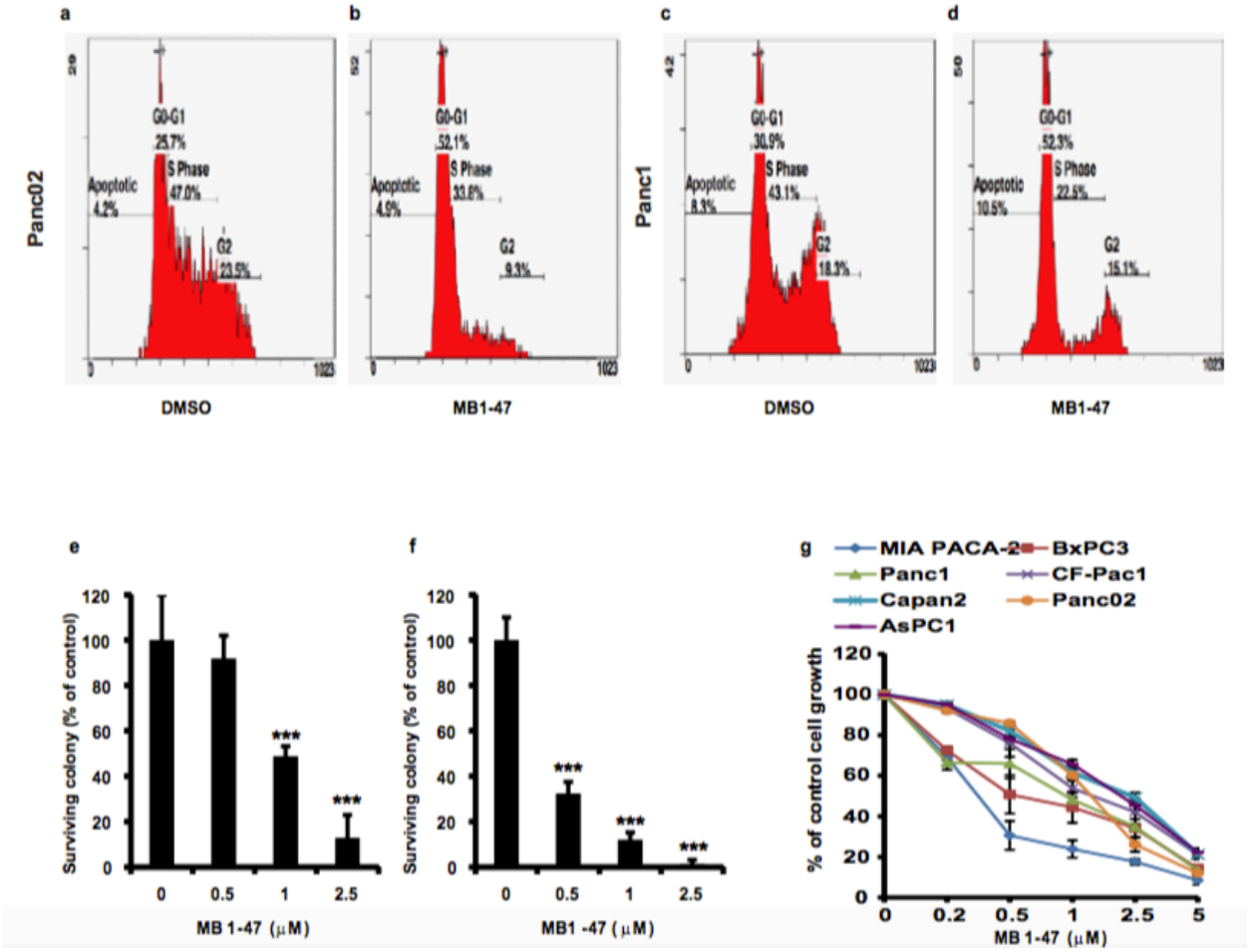

Figure 3.3 MB1-47 affects cell cycle progression, reduce colony formation and inhibit the cell proliferation of pancreatic cancer cells. (**a- d)** MB1-47 arrests the cell cycle of pancreatic cancer cells at G0-G1 phase, Panc02, Panc1 cells treated with 2.5 μM of MB1-47 while the control group treated with DMSO for 48hr. (**e**) MB1-47 reduces the colony survival rate of pancreatic (Panc02 and Panc1) cancer cells. (**f**) MB1-47 inhibits pancreatic cancer cell growth, pancreatic cancer cells treated with different concentrations of MB1-47 for 48h, and cell growth inhibition was detected by sulforhodamine B (SRB) staining. Results from (**a-f)** are shown as means ± SD from

three independent experiments and statistical significance (*P*) between the control and treated cells was determined by student t-test: ***, $P < 0.001$

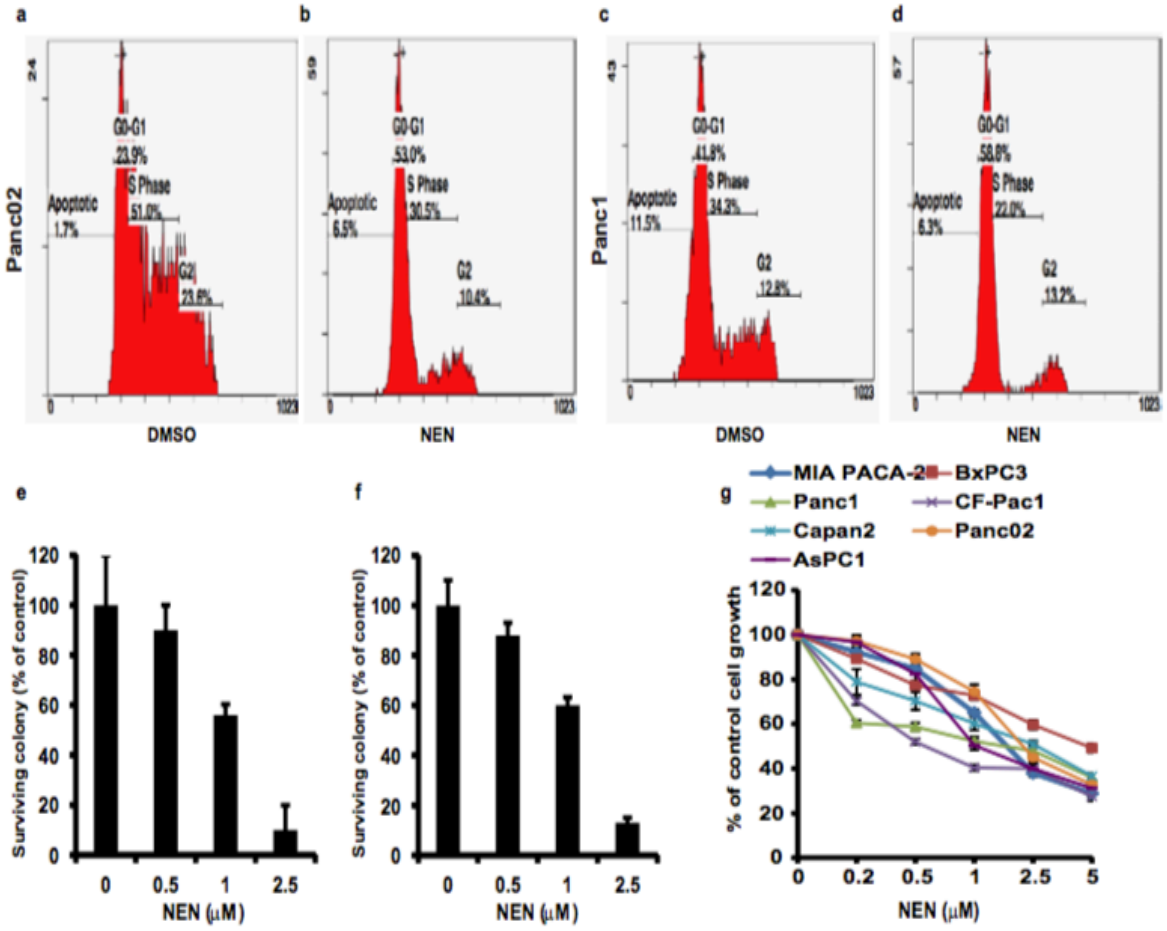

Figure 3.4 NEN arrests cell cycle progression, reduce colony formation and inhibit the cell proliferation of pancreatic cancer cells. (**a- d)** NEN arrests the cell cycle of pancreatic cancer cells at G0-G1 phase, Panc02, Panc1 cells treated with 2.5 μM of NEN while the control group treated with DMSO for 48hr. (**e**) NEN reduces the colony survival rate of pancreatic (Panc02 and Panc1) cancer cells. (**f**) NEN inhibits pancreatic cancer cells, pancreatic cancer cells treated with different concentration of NEN for 48h,

and cell growth inhibition was detected by sulforhodamine B (SRB) staining. Results from (**a-f)** are shown as means ± SD from three independent experiments and statistical significance (*P*) between the control and treated cells was determined by student t-test: ***, $P < 0.001$

3.2.3 MB1-47 and NEN inhibit pancreatic cancer growth in animal models

Next we tested the anticancer effect of MB147 in xenograft animal models of pancreatic cancer. First, C57BL/6j mice were injected intrahepatically with Panc02 on the liver and two days after surgery the mice were randomly divided into two groups, one group fed with normal chow diet, and the second group fed with chow diet containing 750 ppm MB1-47. Our results showed that MB1-47 treatment significantly reduces tumor size compared to control group as shown in (**Figure 3.5 a-e**). Next, we tested also the anticancer effect of NEN against pancreatic tumor growth in mouse model. NEN significantly reduces tumor growth and volume compared to control group as shown in (**Figure 3.6a-e**).

Second, we tested the inhibitory effect of MB1-47 and NEN on pancreatic tumor growth after intrahepatic growth; Panc02 cells were injected intrahepatically into NSG mice. After 10 days the mice were divided into three groups, one group was fed with normal chow diet, and the second and third groups were fed with MB1-47 (750 ppm) and NEN (2000 ppm) respectively for two weeks. MB1-47 and NEN treated groups significantly stopped and inhibited liver tumor growth compared to control group as shown in (**Figure 3.7 a-g**). All together, MB1-47 and NEN have the ability to combat the growth of pancreatic cancer in three different animal models and MB1-shows a strong

anticancer activity with lower dose than NEN in all animal models.

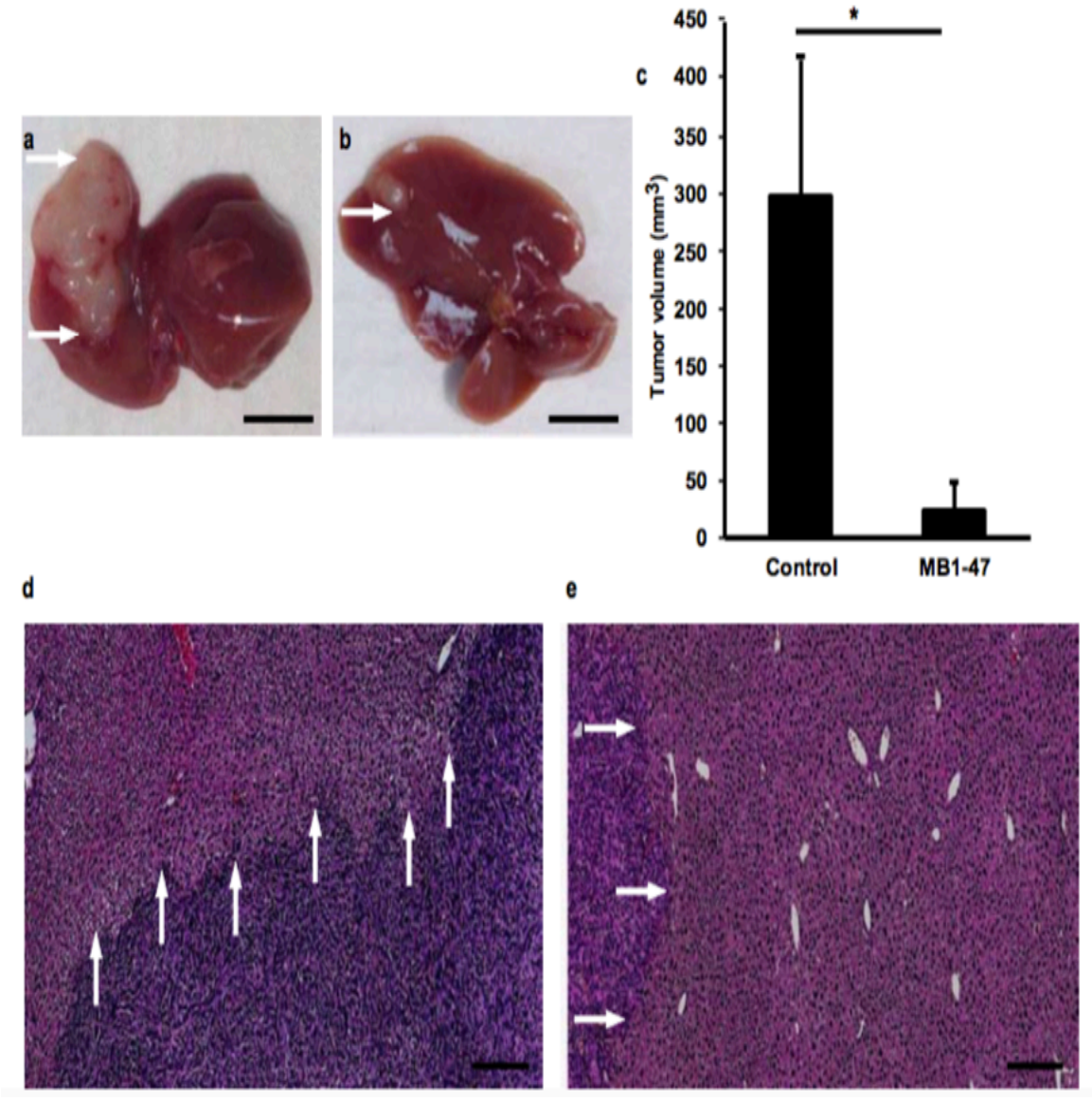

Figure 3.5 MB1-47 inhibits tumor growth of intrahepatic transplantation of pancreatic cancer cells. (a-b) Representative pictures (scale bars, 10 mm) showing the tumors on mouse liver after intrahepatic injection of Panc02 cells into C57bl/6 mice with or without MB1-47 treatment (750 ppm) for 3 weeks. (**c)** Quantification of liver tumor

size (mm^3). (**c-e)** Representative hematoxylin and eosin (H & E), pictures (scale bars, 200 mm), staining of histological section showing the differences between liver mice fed normal diet (**d)** and liver mice fed with diet containing MB1-47 (750 ppm) **(e)**. Data shown as means ± SD. Statistical significance (*P*) was determined by student-*t* test between the control and MB1-47 fed mice. N=6 in each group. **P*<0.05 and ***P*<0.01. The data are representative results from three independent experiments.

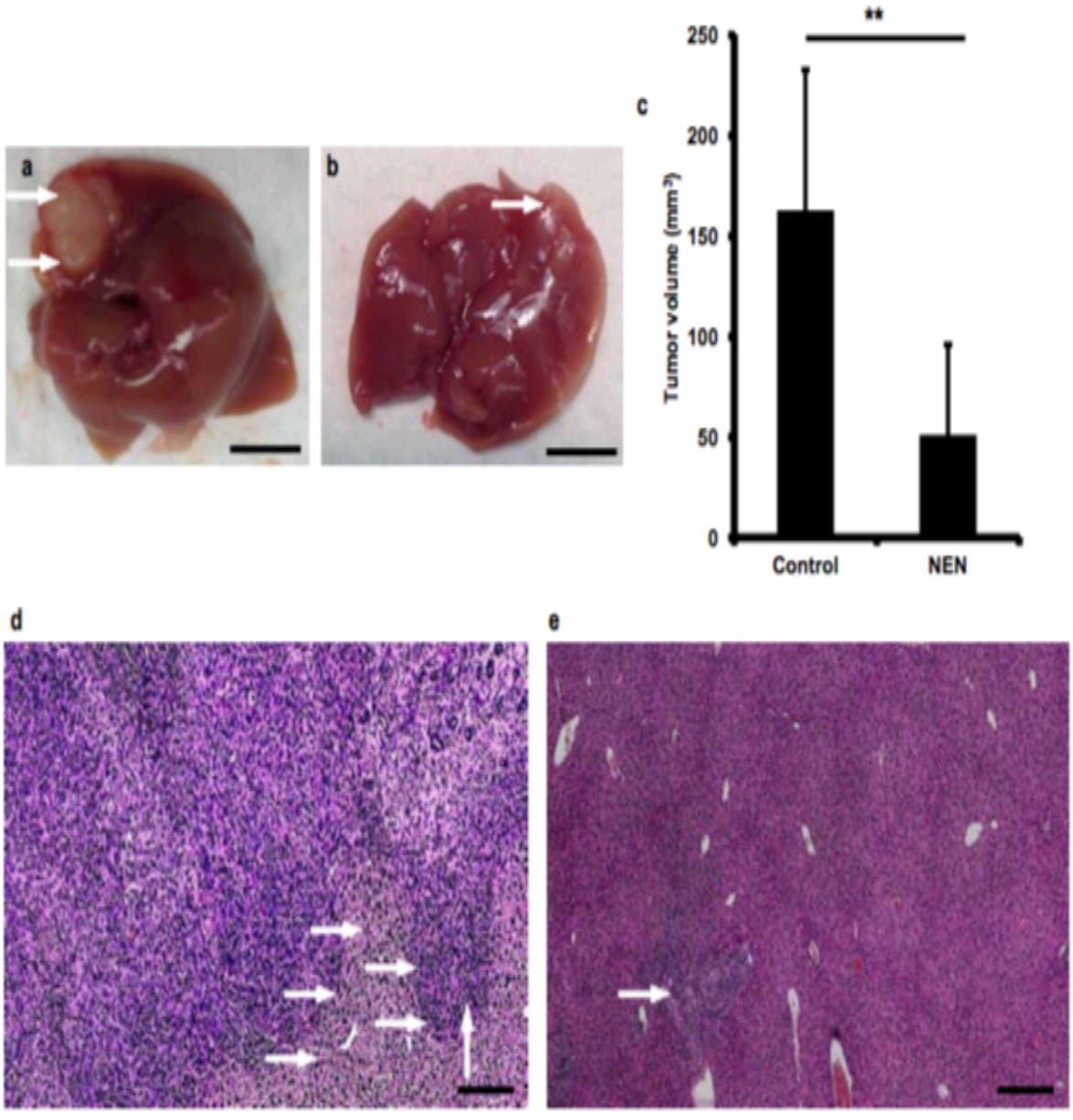

Figure 3.6 NEN inhibits tumor growth of intrahepatic transplantation of pancreatic cancer cells. (a-b) Representative pictures (scale bars, 10 mm) showing the tumors on mouse liver after intrahepatic injection of Panc02 cells into C57bl/6 mice with or without NEN treatment (2000 ppm) for 3 weeks. (**c**) Quantification of liver tumor size (mm^3). (**c-e),** Representative hematoxylin and eosin (H & E), pictures (scale bars, 200 mm), staining of histological section showing the differences between liver mice fed normal diet (**d)** and liver mice fed with diet containing NEN (2000 ppm) **(e)**. Data shown as means ± SD. Statistical significance (*P*) was determined by student-*t* test between the control and NEN fed mice. N=6 in each group. **P*<0.05 and ***P*<0.01. The data are representative results from three independent experiments.

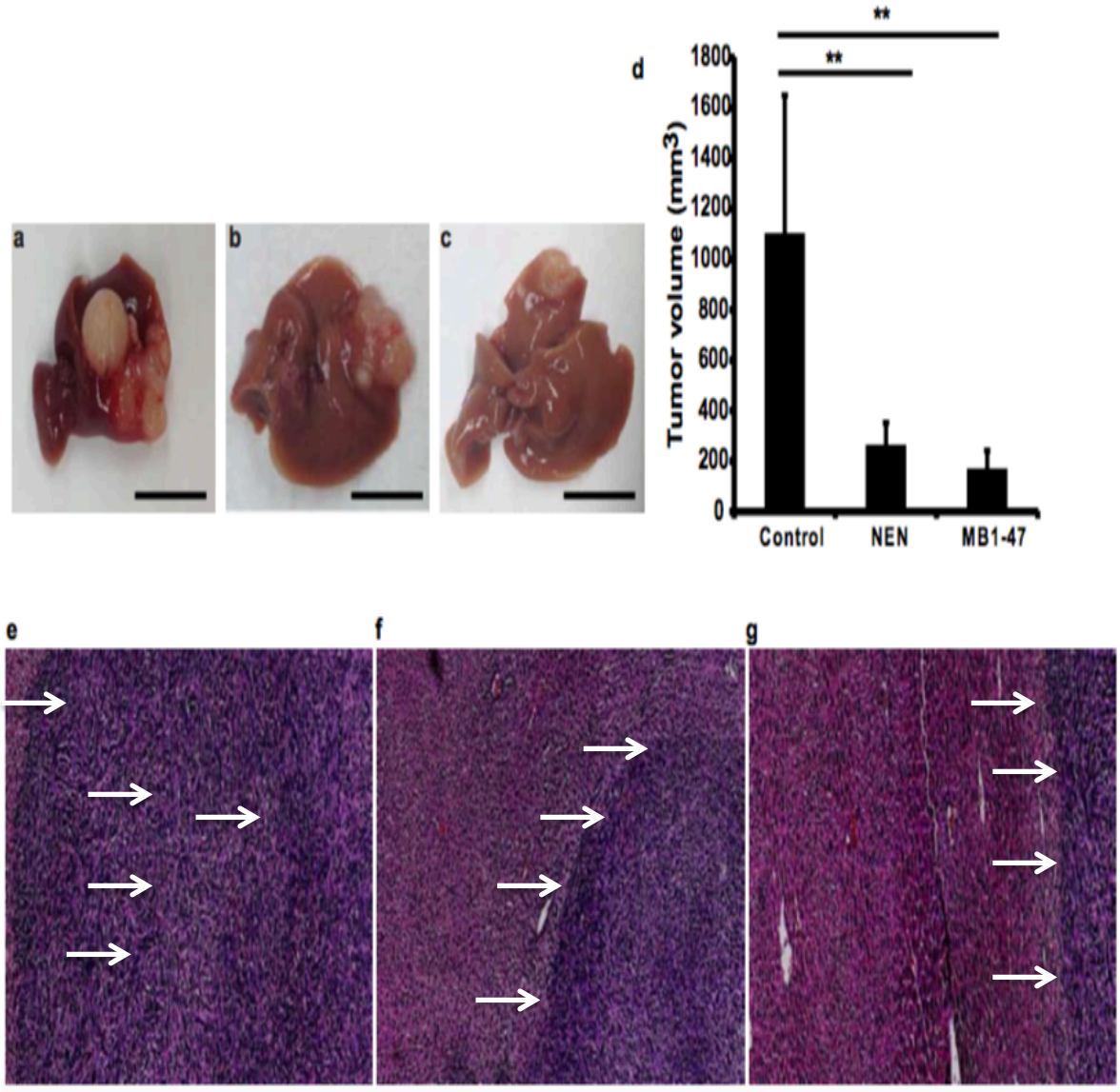

Figure 3.7 MB1-47 and NEN inhibit tumor growth after tumor formation in mouse liver. **(a-c)** Representative pictures showing the tumors on mouse liver after intrahepatic injection of Panc02 cells to C57bl/6 mice and then fed with normal diet (**a**), or diet containing either (2000 ppm) NEN (**b**) or (750 ppm) MB1-47 (**c**) for 2 weeks. **(d)** Quantification of liver tumor size (mm^3) in the mice with or without treatment as indicated. **(e-g)** Representative liver images (H&E) stain (scale bars, 200 mm) showing

the histological differences between DMSO (**e**) and NEN (**f**) or MB1-47 (**g**) respectively. Data shown as means ± SD. Statistical significance (*P*) was determined by student-*t* test between the control and NEN or MB1-47 fed mice. N=6 in each group. ***P*<0.01. The data are representative results from two independent experiments.

3.2.4 MB1-47 impairs or decreases hepatic metastasis of pancreatic cancer

Pancreatic metastasis is the major cause of death in patients with pancreatic tumor; metastases of pancreatic adenocarcinoma are located in lymph nodes liver, lung and peritoneum (204,205). In order to examine the effect of MB1-47 on hepatic metastasis of pancreatic cancer, we used a well-appreciated mouse model (34).

Murine pancreatic (Panc02) cells were injected intrasplenically into immune deficient NSG mice. Ten days after the injection, the mice were divided randomly into two groups, one group fed with normal diet, and second group was fed with diet containing 750 ppm MB1-47. Our result showed that MB1-47 decreases the metastatic tumor nodules to liver and reduces tumor size compared to control chew diet group as shown in (**Figure 3.8 a-g**). In addition, our data showed that NEN reduces the liver metastasis but the data not significant (data not shown) compared to control group. Altogether, MB1-47 significantly stops or decreases the hepatic metastasis after 2 weeks treatment.

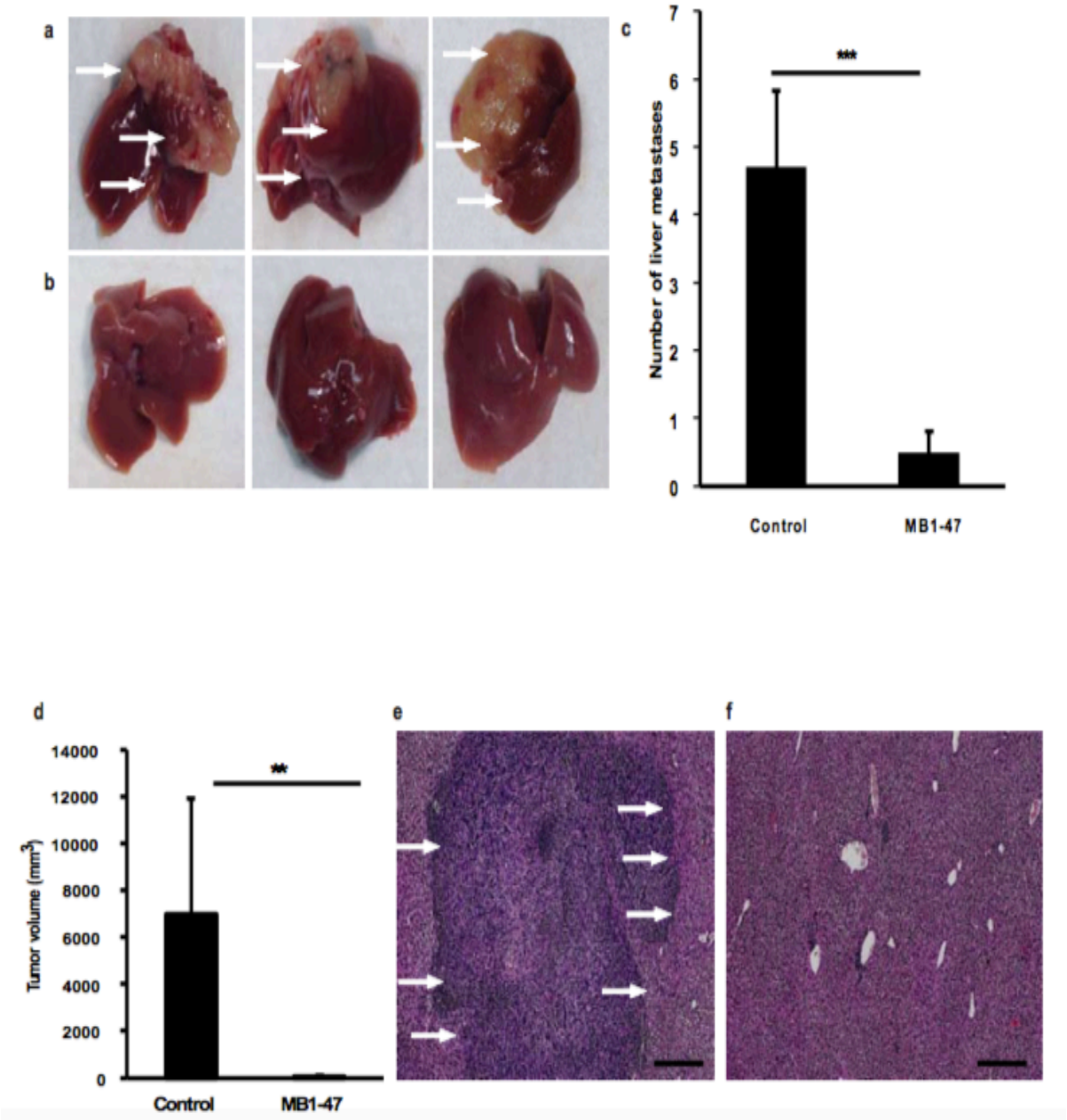

Figure 3.8 MB1-47 inhibits liver metastasis of intrasplenic-injected pancreatic cancer. (a-b) Representative pictures (scale bars, 10 mm) showing the tumors liver nodules after intrasplenic injection of Panc02 cells to NSG mice and then the mice fed with normal chow diet **(a)** or with diet containing (750 p.p.m) MB1-47 **(b)** for 3 weeks.

(c). Quantification of hepatic tumor nodules for mice with or without MB1-47 treatment as indicated. **(d),** The average of hepatic metastasis tumor volume of mice with or without MB1-47 treatment. (**e-f)**, Representative images (H &E), (scale bars, 200 μm) of mouse liver tissues in control and MB1-47 treated mice showing the histological difference between the cancer and normal part of the liver**.** Data shown as means ± SD. Statistical significance (*P*) was determined by student-*t* test between the control and MB1-47 fed mice. N=6 in each group. ***P*<0.01 and ****P*<0.001. The data are representative results from two independent experiments.

3.2.5 MB1-47 and NEN affect the cellular metabolism of pancreatic cancer

To test the effect of MB1-47 and NEN on glucose metabolism especially the pathways that are interconnected with glycolysis as shown in (**Figure 3.10a**). Panc02 cells incubated with label $U^{13}C$ glucose and glucose metabolites analyzed using LC-MS approach. Panc02 cells were incubated with 100% $U^{13}C$ glucose with or without (1μM) of MB1-47 or NEN at a dose that induce mitochondrial uncoupling. Consistent with AMPK activation by MB1-47 or NEN, we assessed the relative pool size of AMP/ATP and ADP/ATP ratios after 1 hrs treatment with/without MB1-47 or NEN. Our results showed that MB1-47 or NEN increases the pool size of AMP/ATP and ADP/ATP as shown in (**Figure 3.10 b and c**) and (**Figure 3.11 b and c**) respectively. It is well know that mitochondrial uncoupling promotes futile cycle and accelerates TCA metabolites inside mitochondrial. We tested the effect of MB1-47 and NEN on TCA metabolites influx, our resulted showed that MB1-47 significantly increases the TCA metabolites

influx into mitochondria as shown here (^{13}C-2C) of Succinate, Fumarate and Malate compared to DMSO control group **(Figure 3.10 d -f).** Similar results we obtained when we used NEN as shown in (**Figure 3.11 d -f**).

To assess the pyruvate level after MB1-47 and we used alanine (^{13}C-3C) level as readout for pyruvate level. As shown in (**Figure 3.9 g**) MB1-47 accelerates alanine flux and oxidation inside mitochondria. NEN also increases alanine flux into mitochondria as shown in (**Figure 3.9 g**). Next, we tested the effect of MB1-47 and NEN on PPP in pancreatic cancer cells. We used UTP pool size as indicator of PPP and the results showed MB1-47 and NEN significantly reduce UTP pool size compared to control group as shown in (**Figure 3.9 h** and **Figure 3.10 h**). Moreover, one carbon pathway also measured by monitoring serine (^{13}C-3C) level. Our data demonstrated that MB1-47 and NEN decreases the serine level as shown in (**Figure 3.9 g** and **Figure 3.10 g**) respectively.

During the aerobic glycolysis under control of Kras oncogene, glucose intermediates rewires to PPP and Hexose Biosynthetic Pathway (HBP) to support pancreatic cancer cell proliferation and growth. As indicated above that MB1-47 and NEN reduce PPP activity. We assessed the inhibitory role of MB1-47 and NEN against HBP. Panc02 treated with (2μM) MB1-47 or NEN for 2hrs, HBP label metabolites measured and our results showed that MB1-47 and NEN reduce the label metabolites of HBP as show in (**Figure 3.9 j-i** and **Figure 3.10 j-1**). All, the results suggested that MB1-47 at effective mitochondrial uncoupling concentration activate AMPK, enhance pyruvate oxidation

inside mitochondria. In addition MB1-47 and NEN accelerate TCA metabolites, reduce PPP and HBP activities.

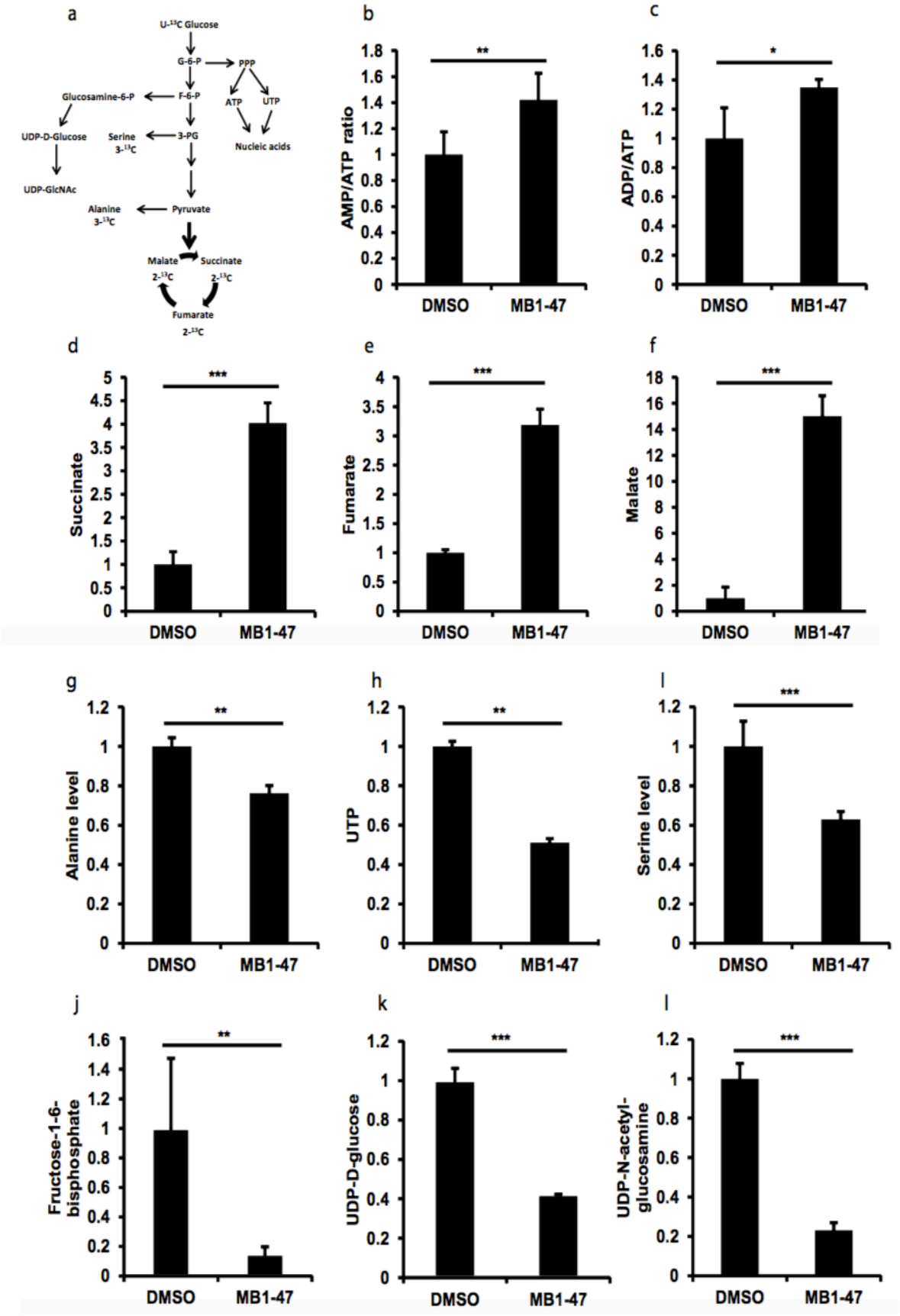
a
U-13C Glucose
G-6-P
PPP
ATP
UTP
Glucosamine-6-P
F-6-P
UDP-D-Glucose
Serine 3-13C
3-PG
Nucleic acids
UDP-GlcNAc
Alanine 3-13C
Pyruvate
Malate
Succinate
2-13C
2-13C
Fumarate 2-13C
b
AMP/ATP ratio
DMSO
MB1-47
c
ADP/ATP
d
Succinate
e
Fumarate
f
Malate
g
Alanine level
h
UTP
i
Serine level
j
Fructose-1-6-bisphosphate
k
UDP-D-glucose
l
UDP-N-acetyl-glucosamine

Figure 3.9 MB1-47 affects pancreatic cancer metabolism. (**a**) Schematic of pathways and molecules measured in metabolomics LC-MS experiment. (**b**) AMP/ATP ratio determined by the pool size of AMP vs pool size of ATP. (**c**) ADP/ATP ratio determined by the pool size of ADP vs pool size of ATP (**d**) Succinate level determined by measuring succinate level at ^{13}C-2C. (**e**) Fumarate level determined by measuring succinate level at ^{13}C-2C. (**f**) Malate level determined by measuring malate level at ^{13}C-2C. (**g**) Relative alanine level determined by measuring alanine at ^{13}C-3C. (**h**) Phosphate Pentose Pathway (PPP) rate determined by measuring UTP pool size. (**i**) Relative serine level determined by measuring serine ^{13}C-3C. (**j**) Relative fructose -1-6- bisphosphate level determined by measuring fructose -1-6-bisphospate at ^{13}C-6C. (**k**) Relative UDP-D-glucose level determined by measuring UDP-N-acetyl-glucosamine at ^{13}C-6C. For (**b-h**) Panc02 cells were grown in medium containing 100% U-^{13}C glucose, treating with 1 μM MB1-47 or vehicle DMSO, while for (**e-k**) Panc02 cells were grown in medium containing 100% U-^{13}C glucose, treating with 2 μM MB1-47 or vehicle DMSO for 2 hrs. The cell metabolites were extracted using cold 40:40:20 methanol:acetonitrile:water w/ 0.5% formic acid (ice cold) mixture. Abbreviations: G6P, glucose-6-phosphate; F6P, fructose-6-phosphate; 3-PG, 3-phosphoglycerate; PPP, Pentose Phosphate Pathway. Results are showed as means ± SD values from three independent experiments and statistical significance (*P*) was determined by student t- test: $*P < 0.05$; $**P < 0.01$; vs. DMSO control

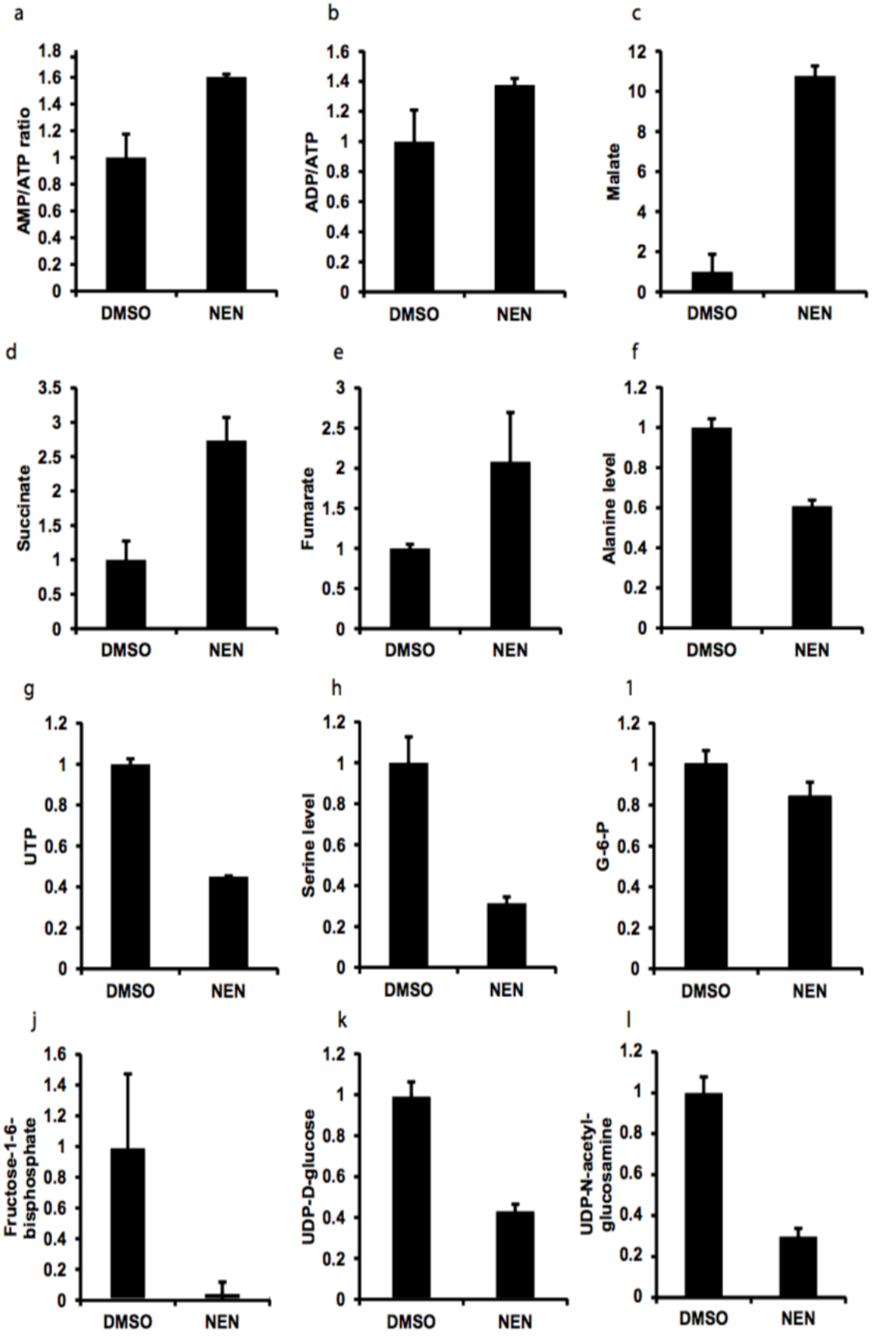
a
AMP/ATP ratio
1.8
1.6
1.4
1.2
1
0.8
0.6
0.4
0.2
0
DMSO
NEN
b
ADP/ATP
1.6
1.4
1.2
1
0.8
0.6
0.4
0.2
0
DMSO
NEN
c
Malate
12
10
8
6
4
2
0
DMSO
NEN
d
Succinate
3.5
3
2.5
2
1.5
1
0.5
0
DMSO
NEN
e
Fumarate
3
2.5
2
1.5
1
0.5
0
DMSO
NEN
f
Alanine level
1.2
1
0.8
0.6
0.4
0.2
0
DMSO
NEN
g
UTP
1.2
1
0.8
0.6
0.4
0.2
0
DMSO
NEN
h
Serine level
1.2
1
0.8
0.6
0.4
0.2
0
DMSO
NEN
I
G-6-P
1.2
1
0.8
0.6
0.4
0.2
0
DMSO
NEN
j
Fructose-1-6-bisphosphate
1.6
1.4
1.2
1
0.8
0.6
0.4
0.2
0
DMSO
NEN
k
UDP-D-glucose
1.2
1
0.8
0.6
0.4
0.2
0
DMSO
NEN
l
UDP-N-acetyl-glucosamine
1.2
1
0.8
0.6
0.4
0.2
0
DMSO
NEN

Figure 3.10 NEN affects pancreatic cancer metabolism. (**a**) Schematic of pathways and molecules measured in metabolomics LC-MS experiment. (**b**) AMP/ATP ratio determined by the pool size of AMP vs pool size of ATP. (**c**) ADP/ATP ratio determined by the pool size of ADP vs pool size of ATP (**d**) Succinate level determined by measuring succinate level at ^{13}C-2C. (**e**) Fumarate level determined by measuring malate level at ^{13}C-2C. (**f**) Malate level determined by measuring succinate level at ^{13}C-2C. (**g**) Relative alanine level determined by measuring alanine at ^{13}C-3C. (h) Phosphate Pentose Pathway (PPP) rate determined by measuring UTP pool size. (**e**) Relative serine level determined by measuring serine ^{13}C-3C. (**j**) Relative fructose -1-6- bisphosphate level determined by measuring fructose -1-6-bisphospate at ^{13}C-6C. (**k**) Relative UDP-D-glucose level determined by measuring UDP-N-acetyl-glucosamine at ^{13}C-6C. For (**b-h**) Panc02 cells were grown in medium containing 100% U-^{13}C glucose, treating with 1 μM MB1-47 or vehicle DMSO, while for (**e-k**) Panc02 cells were grown in medium containing 100% U-^{13}C glucose, treating with 2 μM MB1-47 or vehicle DMSO for 2 hrs. The cell metabolites were extracted using cold 40:40:20 methanol:acetonitrile:water w/ 0.5% formic acid (ice cold) mixture. Abbreviations: G6P, glucose-6-phosphate; F6P, fructose-6-phosphate; 3-PG, 3-phosphoglycerate; PPP, Pentose Phosphate Pathway. Results are showed as means ± SD values from three independent experiments and statistical significance (*P*) was determined by student t- test: $*P < 0.05$; $**P < 0.01$; vs. DMSO control

3.2.6 MB1-47 and NEN increase AMPK activation and reduced lipid synthesis

Cancer cells are highly demanded for glucose utilization compared to normal cells in order to provide the building blocks and reducing agents (NADPH) to generate new cells (28). AMPK is the master regulator for cell energy hemostasis and it is play a crucial role in cell metabolism (101). High AMP/ATP ratio is the activator of AMPK and it is indicator for less energy recourses inside the cells (206). AMPK activation reduces the anabolic signaling pathways and stimulates the catabolic signaling pathways (119). Therefore, AMPK activation impedes the utilization of the energy resources in the highly growing cancer cells.

We tested AMPK activity in pancreatic cancer cells (Panc02 and Panc1) upon treatment with MB1-47 and NEN. As shown in (**Figure 3.11 a-b**) our result showed that MB1-47 and NEN activate AMPK in a dose dependent manner and at concentration that induce mitochondrial uncoupling.

Next, we test the effect of MB1-47 and NEN on AMPK-ACC pathway in vitro cells culture, AMPK activation by MB1-47 and NEN lead to increase in ACC phosphorylation, which diminish ACC activity and decrease the lipid synthesis. Furthermore, MB1-47 and NEN treatment decrease the protein level of fatty acid synthase (FAS) in pancreatic cancer cells as shown in (**Figure 3.11 c-d**).

Taken together, MB1-47 and NEN affect the AMPK-ACC signaling pathway and reduces the lipid synthesis that is necessary for pancreatic cancer cell proliferation and differentiation.

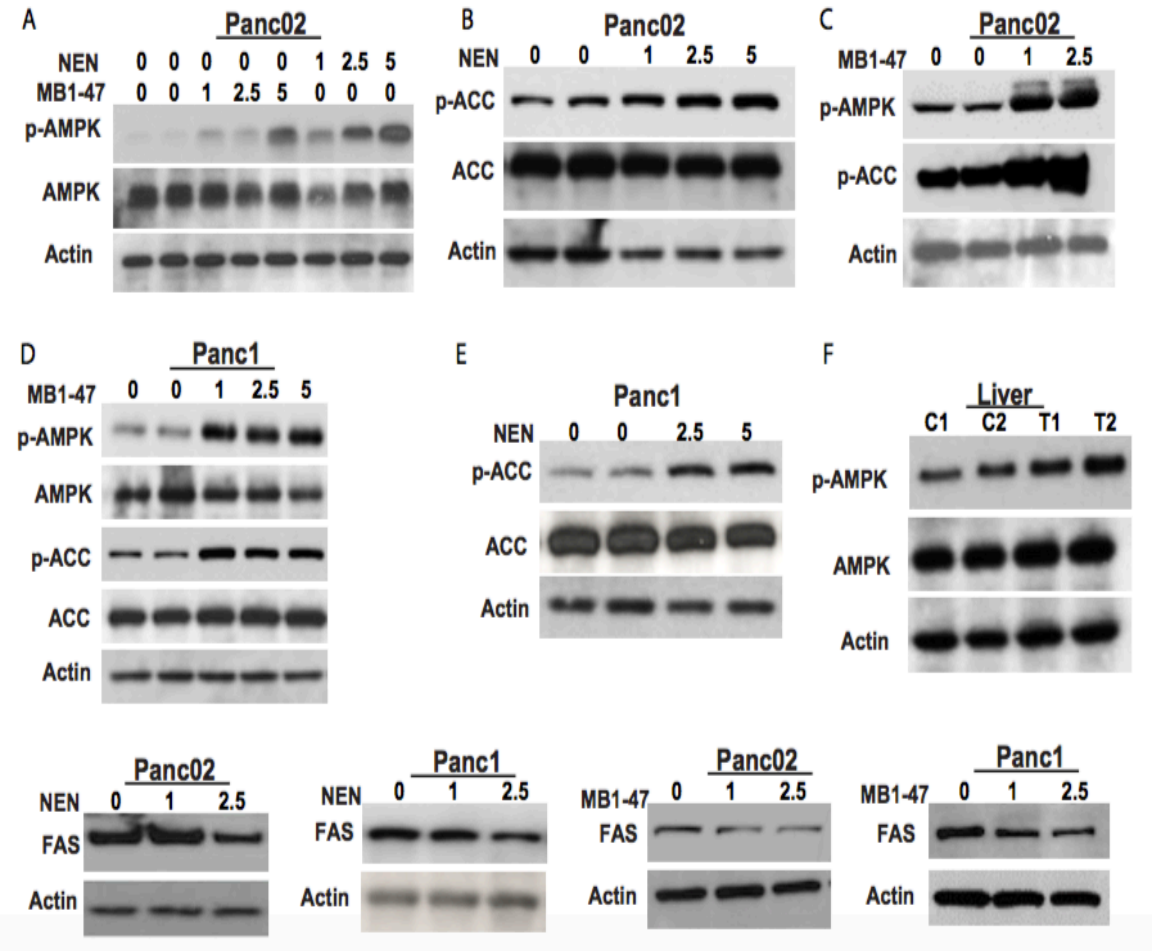

Figure 3.11 MB1-47 and NEN induce AMPK and ACC phosphorylation in pancreatic cancer cells. (a) Immunoblot analyses showing that NEN and MB1-47 increases phosphorylation of AMPK in Panc02 cells. **(a-c),** Immunoblot analyses showing that NEN and MB1-47 increase phosphorylation of ACC in Panc02 cells respectively. **(d-e),** Immunoblot analyses of Panc1 cells showing of that NEN and MB1-47 increase phosphorylation of ACC after 2h treatment respectively. **(g-j)** NEN MB1-47 decreases fatty acid synthase (FAS) expression in the indicated cells. The results are showing data from three independent experiments.

3.2.7 MB1-47 and NEN downregulate mTOR and other signaling pathways on pancreatic cancer

Pancreatic cancer cells are characterized by common mutations in KRAS and massive deregulation of many signaling pathways, which are involved on the pancreatic cancer progression (207). Mammalian target of rapamycin (mTOR) is an activated downstream kinase of RAS signaling and perhaps is a main mediator of RAS induced oncognesis(208). Furthermore, activated AMPK downregulates mTOR activity because mTOR is the major downstream target of AMPK(114). As shown in (**Figure 3.12 a-d**) we sought that MB1-47 and NEN treatment decrease the phosphorylation of P70S6K and 4E-BP1(downregulation of mTOR activity) in a dose dependent manner and this lead to arrest the cell cycle and decrease the cells proliferation. Next, we sought to study the effect of NEN and MB1-47 on AKT, ERK1/2 and, GSK signaling pathways. Our Western analysis data demonstrated that MB1-47 and NEN decreased the activity of AKT, ERK1/2 and GSK signaling pathways in cancer pancreatic cancer cells.

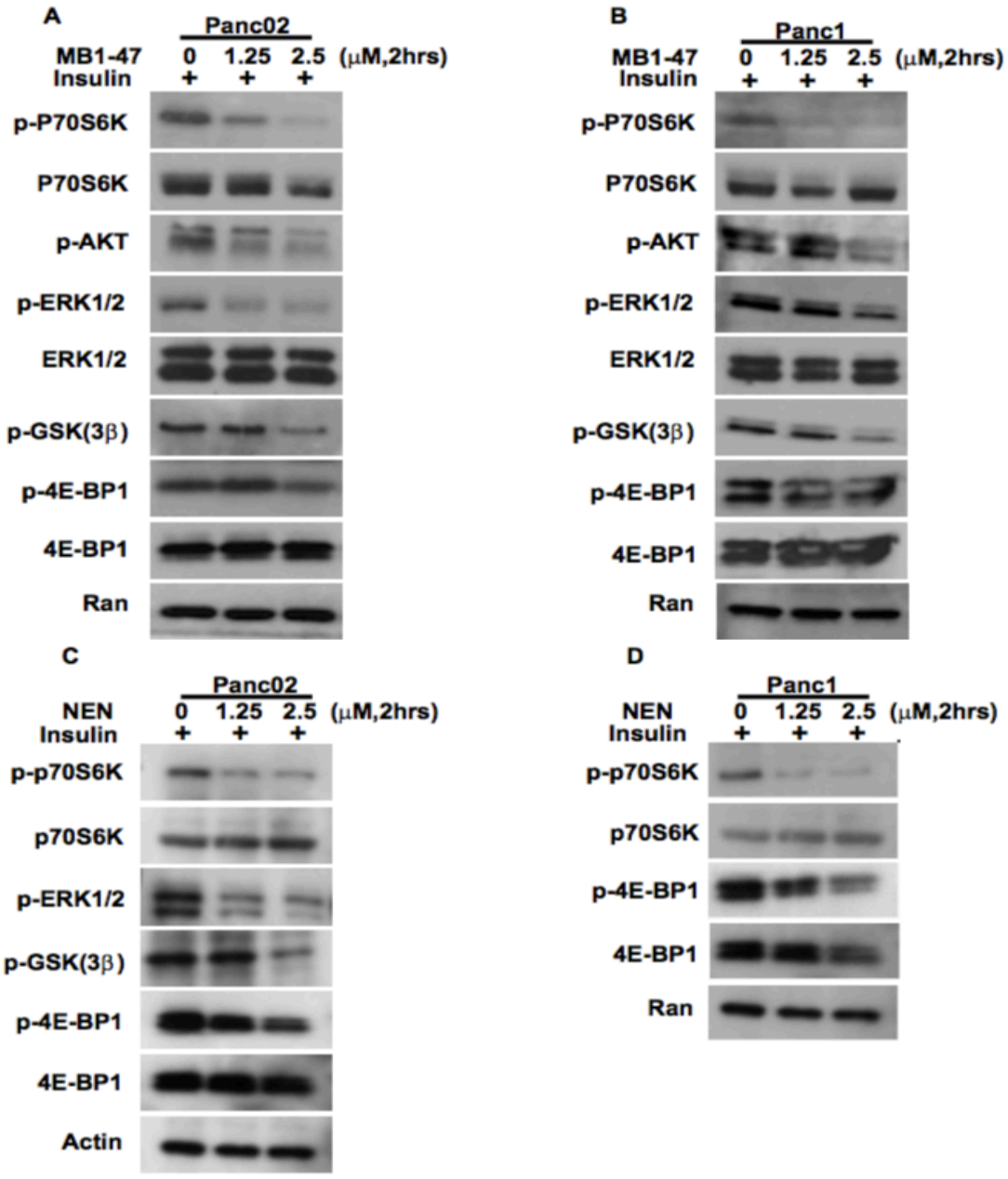

Figure 3.12 MB1-47 and NEN reduce the activity of some signaling pathways related to pancreatic cancer cells growth and proliferation. (a-d) Immunoblot analyses of Panc02 and Panc1 cells respectively. The results are showing that MB1-47 and NEN reduce the mTOR activity, AKT, ERK and GSK (3β) phosphorylation. The results are showing data from two independent experiments.

Chapter IV

4. Materials and Methods

4.1 Cell lines

Murine colon adenocarcinoma cell line (MC38) was a kind gift from Dr. Harvey Roy Herschman (University of California Los Angeles, CA), Human colon carcinoma cell line HCT116 and Human pancreatic cancer cell line Panc1were a gift from Dr. Steven Zheng (Rutgers University of New Jersey), MIA PACA-2, BxPC3, AsPC1, Capan2, and CFPAC-1 cells were kind gifts from Dr. Caprizo (Cinj-Rutgers University of New Jersey), Murine Pancreatic adenocarcinoma (Panc02) and Mouse myoblast cells (C2C12) were purchased from the American Type Culture Collection (ATCC, Manassas, VA, USA). MC38, HCT116, C2C12, MIA PACA-2, and Panc1 cells were cultured in Dulbecco's modified Eagle's medium (DMEM) containing (10% FBS, 2.5% horse serum (HS) for MIA PACA-2. Panc1 and CFPAC-1 cells were maintained in DMEM containing 10% FBS, 10 U/ml penicillin and 10 μg/ml streptomycin and 0.1 mM nonessential amino acids, and 1.0 mM sodium pyruvate for (MC 38 cells), Panc02, AsPC1, and BxPC3 were maintained in RPMI-1640 medium supplemented with fetal bovine serum (10% for Panc02, Capan-1 and Bx-PC3, 20% for AsPC1), 100 U/ml penicillin, 100mg/ml streptomycin and 1% sodium pyruvate and all cells were incubated at 37 °C and 5% CO_2.

4.2 Reagents and Antibodies

NEN (niclosamide 5-chloro-salicyl-(2-chloro-4-nitro) anilide 2-aminoethanol salt), was purchased from 2A PharmaChem (Lisle, IL). Oxyclozanide, trypan blue, crystal violet, glucose and DSS (4,4-dimethyl-4-silapentane-1-sulfonic acid) propidium iodide (PI), RNAse A, sulforhodamine B, Trichloroacetic acid (TCA), Insulin, NH_4HCO_3, methanol, acetonitrile, and formic acid purchased from Sigma (St. Louis, MO). [U-^{13}C] glucose and 99.9% enriched D_2O (Cambridge Isotope Laboratories, Tewksbury, MA). Dialyzed serum (SH3007903) was purchased from Fisher. pAMPK- (Thr172) monoclonal antibody (mAb) and AMPK-mAb, phospho-p70S6 kinase (Thr-389)P70S6K, p4E-Bp1 and 4E-Bp1, pERK1/2,ERK1/2, pGSK(3B), AKT, p-ACC and ACC were purchased from Cell Signaling Technology (Danvers, MA), we used 1:1,000 dilution for immunoblotting experiment. Ran, Actin antibodies were purchased from Santa Cruz Biotechnology (Dallas, TX), and we used 1:1,000 dilution for immunoblotting experiments.

4.3 Mitochondrial uncoupling analysis

To perform the mitochondrial uncoupling analysis with cancer cells, murine and human colon and pancreatic adenocarcinoma cells (MC38, HCT116, Panc02 and Panc1) were seeded onto six-well plates and maintained in DMEM until reaching log phase. Then, cells were incubated with different concentrations of NEN or oxyclozanide for (MC38 and HCT116) cells, NEN or MB1-47 for (Panc02 and Panc1) for 2hrs followed by staining with 100 nM tetramethylrhodamine ethyl ester (TMRE) for 10-15 min.

Finally, cells were rinsed once with DPBS and then observed under fluorescence microscopy.

4.4 Cell culture medium for NMR labeling experiment

Prior to the experiment, MC38 cells were maintained in DMEM containing 10% FBS, 1% penicillin-streptomycin, 0.1 mM nonessential amino acids, and 1.0 mM sodium pyruvate. For NMR labeling experiment, MC38 cells were seeded into 150 mm dish at a density 6 x 10^6 cell per dish. After overnight incubation, the medium was replaced with labeled DMEM phenol – free medium containing 10% FBS, 1% penicillin-streptomycin, 2mm of L-glutamine, 1 g/l glucose (Sigma), 1 g/l [U-^{13}C] glucose (Cambridge Isotope Laboratories, Tewksbury, MA). One plate was treated with 2μM NEN while a second plate (control) was treated with DMSO for 6 or 12 hours. After these two incubation time points were performed, cells were harvested and metabolites were extracted using cold methanol- chloroform extraction method as previously described (27). Briefly, cell were washed twice with ice-cold phosphate buffer solution, and then trypsinized to collect the cell pellets. After that, the cell pellets were extracted with ice-cold methanol–chloroform-water (2-1-1) and centrifuge at (18.000g) for 15 minutes at 4°C. Next, aqueous supernatants were collected and dried by using an evaporator. Samples were stored at -20 °C until NMR analysis.

4.4.1 NMR analysis

Cell extracts were redisloved in 600 μl of deuterium oxide (D_2O) containing 10% 4,4-dimethyl-4-silapentane-1-sulfonic acid (DSS), used as references standard for proton and carbon NMR spectroscopy, and the samples were filter by using 0.2 μm pore size filter.

NMR (2D) C-H-HSQC spectra were acquired on a 800 MHz spectrometer Bruker (Bruker, Karlsruhe, Germany) equipped with a 5mm cryoprobe at 25°C. 2048 complex points were acquired along the H- dimension for each of the 64 complex points in aliphatic ^{13}C dimension. The sweep width in proton dimension was 13 ppm with the carrier on water while 120 ppm was used for carbon with the carrier at 60 ppm. The data were processed using NMR pipeline and then analyzed using Sparky 3.2 (University of California, San Francisco).

4.5 Cell culture preparation for LC-MS metabolomics experiment

Prior to the experiment, Panc02 cells were maintained in RPMI-1640 medium. For LC-MS labeling experiments, Panc02 cells were seeded into 100 mm dish at a density 6 x 10^6 cell per dish. 24-48 hrs prior to metabolite collection, the medium was replaced with DMEM phenol– free medium containing 10% dialyzed serum (SH3007903 from Fisher), 2mm of L-glutamine, and 4.5 g/l glucose (Sigma). Then, 1-2 h prior to metabolite collection, aspirate of all medium and replace with 10 ml new of respective medium. Next, the cells were switched to labeled medium containing 10% dialyzed serum, 2mm of L-glutamine, and 4.5 g/l [U-^{13}C] labeled glucose (Cambridge Isotope Laboratories) (Tewksbury, MA) labeled glucose (Cambridge) for 2 hr with (2 μM) NEN and MB1-47 for the treated groups and dimethyl sulfoxide (DMSO) for control group. After 2 hrs treatment, cell lysate was collected and the cells metabolites were obtained using 1 ml of lysis buffer containing (40:40:20 methanol:acetonitrile:water w/ 0.5% formic acid (ice cold) mixture. Immediately, the plates were transferred to ice and incubated for 5 minutes

and 50 of 15% NH4HCO3 was added to each plate. After that, cell lysate was collected with centrifuged at 15,000g for 10 minutes in cold room to pellet cell debris and proteins. Then, 700 µl of supernatant was transferred to 1.5 ml tube and all the samples were stored at -80 °C until they were used for LC-MS analysis.

LC-MS analysis

LC−MS analysis the cellular metabolites was performed on the Q Exactive PLUS hybrid quadrupole-orbitrap mass spectrometer (Thermo Scientific) coupled to hydrophilic interaction chromatography (HILIC). The LC separation was performed on UltiMate 3000 UHPLC system with an XBridge BEH Amide column (150 mm × 2.1 mm, 2.5 µM particle size, Waters, Milford, MA) with the corresponding XP VanGuard Cartridge. The liquid chromatography used a gradient of solvent A (95%: 5% H2O: acetonitrile with 20 mM ammonium acetate, 20 mM ammonium hydroxide, pH 9.4), and solvent B (20%: 80% H2O: acetonitrile with 20 mM ammonium acetate, 20 mM ammonium hydroxide, pH 9.4). The gradient was 0 min, 100% B; 3 min, 100% B; 3.2 min, 90% B; 6.2 min, 90% B; 6.5 min, 80% B; 10.5 min, 80% B; 10.7 min, 70% B; 13.5 min, 70% B; 13.7 min, 45% B; 16 min, 45% B; 16.5 min, 100% B. The flow rate was 300 µl/min. Injection volume was 5 µL and column temperature 25 °C. The MS scans were in negative ion mode with a resolution of 70,000 at m/z 200. The automatic gain control (AGC) target was 3×10^6 and the scan range was 75−1000. Metabolite features were extracted in MAVEN (Cite: PMID 21049934) with the labeled isotope specified and a mass accuracy window of 5 ppm. The ^{13}C isotope natural abundance and impurity of labeled substrate was corrected using AccuCor written in R (Cite: PMID 28471646).

4.6 Cell viability assay

To assess cell viability during drug treatment, MC38 cells were plated in 6 well plates at 1x 10^5cells/ 2 ml medium in each well and incubated overnight. After overnight culture, drugs were added at different concentrations and vehicle control was included for each plate. Each experiment was done in triplicate. After 24 h incubation with drug at 37°C, cell viability were detected through staining with trypan blue. To distinguish between the live and dead cells, the viable cell numbers were counted by heamocytometer under normal light microscope.

4.7 Clonogenic assay

MC38, HCT116, Panc02, Panc1, MIA-PACA2 cells were plated in 6-well plates at 200 cells per well in 2 ml with respective medium. MC38, HC116 cells were treated with different concentration of NEN or oxyclozanide, Panc02, Panc1, and MIA-PACA2 were treated with various concentrations of MB1-47 or NEN for 24 or 48 h. After incubation, drugs were kept with medium for whole experiment period. Cells were kept with changing the medium plus drugs for 7 to10 days. The colonies were then fixed in 1:3 Acetic–Methanol solution for 5 minutes, stained with 0.02% crystal violet for 20 minutes and counted under normal light microscopy.

4.8 Cell cycle profile

To test the toxic effect of mitochondrial uncoupler compounds (NEN, oxyclozanide, and MB1-47) on cell cycle profile of colon and pancreatic cancer cells, MC38 and HCT116 cells were treated with different concentrations of NEN or oxyclozanide for 24

h whereas Panc02, Panc1, MIA-PACA2, and BxPC3 were treated with (2.5) μM NEN or MB1-47 for 48hrs. Control group was treated with DMSO. Then, the cells were fixed with ice-cold 70% ethanol in ice for 30 minutes. After that, 5 ml of propidium iodide (PI) (Sigma, P 4170) (1 μg/ml) solution and 50 μl of RNAse A (Sigma, R- 4875) solutions were added to the fixed cells and then kept for 30 minutes in dark at room temperature prior analysis by flow cytometry.

4.9 Determination 50 % of growth inhibition (GI)

Pancreatic cell lines (Panc02, Panc1, MIA PACA-2, Bx-PC3, AsPC1, Capan2, and CFPAC-1) were seeded at densities 5000-20.000 cells/well in 96-well plates. After 24 hr, the cells were treated with various concentrations of the NEN and MB1-47 while control wells incubated with DMSO for 48hr. The growth inhibition was assessed by using sulforhodamine B (SRB) staining assay as previously (209) with some modification. Briefly, after 48 hr treatment with NEN and MB1-47 the medium was discarded, and the adherent cells were fixed by adding 50 ml of cold Trichloroacetic acid TCA (10% (w/v) to each well and incubating for 1hr at 4 °C. Then, the plates were washed 5 times with deionized water and air-dried. After that, 200 ml of SRB solution (0.4% w/v in 1% acetic acid) was added to each well and the plates were incubated for 10 min at room temperature. Then, the plates were washed 5 times with 1% acetic acid to remove unbound SRD and the plates were air dried. SRD Bound stain was solubilized with 200 ml Tris base (10 mM) (pH 10.5) for 10-20 minutes. The optical intensities were read using a microplate reader at 492 nm. Triplicate wells were used for each analysis. The percentage of growth inhibition (%IG50) was estimated using this equation: % GI = (1-

Nt/Nc) X 100, where Nt: and Nc represent the reading absorbance in treated and control well respectively.

4.10 Oxygen Consumption Rate (OCR)

OCR analyses were performed using the SeaHorse XF24 cartridge according to the instructions from Agilent technologies. Briefly, 40,000-50,000 Mouse myoblast cells (C2C12), murine pancreatic adenocarcinoma cells (Panc02) were seeded in a Seahorse 24XF cell culture microplate and cultured in DMEM medium. Before the analyses, cells were washed with DMEM media and placed in a non-CO_2 37 °C incubator for at least one hour. OCR of the cells was analyzed by stepwise injections of (5 μM) Oligomycin, (2.5 μM) Rotenone, with either (2.5 μM) of NEN or MB1-47 into each well.

4.11 Immunoblotting assay

MC38, Panc02, and Panc1 cells were plated onto six-well plate and maintained with DMEM to the 70% confluence. MC 38 cells were incubated with NEN, oxyclozanide at different concentrations for 2hr, Panc02, and Panc1 cells were incubated also with different concentration of MB1-47 or NEN for 2 hr for AMPK phosphorylation. For mTOR phosphorylation experiments in Panc02, and Panc1 prior treated with 10 mg/ml insulin for 1hr and then different concentrations from MB1-47 or NEN was added. The protein was extracted, separated through SDS-PAGE, and moved to polyvinylidene difluoride (PVDF) membranes (Millipore, Billerica, MA) as previously described (27). Immunoblotting was made for pAMPK- (Thr172) monoclonal antibody (mAb) and AMPK-mAb, phospho-p70S6 kinase (Thr-389)P70S6K, p4E-Bp1 and 4E-Bp1,

pERK1/2,ERK1/2, pGSK(3B), AKT, p-ACC and ACC followed by secondary antibodies (Santa Cruz Biotechnology, Dallas, TX). Ran and Actin were used as a control and proteins were visualized using western blotting and chemiluminescence reagents (Amersham, Piscataway, NJ).

4.12 Cell invasion assay

Invasion assay was performed with Boyden chamber assay (Corning, Corning, NY). Prior to experiment, MC38 cells were plated at concentration of $2x10^6$ per 10 cm dish and incubated for 24 hr. Cells were rinsed twice with PBS and then maintained with serum – free medium and 1ml NEN or DMSO for 4 hr. Cells were trypsinized, and pelleted at 1500 x g for 5 min. Cells were resuspended and 2×10^5 (200 μL) were seeded into serum - free medium with 1mM NEN or DMSO in each transwell. 700 ml of complete medium supplemented with 1ml NEN or DMSO was added to the lower chambers. Plates were kept at 37°C and 5% CO_2 for 18 hours. Afterwards, the inserts were removed and cells were fixed with 70% cold methanol for 5 minutes, followed by incubation with 0.2% crystal blue for 10 minutes in the dark. Inserts were then washed twice with PBS and left to completely dry. Invaded cells were counted in 4 different fields by using Neubauer chambers slide. Each invasion experiment was performed in duplicate.

4.13 Wound healing assay

MC38 and HCT116 cells were plated in six-well plates to confluence level in 2 ml of DMEM. Wounds were made by using a 10ml pipette tip to scratch through confluent cell monolayer. Fresh medium was added to the plates and the initial wound was

recorded by taking images at (0h) time. The first and second groups were treated with various concentrations of NEN or oxyclozanide at different time points whereas the control group was treated with DMSO. Images of each time point were recorded. Wound closure percentage was determined by comparing the wound closure size between the initial wound and the different time points in control versus treated groups.

4.14 AMPK activation in vivo

For AMPK activation in vivo, NEN or Oxyclozanide was suspended in 0.5% methyl cellulose and then administered to male C57BL/6J mice (n = 2) by oral gavage at a dose of 40 or 80 mg per kg body weight respectively. The mice were euthanized after 2 hours for NEN 6 hours for Oxyclozanide. Liver samples were kept in liquid nitrogen for future western blot analysis.

4.15 Tumor xenograft experiments

Male NOD.Cg-*Prkdc*^{scid} *Il2rg*^{tm1Wjl}*/SzJ* mice, also known as NOD scid gamma (NSG) mice were purchased from The Jackson Laboratory (Farmington, CT). The mice were kept at the Rutgers -Robert Wood Johnson Medical School. All experiments were done following a protocol approved by the Institutional Animal Care and Use Committees (IACUCs). Sub-confluent culture of MC38 or Panc02 cells were harvested with trypsin-EDTA solution. Collected cells were washed and suspended in serum-free medium at a concentration of $1x10^5$ cells / ml.

For intrasplenic injections, 30 male NOD mice were used. Mice were injected (0.1 mg/kg) buprenorphine subcutaneously for analgesia 30 minutes before the surgery. Then,

the mice were injected anesthetic drugs i.p. (Acepromazine 5 mg/kg, and ketamin 100 mg/kg body weight). After anesthesia, the surgical site was cleaned and aseptically prepared by using iodophor and 70% alcohol. The spleen was pulled out the body of mice. The lower end of the spleen was circled with a 5/0 silk synthetic suture, and $1x10^5$ murine colon adenocarcinoma cells (MC38) in 0.2 ml medium were injected into the lower pole of the spleen and then we were waited for 10 minutes. Then, the spleen was ligated and the whole spleen was completely removed from the mouse body. The abdominal wall was closed with two layers of sutures. Postoperatively, mice were kept warm on a heating pad, which was disinfected with 70% ethanol in advance, and returned to their cages when completely awake. 10 hours later, all mice received the second dose of (0.1mg/kg) buprenorphine. Animals were assigned into three groups: control group was fed with normal control diet (AIN-93M) (Research Diet, New Brunswick, NJ) while the first and second treated groups were fed with AIN- 93M containing 800 ppm oxyclozanide or with AIN- 93M containing 2000 ppm NEN respectively. Three weeks after the surgery, mice were sacrificed by cervical dislocation. Liver tissue was obtained and imaged. Tumor metastases were counted, tumor volume (in mm^3) was calculated from recently excised liver by using an electronic caliper, using the following equation: [volume = 0.52 x $(width)^2$ X length] (210). Immediately a section of each normal tissue or tumor was fixed 10% neutral formalin for 24 h and then processed for histological and immunohistochemistry analysis, whereas the remaining liver tissue was kept in liquid nitrogen for Western blot or other analyses.

For intrasplenic injection of Panc02 in (NSG) mice, we performed the same procedure like MC38 cells injection with little change. Briefly, 16 male NOD mice were

used and Panc02 cell number was (2.5 x10^5 cell/ml). Mice after injection and recovery were divided randomly into two different groups: control group was fed with normal control diet (AIN-93M) (Research Diet, New Brunswick, NJ) while the first and second treated groups were fed with AIN- 93M containing MB1-47 (750 ppm) for two weeks.

For (Panc02) intrahepatic injection, female C57BL6/J (18) mice aged 8-12 weeks were used; Panc02 cells (1x10^5 cell/ml) were injected into liver of recipient mice. After recovery, the mice were divided randomly into control group fed with normal control diet (AIN-93M) and, the treated group fed with AIN- 93M containing either NEN (2000 ppm), or MB1-47 (750 ppm) respectively. Tumor occurrence and volume were recorded after three weeks of treatment.

For reversal tumor growth inhibition experiment, Panc02 cells (1 x10^5 cell/ml)) were injected intrahepatically of recipient mice. After 10 days, the mice were divided randomly into control group fed with normal control diet (AIN-93M) and, the treated group fed with AIN- 93M containing NEN (2000 ppm), MB1-47 (750ppm) respectively for two weeks. Tumor growth and volume were recorded and liver was imaged.

4.16 Liver histology

Tissues from liver were collected after the mice were euthanized. Samples were kept in 10% neutral buffered formalin for 24 h, changed to 70% ethanol alcohol and later implanted in paraffin. Liver tissue sections were completed and stained with H&E stain. Images were taken with a Carl Zeiss Universal Microscope imaging system with different phase-contrast objectives.

4.17 Statistical analysis

Results are presented as means ± SD experiments. Data were assessed using student *t* test to compare the control group and drug treated group, statistical significance *P* values were denoted as *, $P < 0.05$; **, $\boldsymbol{P} < 0.01$; and ***, $P < 0.001$.

Chapter V

5. Discussion and Conclusions

Otto Warburg found that cancer cells tend to "ferment" glucose into lactate even in the presence of sufficient oxygen. This phenomenon of aerobic glycolysis is called "the Warburg effect" (1,3,154). Recent work in cancer cell metabolism has led to the elucidation of the significance of the Warburg effect to cancer. In essence, glycolysis in non-dividing cells is followed by complete oxidation of pyruvate in mitochondria, with the end product of CO_2. This leads to a complete oxidation of glucose without biomass accumulation. In contrast, in cancer cells, the pyruvate flux into mitochondria is reduced as the result of aerobic glycolysis. It is assessed that pyruvate entering mitochondria for complete oxidation only is ~5% of glucose metabolism, while a main of pyruvate undergoes "fermentation" to lactate, which represents 85% of glucose metabolism. The residual ~10% of glucose metabolism is rewired to other metabolic pathways, such as the pentose phosphate pathway (PPP). These pathways generate reducing agents (NADPH) and metabolic intermediates such as ribose, providing the reducing agent and building blocks for biosynthesis required for biomass accumulation needed for cell proliferation (4,5,15,211,212). Thus, targeting aerobic glycolysis, which in turn reduces the production of reducing agents and building blocks for cancer cell biosynthesis, can be an effective and possible universal anti-cancer strategy.

Pyruvate generated from glycolysis influxes into mitochondria in the presence of oxygen, where it is converted to acetyl-CoA and this happened in differentiated cells. Then, acetyl-CoA is metabolized to CO_2 through TCA cycle, and energy is extracted and

stored in the form of high-energy electrons in NADH and FADH. Then, The electrons feed into the electron transport chain (ETC) reside in the mitochondrial inner membrane, which pumps H^+ protons out the membrane and generates a proton gradient. Protons enter the mitochondrial matrix through ATP synthase, driving ATP production. Usually, ETC activity is coupled to the energy requirement of the cells. When the energetic requirement is met, ETC and oxidation of acetyl-CoA are shut down, along with pyruvate flux into mitochondria.

Mitochondrial uncoupling is a process that leads to proton influx across the mitochondrial inner membrane without passing through ATP synthase. This process de-couples mitochondrial oxidation from ATP synthesis, leading to a futile cycle, i.e. complete oxidation of acetyl-CoA without generating ATP. As a result, energy efficiency of mitochondria is dissipated. To meet the cellular energy demand, the flux of pyruvate into mitochondria is expected to accelerate, which promotes the complete oxidation of glucose. This mode of metabolic change induced by mitochondrial uncoupling could potentially diminish the anabolic effect of aerobic glycolysis.

Niclosamide was an FDA approved anthelmintic drug for treating tapeworm infection. Its mechanism of action is to uncouple mitochondria (213). NEN (niclosamide ethanolamine) is the ethanolamine salt of niclosamide, which has a similar excellent safety profile as niclosamide (188) . Oxyclozanide is another mitochondrial uncoupling anthelmintic drug approved for veterinary use and assess their potential use in cells and *in vivo* models for treating and preventing hepatic metastatic of colon cancer. Oxyclozanide is veterinary anthelmintic drug; mainly it is used for treatment and control flatworms in farm animal and it has a longer half-life and it is metabolized in liver (191). We decided

to use NEN and oxyclozanide as prototype drugs to examine the impact of mitochondrial uncoupling on cancer glucose metabolism and to determine their potential anti-cancer activities.

First, we used NEN and oxyclozanide to target the metabolism of colon cancer. We performed metabolomics NMR experiment to study the effect of NEN on glucose metabolism in cancer cells. Our metabolomics NMR results directly demonstrated that mitochondrial uncoupling by NEN dramatically increases pyruvate flux into mitochondria, increases mitochondrial oxidation, reduces lactate production, and reduces biosynthetic PPP pathway.

We then investigated the antitumor effects of NEN and as well as oxyclozanide on colon cancer in cell culture models. NEN and oxyclozanide inhibits cell proliferation and reduces clonogenicity of cancer cells. Moreover, NEN and oxyclozanide also inhibited cell migration and invasion. These effects were associated with the activation of AMPK and downregulation of mTOR signaling pathway *in vitro* and *in vivo*.

We further examined the in vivo anti-cancer effect of NEN and oxyclozanide using mouse metastatic cancer models. Then, we tested if the uncouplers are effective in inhibiting cancer growth. The colon cancer MC38 cells were injected into the liver of NSG mice. Oral treatment of oxyclozanide significantly reduced tumor size and tumor incidence in mouse liver.

We then tested if these drugs could inhibit tumor metastasis. MC38 cells were intrasplenically injected into the mice and the tumor metastasis to liver was analyzed. Oral NEN or oxyclozanide either totally prevented tumor metastasis to liver or drastically

reduced metastatic tumor numbers and tumor volume.

Second, We further investigated the effect of MB1-47 (NEN's analogue) and NEN on pancreatic cancer metastasis to liver. MB1-47 is a new mitochondrial uncoupling compound and it is synthesized and developed in collaboration between our lab and medicinal chemistry lab at Pharmacy School-Rutgers. MB1-47 is characterized by higher blood exposure, longer half-life, more potent, relative more soluble in water compared to NEN. MB1-47 and NEN have similar toxicity profile.

Our data showed that MB1-47 and NEN uncouple mitochondria by increasing oxygen consumption rate, and reduce the membrane potential of murine and human pancreatic cancer cells. We then studied the antitumor effects of MB1-47 and NEN on murine and human pancreatic cancers in vitro cell models. MB1-47 and NEN arrest cell cycle at G0-G1 phase, reduce clonogenicity and inhibit cell growth of murine and human PDA cells at the same concentration that induces the uncoupling effect.

Moreover, in mouse xenograft models, MB1-47 and NEN reduce tumor growth and tumor occurrence after intrahepatic transplantation into (NSG) mice models. Moreover, MB1-47 diminishes hepatic metastasis when PDA cells are transplanted intrasplenically into NSG mice.

These results are concomitant with LC-MS metabolic data, which are characterized by increased AMP/ATP and ADP/ATP ratios, reduction in PPP metabolites, accelerate TCA metabolites flux to mitochondria, increase pyruvate oxidation inside mitochondria. In addition, Hexose Biosynthetic Pathway (HBP) and one carbon pathway (Serine) also inhibit upon treatment with MB1-47 and NEN.

Higher AMP/ATP and ADP/ATP ratios are the activator of AMPK activation and this happened as consequence of mitochondrial uncoupling effect. Our Western blot analysis confirmed that MB1-47 and NEN activate AMPK in both *in vitro* and *in vivo* models and latter effect of AMPK arrests cell cycle of pancreatic cancer cells.

Furthermore, MB1-47 and NEN downregulate mTOR activity, and other signaling pathways that are related to pancreatic cancer cell growth and proliferation. In addition, AMPK activation by MB1-47 and NEN led to downregulate the activity of ACC reduces the Fatty Acid Synthase (FAS) and this consequently inhibits the lipid biosynthesis in pancreatic cancer cells. Our data highlight a unique approach for treating PDA, and provide novel experimental drug leads for future investigation.

The main mechanism for pyruvate entrance into mitochondria to meet the energy requirement is through Pyruvate Dehydrogenase (PDH) feed back control. PDH controls pyruvate conversion to acetyl CoA and its activity inhibited by acetyl CoA (83,213). Acetyl CoA activates Pyruvate Dehydrogenase (PDH), which phosphorylates PDH and inhibits its activity (213,214). Low cellular level of ATP or high cellular level of ADP stimulates mitochondrial oxidative phosphorylation that accelerates TCA cycle and enhances Acetyl CoA oxidation inside mitochondria. Thus, PDH inhibition is reduced that stimulates pyruvate influx into mitochondria. Mitochondrial uncoupler inhibits ATP synthesis from ETC and creates futile cycle that enhances mitochondrial oxidation of Acetyl CoA and decreases mitochondrial pool size of Acetyl CoA, thus activates PDH and pyruvate influx. This is well-known negative feedback loop mechanism under the observed effects of mitochondrial uncoupling to enhance pyruvate influx and oxidation inside mitochondria in cancer cells.

NEN (niclosamide ethanolamine) is the ethanolamine salt of niclosamide that has a similar tremendous safety profile like niclosamide (167,186-188) and has good water solubility and systemic exposure (188). Our recent studies showed that NEN has high levels of distribution in the liver after oral administration (142). In addition, oxyclozanide is also enriched in liver after oral administration. Thus, we choose liver as a therapeutic site for mitochondrial uncoupler compounds. Liver is one of the most important target organs for metastatic cancers, in particular for colorectal and pancreatic cancers.

Several previous studies showed that niclosamide has a robust in vitro anticancer activity against many of cancer cells like breast cancer (169,170), colon cancer (140,171,172), adrenocortical carcinoma (173), hepatocellular carcinoma(174), prostate cancer (175,176) ovarian cancer(177,178), and other types of cancers (179-182). There is no specific target of niclosamide was recognized on the previous studies and many possible anticancer mechanism/pathway were suggested, including S100A4(171), Wnt/b-catenin(170,178,183), CDC37 (174), State3 (184), NF-kB (185) and other signaling pathways (174,181).

In addition, we submitted a number of structurally unrelated mitochondrial uncouplers to NCI for testing anti-cancer effect using NCI-60 cancer cell panel (60 different human cancer cell lines). The results showed that the mitochondrial uncouplers have inhibitory effect on cell growth and proliferation on all cell lines at concentrations that exhibit mitochondrial uncoupling activity for each compound (215).

In summary, our results have revealed that mitochondrial uncouplers compounds modify the cell metabolism of colon and pancreatic cancers, which prevent the anabolic

effect of aerobic glycolysis. Furthermore, our results demonstrated that mitochondrial uncoupler compounds (NEN, oxyclozanide and MB1-47) have antitumor activities for preventing and treating hepatic metastasis of colon and pancreatic cancers in NSG mouse model respectively. These results also suggest a new strategy for targeting the functional significant of Warburg effect. Our project provided new anticancer experimental compounds leads for future investigation.

Abbreviations

ATP	Adenine Triphosphate
NADPH	Nicotinamide adenine dinucleotide phosphate
PPP	Pentose Phosphate Pathway
OXPHOS	Oxidative Phosphorylation
NEN	Niclosamide ethanolamine
TCA	Tricarboxylic Acid
NAD	Nicotinamide adenine dinucleotide
PI3K	Phosphatidylinositol 3-kinase
TMRE	Tetramethylrhodamine ethyl ester
mTOR	mammalian Target Of Rapamycin
PBS	Phosphate Buffer Saline
CLSI	Clinical and Laboratory Standards Institute
PI	Propidium iodide
DMEM	Dulbecco's Modified Eagle Medium
FDA	Food And Drug Administration
ETC	Electron Transport Chain
AMPK	AMP-activated protein kinase
OCR	Oxygen Consumption Rate (OCR)

References

1. Warburg O. On the origin of cancer cells. Science **1956**;123(3191):309-14.

2. Vander Heiden MG, Cantley LC, Thompson CB. Understanding the Warburg effect: the metabolic requirements of cell proliferation. science **2009**;324(5930):1029-33.

3. Warburg O, Minami S. Versuche an Überlebendem Carcinom-gewebe. Journal of Molecular Medicine **1923**;2(17):776-7.

4. Lunt SY, Vander Heiden MG. Aerobic glycolysis: meeting the metabolic requirements of cell proliferation. Annu Rev Cell Dev Biol **2011**;27:441-64 doi 10.1146/annurev-cellbio-092910-154237.

5. Koppenol WH, Bounds PL, Dang CV. Otto Warburg's contributions to current concepts of cancer metabolism. Nature Reviews Cancer **2011**;11(5):325-37.

6. Tochigi T, Shuto K, Kono T, Ohira G, Tohma T, Gunji H*, et al.* Heterogeneity of Glucose Metabolism in Esophageal Cancer Measured by Fractal Analysis of Fluorodeoxyglucose Positron Emission Tomography Image: Correlation between Metabolic Heterogeneity and Survival. Digest Surg **2017**;34(3):186-91 doi 10.1159/000447751.

7. Larson SM. Positron emission tomography-based molecular imaging in human cancer: Exploring the link between hypoxia and accelerated glucose metabolism. Clinical Cancer Research **2004**;10(7):2203-4 doi Doi 10.1158/1078-0432.Ccr-0002-4.

8. Hanahan D, Weinberg RA. Hallmarks of cancer: the next generation. Cell **2011**;144(5):646-74 doi 10.1016/j.cell.2011.02.013.

9. DeBerardinis RJ, Chandel NS. Fundamentals of cancer metabolism. Science advances **2016**;2(5) doi UNSP e1600200 10.1126/sciadv.1600200.

10. Ward PS, Thompson CB. Metabolic reprogramming: a cancer hallmark even warburg did not anticipate. Cancer Cell **2012**;21(3):297-308 doi 10.1016/j.ccr.2012.02.014.

11. Gentric G, Mieulet V, Mechta-Grigoriou F. Heterogeneity in Cancer Metabolism: New Concepts in an Old Field. Antioxid Redox Sign **2017**;26(9):462-85 doi 10.1089/ars.2016.6750.

12. Villa E, Ricci JE. How does metabolism affect cell death in cancer? Febs Journal **2016**;283(14):2653-60 doi 10.1111/febs.13570.

13. Zielinski DC, Jamshidi N, Corbett AJ, Bordbar A, Thomas A, Palsson BO. Systems biology analysis of drivers underlying hallmarks of cancer cell metabolism. Scientific Reports **2017**;7 doi ARTN 4124110.1038/srep41241.

14. Tran Q, Lee H, Park J, Kim SH, Park J. Targeting Cancer Metabolism - Revisiting the Warburg Effects. Tox Research **2016**;32(3):177-93 doi 10.5487/Tr.2016.32.3.177.

15. Hsu PP, Sabatini DM. Cancer cell metabolism: Warburg and beyond. Cell **2008**;134(5):703-7 doi 10.1016/j.cell.2008.08.021.

16. Li ZY, Zhang HF. Reprogramming of glucose, fatty acid and amino acid metabolism for cancer progression. Cell Mol Life Sci **2016**;73(2):377-92 doi 10.1007/s00018-015-2070-4.

17. Kim SY. Cancer Energy Metabolism: Shutting Power off Cancer Factory. Biomol Ther **2018**;26(1):39-44 doi 10.4062/biomolther.2017.184.

18. Corbet C, Feron O. Cancer cell metabolism and mitochondria: Nutrient plasticity for TCA cycle fueling. Bba-Rev Cancer **2017**;1868(1):7-15 doi 10.1016/j.bbcan.2017.01.002.

19. Weinberg F, Chandel NS. Mitochondrial Metabolism and Cancer. Ann Ny Acad Sci **2009**;1177:66-73 doi 10.1111/j.1749-6632.2009.05039.

20. DeBerardinis RJ, Mancuso A, Daikhin E, Nissim I, Yudkoff M, Wehrli S*, et al.* Beyond aerobic glycolysis: transformed cells can engage in glutamine metabolism that exceeds the requirement for protein and nucleotide synthesis. Proceedings of the National Academy of Sciences **2007**;104(49):19345-50.

21. Shaw RJ. Glucose metabolism and cancer. Curr Opin Cell Biol **2006**;18(6):598-608 doi S0955-0674(06)00158.

22. DeNicola GM, Cantley LC. Cancer's Fuel Choice: New Flavors for a Picky Eater. Molecular cell **2015**;60(4):514-23 doi 10.1016/j.molcel.2015.10.018.

23. Lunt SY, Vander Heiden MG. Aerobic glycolysis: meeting the metabolic requirements of cell proliferation. Annual review of cell and developmental biology **2011**;27:441-64.

24. DeBerardinis RJ, Lum JJ, Hatzivassiliou G, Thompson CB. The biology of cancer: metabolic reprogramming fuels cell growth and proliferation. Cell Metab **2008**;7(1):11-20 doi S1550-4131(07)00295-1.

25. Zhao LQ, Mao YT, Zhao YL, Cao Y, Chen X. Role of multifaceted regulators in cancer glucose metabolism and their clinical significance. Oncotarget **2016**;7(21):31572-85 doi 10.18632/oncotarget.7765.

26. Koppenol WH, Bounds PL, Dang CV. Otto Warburg's contributions to current concepts of cancer metabolism. Nat Rev Cancer **2011**;11(5):325-37 doi 10.1038/nrc3038.

27. Vander Heiden MG. Targeting cancer metabolism: a therapeutic window opens. Nat Rev Drug Discov **2011**;10(9):671-84 doi 10.1038/nrd3504.

28. Vander Heiden MG, Locasale JW, Swanson KD, Sharfi H, Heffron GJ, Amador-Noguez D*, et al.* Evidence for an alternative glycolytic pathway in rapidly proliferating cells. Science **2010**;329(5998):1492-9 doi 329/5998/1492 [pii] 10.1126/science.1188015.

29. Kalyanaraman B, Cheng G, Hardy M, Ouari O, Lopez M, Joseph J*, et al.* A review of the basics of mitochondrial bioenergetics, metabolism, and related signaling pathways in cancer cells: Therapeutic targeting of tumor mitochondria with lipophilic cationic compounds. Redox Biol **2018**;14:316-27 doi 10.1016/j.redox.2017.09.020.

30. Stepien M, Duarte-Salles T, Fedirko V, Floegel A, Barupal DK, Rinaldi S*, et al.* Alteration of amino acid and biogenic amine metabolism in hepatobiliary cancers: Findings from a prospective cohort study. International Journal of Cancer **2016**;138(2):348-60 doi 10.1002/ijc.29718.

31. Frezza C. CANCER METABOLISM Addicted to serine. Nature Chemical Biology **2016**;12(6):389-90 doi 10.1038/nchembio.2086.

32. Zhang J, Pavlova NN, Thompson CB. Cancer cell metabolism: the essential role of the nonessential amino acid, glutamine. Embo J **2017**;36(10):1302-15 doi 10.15252/embj.201696151.

33. Altman BJ, Stine ZE, Dang CV. From Krebs to clinic: glutamine metabolism to cancer therapy. Nature Reviews Cancer **2016**;16(10):619-34 doi 10.1038/nrc.2016.71.

34. Choi YK, Park KG. Targeting Glutamine Metabolism for Cancer Treatment. Biomol Ther **2018**;26(1):19-28 doi 10.4062/biomolther.2017.178.

35. Hensley CT, Wasti AT, DeBerardinis RJ. Glutamine and cancer: cell biology, physiology, and clinical opportunities. Journal of Clinical Investigation **2013**;123(9):3678-84 doi 10.1172/Jci69600.

36. Lukey MJ, Cerione RA. The regulation of cancer cell glutamine metabolism. Transl Cancer Res **2016**;5:S1297-S8 doi 10.21037/tcr.2016.11.39.

37. Nicklin P, Bergman P, Zhang BL, Triantafellow E, Wang H, Nyfeler B*, et al.* Bidirectional Transport of Amino Acids Regulates mTOR and Autophagy. Cell **2009**;136(3):521-34 doi 10.1016/j.cell.2008.11.044.

38. Wise DR, DeBerardinis RJ, Mancuso A, Sayed N, Zhang XY, Pfeiffer HK*, et al.* Myc regulates a transcriptional program that stimulates mitochondrial glutaminolysis and leads to glutamine addiction. Proc Natl Acad Sci U S A **2008**;105(48):18782-7 doi 0810199105.

39. Yuneva M, Zamboni N, Oefner P, Sachidanandam R, Lazebnik Y. Deficiency in glutamine but not glucose induces MYC-dependent apoptosis in human cells. J Cell Biol **2007**;178(1):93-105 doi jcb.200703099.

40. Bott AJ, Peng IC, Fan YJ, Faubert B, Zhao L, Li JY*, et al.* Oncogenic Myc Induces Expression of Glutamine Synthetase through Promoter Demethylation. Cell Metab **2015**;22(6):1068-77 doi 10.1016/j.cmet.2015.09.025.

41. Vazquez A, Kamphorst JJ, Markert E, Schug ZT, Tardito S, Gottlieb E. Cancer metabolism at a glance. J Cell Sci **2016**;129(18):3367-73 doi 10.1242/jcs.181016.

42. Xiang Y, Stine ZE, Xia JS, Lu YQ, O'Connor RS, Altman BJ*, et al.* Targeted inhibition of tumor-specific glutaminase diminishes cell-autonomous tumorigenesis. Journal of Clinical Investigation **2015**;125(6):2293-306 doi 10.1172/Jci75836.

43. Shroff EH, Eberlin LS, Dang VM, Gouw AM, Gabay M, Adam SJ*, et al.* MYC oncogene overexpression drives renal cell carcinoma in a mouse model through glutamine metabolism. Proceedings of the National Academy of Sciences of the United States of America **2015**;112(21):6539-44 doi 10.1073/pnas.1507228112.

44. Yuan TL, Cantley LC. PI3K pathway alterations in cancer: variations on a theme. Oncogene **2008**;27(41):5497-510 doi onc2008245.

45. Dibble CC, Manning BD. Signal integration by mTORC1 coordinates nutrient input with biosynthetic output. Nature cell biology **2013**;15(6):555-64 doi DOI 10.1038/ncb2763.

46. Osaki M, Oshimura M, Ito H. PI3K-Akt pathway: Its functions and alterations in human cancer. Apoptosis **2004**;9(6):667-76 doi DOI 10.1023/B:APPT.0000045801.15585.dd.

47. Miller DM, Thomas SD, Islam A, Muench D, Sedoris K. c-Myc and Cancer Metabolism. Clinical Cancer Research **2012**;18(20):5546-53 doi 10.1158/1078-0432.Ccr-12-0977.

48. Yuneva M, Zamboni N, Oefner P, Sachidanandam R, Lazebnik Y. Deficiency in glutamine but not glucose induces MYC-dependent apoptosis in human cells. J Cell Biol **2007**;178(1):93-105 doi DOI 10.1083/jcb.200703099.

49. Yuan LW, Yamashita H, Seto Y. Glucose metabolism in gastric cancer: The cutting-edge. World J Gastroentero **2016**;22(6):2046-59 doi 10.3748/wjg.v22.i6.2046.

50. Hsieh AL, Walton ZE, Altman BJ, Stine ZE, Dang CV. MYC and metabolism on the path to cancer. Semin Cell Dev Biol **2015**;43:11-21 doi 10.1016/j.semcdb.2015.08.003.

51. Kerr EM, Gaude E, Turrell FK, Frezza C, Martins CP. Mutant Kras copy number defines metabolic reprogramming and therapeutic susceptibilities. Nature **2016**;531(7592):110-3 doi 10.1038/nature16967.

52. Hollstein M, Sidransky D, Vogelstein B, Harris CC. p53 mutations in human cancers. Science **1991**;253(5015):49-53.

53. Chun SY, Johnson C, Washburn JG, Cruz-Correa MR, Dang DYT, Dang LH. Oncogenic KRAS modulates mitochondrial metabolism in human colon cancer cells by inducing HIF-1 alpha and HIF-2 alpha target genes. Molecular Cancer **2010**;9 doi Artn 29310.1186/1476-4598-9-293.

54. Yun J, Rago C, Cheong I, Pagliarini R, Angenendt P, Rajagopalan H*, et al.* Glucose deprivation contributes to the development of KRAS pathway mutations in tumor cells. Science **2009**;325(5947):1555-9 doi 1174229 [pii] 10.1126/science.1174229.

55. Jiang L, Kon N, Li TY, Wang SJ, Su T, Hibshoosh H*, et al.* Ferroptosis as a p53-mediated activity during tumour suppression. Nature **2015**;520(7545):57-+ doi 10.1038/nature14344.

56. Jin S, Levine AJ. The p53 functional circuit. J Cell Sci **2001**;114(Pt 23):4139-40.

57. Li TY, Kon N, Jiang L, Zhao Y, Baer R, Gu W. Tumor suppression in the absence of p53-mediated cell cycle arrest, apoptosis, and senescence. Cancer Research **2013**;73(8) doi 10.1158/1538-7445.Am2013-Sy02-02.

58. Li TY, Kon N, Jiang L, Tan MJ, Ludwig T, Zhao YM*, et al.* Tumor Suppression in the Absence of p53-Mediated Cell-Cycle Arrest, Apoptosis, and Senescence. Cell **2012**;149(6):1269-83 doi 10.1016/j.cell.2012.04.026.

59. Napoli M, Flores ER. The p53 family orchestrates the regulation of metabolism: physiological regulation and implications for cancer therapy. Brit J Cancer **2017**;116(2):149-55 doi 10.1038/bjc.2016.384.

60. Jiang P, Du W, Wang X, Mancuso A, Gao X, Wu M*, et al.* p53 regulates biosynthesis through direct inactivation of glucose-6-phosphate dehydrogenase. Nature cell biology **2011**;13(3):310-6 doi ncb2172.

61. Zhou S, Kachhap S, Singh KK. Mitochondrial impairment in p53-deficient human cancer cells. Mutagenesis **2003**;18(3):287-92 doi DOI 10.1093/mutage/18.3.287.

62. Guo AK, Hou YY, Hirata H, Yamauchi S, Yip AK, Chiam KH*, et al.* Loss of p53 Enhances NF- kB- Dependent Lamellipodia Formation. J Cell Physiol **2014**;229(6):696-704 doi 10.1002/jcp.24505.

63. Sullivan LB, Chandel NS. Mitochondrial metabolism in TCA cycle mutant cancer cells. Cell Cycle **2014**;13(3):347-8 doi 10.4161/cc.27513.

64. Harman D. The biologic clock: the mitochondria? J Am Geriatr Soc **1972**;20(4):145-7.

65. Ahn CS, Metallo CM. Mitochondria as biosynthetic factories for cancer proliferation. Cancer Metab **2015**;3 doi ARTN 110.1186/s40170-015-0128-2.

66. Wallace DC. Mitochondria, bioenergetics, and the epigenome in eukaryotic and human evolution. Cold Spring Harb Symp Quant Biol **2009**;74:383-93 doi sqb.2009.74.031.

67. Dang CV. Links between metabolism and cancer. Genes & Development **2012**;26(9):877-90 doi 10.1101/gad.189365.112.

68. Comerford SA, Huang Z, Du X, Wang Y, Cai L, Witkiewicz AK*, et al.* Acetate Dependence of Tumors. Cell **2014**;159(7):1591-602 doi 10.1016/j.cell.2014.11.020.

69. Fan TW, Lane AN, Higashi RM, Farag MA, Gao H, Bousamra M*, et al.* Altered regulation of metabolic pathways in human lung cancer discerned by (13)C stable isotope-resolved metabolomics (SIRM). Mol Cancer **2009**;8:41 doi 10.1186/1476-4598-8-41.

70. Newman AC, Maddocks ODK. One-carbon metabolism in cancer. Brit J Cancer **2017**;116(12):1499-504 doi 10.1038/bjc.2017.118.

71. Konn M, Asai A, Kawamoto K, Nishida N, Satoh T, Doki Y*, et al.* The one-carbon metabolism pathway highlights therapeutic targets for gastrointestinal cancer (Review). Int J Oncol **2017**;50(4):1057-63 doi 10.3892/ijo.2017.3885.

72. Gaude E, Frezza C. Defects in mitochondrial metabolism and cancer. Cancer Metab **2014**;2:10 doi 10.1186/2049-3002-2-10.

73. Kaelin WG, Ratcliffe PJ. Oxygen sensing by metazoans: The central role of the HIF hydroxylase pathway. Molecular cell **2008**;30(4):393-402 doi 10.1016/j.molcel.2008.04.009.

74. Schito L, Rey S, Pawling J, Dennis JW, Wouters BG, Koritzinsky M. Fumarate hydratase deficiency redirects glucose metabolism of hypoxic cancer cells into the pentose phosphate pathway. Cancer Research **2016**;76 doi 10.1158/1538-7445.Am2016-1031.

75. Chen YY, Li P. Fatty acid metabolism and cancer development. Sci Bull **2016**;61(19):1473-9 doi 10.1007/s11434-016-1129-4.

76. Santos CR, Schulze A. Lipid metabolism in cancer. Febs Journal **2012**;279(15):2610-23 doi 10.1111/j.1742-4658.2012.08644.x.

77. Cantor JR, Sabatini DM. Cancer Cell Metabolism: One Hallmark, Many Faces. Cancer Discov **2012**;2(10):881-98 doi 10.1158/2159-8290.Cd-12-0345.

78. Martinez-Outschoorn UE, Peiris-Pages M, Pestell RG, Sotgia F, Lisanti MP. Cancer metabolism: a therapeutic perspective. Nat Rev Clin Oncol **2017**;14(1):11-31 doi 10.1038/nrclinonc.2016.60.

79. McCracken AN, Edinger AL. Nutrient transporters: the Achilles' heel of anabolism. Trends Endocrin Met **2013**;24(4):200-8 doi 10.1016/j.tem.2013.01.002.

80. Selwan EM, Edinger AL. Branched chain amino acid metabolism and cancer: the importance of keeping things in context. Transl Cancer Res **2017**;6:S578-S84 doi 10.21037/tcr.2017.05.05.

81. DeBerardinis RJ, Cheng T. Q's next: the diverse functions of glutamine in metabolism, cell biology and cancer. Oncogene **2010**;29(3):313-24 doi 10.1038/onc.2009.358.

82. Laplante M, Sabatini DM. mTOR Signaling in Growth Control and Disease. Cell **2012**;149(2):274-93 doi 10.1016/j.cell.2012.03.017.

83. Randle PJ. Regulatory interactions between lipids and carbohydrates: the glucose fatty acid cycle after 35 years. Diabetes Metab Rev **1998**;14(4):263-83.

84. Ray U, Roy SS. Aberrant lipid metabolism in cancer cells - the role of oncolipid-activated signaling. Febs Journal **2018**;285(3):432-43 doi 10.1111/febs.14281.

85. Mullen AR, Wheaton WW, Jin ES, Chen PH, Sullivan LB, Cheng T*, et al.* Reductive carboxylation supports growth in tumour cells with defective mitochondria. Nature **2012**;481(7381):385-U171 doi 10.1038/nature10642.

86. Metallo CM, Gameiro PA, Bell EL, Mattaini KR, Yang JJ, Hiller K*, et al.* Reductive glutamine metabolism by IDH1 mediates lipogenesis under hypoxia. Nature **2012**;481(7381):380-U166 doi 10.1038/nature10602.

87. Wise DR, Ward PS, Shay JES, Cross JR, Gruber JJ, Sachdeva UM*, et al.* Hypoxia promotes isocitrate dehydrogenase-dependent carboxylation of alpha-ketoglutarate to citrate to support cell growth and viability. Proceedings of the National Academy of Sciences of the United States of America **2011**;108(49):19611-6 doi 10.1073/pnas.1117773108.

88. Schug ZT, Peck B, Jones DT, Zhang QF, Grosskurth S, Alam IS*, et al.* Acetyl-CoA Synthetase 2 Promotes Acetate Utilization and Maintains Cancer Cell Growth under Metabolic Stress. Cancer Cell **2015**;27(1):57-71 doi 10.1016/j.ccell.2014.12.002.

89. Green CR, Wallace M, Divakaruni AS, Phillips SA, Murphy AN, Ciaraldi TP*, et al.* Branched-chain amino acid catabolism fuels adipocyte differentiation and lipogenesis. Nature Chemical Biology **2016**;12(1):15-+ doi 10.1038/Nchembio.1961.

90. Kannan R, Lyon I, Baker N. Dietary control of lipogenesis in vivo in host tissues and tumors of mice bearing Ehrlich ascites carcinoma. Cancer Res **1980**;40(12):4606-11.

91. Lewis CA, Parker SJ, Fiske BP, McCloskey D, Gui DY, Green CR*, et al.* Tracing Compartmentalized NADPH Metabolism in the Cytosol and Mitochondria of Mammalian Cells. Molecular cell **2014**;55(2):253-63 doi 10.1016/j.molcel.2014.05.008.

92. Fan J, Ye JB, Kamphorst JJ, Shlomi T, Thompson CB, Rabinowitz JD. Quantitative flux analysis reveals folate-dependent NADPH production (vol 510, pg 298, 2014). Nature **2014**;513(7519):574- doi 10.1038/nature13675.

93. Horton JD, Goldstein JL, Brown MS. SREBPs: activators of the complete program of cholesterol and fatty acid synthesis in the liver. Journal of Clinical Investigation **2002**;109(9):1125-31 doi 10.1172/Jci200215593.

94. Duvel K, Yecies JL, Menon S, Raman P, Lipovsky AI, Souza AL*, et al.* Activation of a Metabolic Gene Regulatory Network Downstream of mTOR Complex 1. Molecular cell **2010**;39(2):171-83 doi 10.1016/j.molcel.2010.06.022.

95. DeBerardinis RJ, Lum JJ, Thompson CB. Phosphatidylinositol 3-kinase-dependent modulation of carnitine palmitoyltransferase 1A expression regulates lipid metabolism during hematopoietic cell growth. Journal of Biological Chemistry **2006**;281(49):37372-80 doi 10.1074/jbc.M608372200.

96. Hao YJ, Samuels Y, Li QL, Krokowski D, Brunengraber H, Hatzoglou M*, et al.* Oncogenic PIK3CA mutations reprogram glutamine metabolism in colorectal cancers. Cancer Research **2015**;75 doi 10.1158/1538-7445.Am2015-1125.

97. Kuma A, Hatano M, Matsui M, Yamamoto A, Nakaya H, Yoshimori T*, et al.* The role of autophagy during the early neonatal starvation period. Nature **2004**;432(7020):1032-6 doi 10.1038/nature03029.

98. Stincone A, Prigione A, Cramer T, Wamelink MMC, Campbell K, Cheung E*, et al.* The return of metabolism: biochemistry and physiology of the pentose phosphate pathway. Biol Rev **2015**;90(3):927-63 doi 10.1111/brv.12140.

99. Aird KM, Zhang RG. Nucleotide metabolism, oncogene-induced senescence and cancer. Cancer Letters **2015**;356(2):204-10 doi 10.1016/j.canlet.2014.01.017.

100. Ben-Sahra I, Howell JJ, Asara JM, Manning BD. Stimulation of de Novo Pyrimidine Synthesis by Growth Signaling Through mTOR and S6K1. Science **2013**;339(6125):1323-8 doi 10.1126/science.1228792.

101. Wang W, Guan KL. AMP-activated protein kinase and cancer. Acta Physiol (Oxf) **2009**;196(1):55-63.

102. Canto C, Auwerx J. Calorie restriction: is AMPK a key sensor and effector? Physiology **2011**;26(4):214-24.

103. Klaus S, Keipert S, Rossmeisl M, Kopecky J. Augmenting energy expenditure by mitochondrial uncoupling: a role of AMP-activated protein kinase. Genes Nutr **2012**;7(3):369-86 doi 10.1007/s12263-011-0260-8.

104. Fujii N, Aschenbach WG, Musi N, Hirshman MF, Goodyear LJ. Regulation of glucose transport by the AMP-activated protein kinase. Proc Nutr Soc **2004**;63(2):205-10 .

105. Haurie V, Boucherie H, Sagliocco F. The snf1 protein kinase controls the induction of genes of the iron uptake pathway at the diauxic shift in Saccharomyces cerevisiae. Journal of Biological Chemistry **2003**;278(46):45391-6 doi 10.1074/jbc.M307447200.

106. Zhou G, Myers R, Li Y, Chen Y, Shen X, Fenyk-Melody J*, et al.* Role of AMP-activated protein kinase in mechanism of metformin action. J Clin Invest **2001**;108(8):1167-74.

107. Hawley SA, Fullerton MD, Ross FA, Schertzer JD, Chevtzoff C, Walker KJ*, et al.* The Ancient Drug Salicylate Directly Activates AMP-Activated Protein Kinase. Science **2012**;336(6083):918-22 doi 10.1126/science.1215327.

108. Daurio NA, Tuttle SW, Worth AJ, Song EY, Davis JM, Snyder NW*, et al.* AMPK Activation and Metabolic Reprogramming by Tamoxifen through Estrogen Receptor-Independent Mechanisms Suggests New Uses for This Therapeutic Modality in Cancer Treatment. Cancer Research **2016**;76(11):3295-306 doi 10.1158/0008-5472.Can-15-2197.

109. Xiao B, Heath R, Saiu P, Leiper FC, Leone P, Jing C*, et al.* Structural basis for AMP binding to mammalian AMP-activated protein kinase. Nature **2007**;449(7161):496-U14 doi 10.1038/nature06161.

110. Scott JW, Hawley SA, Green KA, Anis M, Stewart G, Scullion GA*, et al.* CBS domains form energy-sensing modules whose binding of adenosine ligands is disrupted by disease mutations. Journal of Clinical Investigation **2004**;113(2):274-84 doi 10.1172/Jci200419874.

111. Gowans GJ, Hawley SA, Ross FA, Hardie DG. AMP Is a True Physiological Regulator of AMP-Activated Protein Kinase by Both Allosteric Activation and Enhancing Net Phosphorylation. Cell Metab **2013**;18(4):556-66 doi 10.1016/j.cmet.2013.08.019.

112. Hardie DG. Molecular Pathways: Is AMPK a Friend or a Foe in Cancer? Clinical Cancer Research **2015**;21(17):3836-40 doi 10.1158/1078-0432.Ccr-14-3300.

113. Hay N, Sonenberg N. Upstream and downstream of mTOR. Genes & development **2004**;18(16):1926-45.

114. Xu J, Ji J, Yan X-H. Cross-talk between AMPK and mTOR in regulating energy balance. Critical reviews in food science and nutrition **2012**;52(5):373-81.

115. Faubert B, Vincent EE, Griss T, Samborska B, Izreig S, Svensson RU*, et al.* Loss of the tumor suppressor LKB1 promotes metabolic reprogramming of cancer cells via HIF-1alpha. Proc Natl Acad Sci U S A **2014**;111(7):2554-9 doi 10.1073/pnas.1312570111.

116. El-Masry OS, Brown BL, Dobson PRM. Effects of activation of AMPK on human breast cancer cell lines with different genetic backgrounds. Oncol Lett **2012**;3(1):224-8 doi 10.3892/ol.2011.458.

117. Hadad SM, Baker L, Quinlan PR, Robertson KE, Bray SE, Thomson G*, et al.* Histological evaluation of AMPK signalling in primary breast cancer. Bmc Cancer **2009**;9 doi Artn 30710.1186/1471-2407-9-307.

118. Lee CW, Wong LLY, Tse EYT, Liu HF, Leong VYL, Lee JMF*, et al.* AMPK Promotes p53 Acetylation via Phosphorylation and Inactivation of SIRT1 in Liver Cancer Cells. Cancer Research **2012**;72(17):4394-404 doi 10.1158/0008-5472.Can-12-0429.

119. Faubert B, Boily G, Izreig S, Griss T, Samborska B, Dong Z*, et al.* AMPK is a negative regulator of the Warburg effect and suppresses tumor growth in vivo. Cell Metab **2013**;17(1):113-24.

120. Hawley SA, Pan DA, Mustard KJ, Ross L, Bain J, Edelman AM*, et al.* Calmodulin-dependent protein kinase kinase-beta is an alternative upstream kinase for AMP-activated protein kinase. Cell Metab **2005**;2(1):9-19 doi 10.1016/j.cmet.2005.05.009.

121. Sanchez-Cespedes M, Parrella P, Esteller M, Nomoto S, Trink B, Engles JM*, et al.* Inactivation of LKB1/STK11 is a common event in adenocarcinomas of the lung. Cancer Research **2002**;62(13):3659-62.

122. Ji HB, Ramsey MR, Hayes DN, Fan C, McNamara K, Kozlowski P*, et al.* LKB1 modulates lung cancer differentiation and metastasis. Nature **2007**;448(7155):807-U7 doi 10.1038/nature06030.

123. Wingo SN, Gallardo TD, Akbay EA, Liang MC, Contreras CM, Boren T*, et al.* Somatic LKB1 Mutations Promote Cervical Cancer Progression. Plos One **2009**;4(4) doi ARTN e513710.1371/journal.pone.0005137.

124. Hawley SA, Ross FA, Gowans GJ, Tibarewal P, Leslie NR, Hardie DG. Phosphorylation by Akt within the ST loop of AMPK-alpha 1 down-regulates its activation in tumour cells. Biochemical Journal **2014**;459:275-87 doi 10.1042/Bj20131344.

125. Horman S, Vertommen D, Heath R, Neumann D, Mouton V, Woods A*, et al.* Insulin antagonizes ischemia-induced Thr172 phosphorylation of AMP-

activated protein kinase alpha-subunits in heart via hierarchical phosphorylation of Ser485/491. J Biol Chem **2006**;281(9):5335-40 doi 10.1074/jbc.M506850200.

126. Zheng B, Jeong JH, Asara JM, Yuan YY, Granters SR, Chin L*, et al.* Oncogenic B-RAF Negatively Regulates the Tumor Suppressor LKB1 to Promote Melanoma Cell Proliferation. Molecular cell **2009**;33(2):237-47 doi 10.1016/j.molcel.2008.12.026.

127. Hay N, Sonenberg N. Upstream and downstream of mTOR. Genes Dev **2004**;18(16):1926-45.

128. Harris TE, Lawrence JC, Jr. TOR signaling. Sci STKE **2003**;2003(212):re15.

129. Abu el Maaty MA, Wolfl S. Vitamin D as a Novel Regulator of Tumor Metabolism: Insights on Potential Mechanisms and Implications for Anti-Cancer Therapy. Int J Mol Sci **2017**;18(10) doi ARTN 218410.3390/ijms18102184.

130. Li ZR. mTOR signaling coordinates glucose and lipid metabolisms in liver. Faseb J **2016**;30.

131. Yin G, Liang Y, Wang Y, Yang Y, Yang M, Cen XM*, et al.* mTOR complex 1 signalling regulates the balance between lipid synthesis and oxidation in hypoxia lymphocytes. Bioscience Rep **2017**;37 doi Artn Bsr20160479 10.1042/Bsr20160479.

132. Suter U. LIPID BIOSYNTHESIS, mTOR SIGNALING AND MYELINATION. Glia **2013**;61:S37-S.

133. Han CC, Wei SH, He F, Liu DD, Wan HF, Liu HH*, et al.* The Regulation of Lipid Deposition by Insulin in Goose Liver Cells Is Mediated by the PI3K-AKT-mTOR Signaling Pathway. Plos One **2015**;10(5) doi ARTN e0098759 10.1371/journal.pone.0098759.

134. Saxton RA, Sabatini DM. mTOR Signaling in Growth, Metabolism, and Disease. Cell **2017**;168(6):960-76 doi 10.1016/j.cell.2017.02.004.

135. Robitaille AM, Christen S, Shimobayashi M, Cornu M, Fava LL, Moes S*, et al.* Quantitative Phosphoproteomics Reveal mTORC1 Activates de Novo Pyrimidine Synthesis. Science **2013**;339(6125):1320-3 doi 10.1126/science.1228771.

136. Houede N, Pourquier P. Targeting the genetic alterations of the PI3K-AKT-mTOR pathway: Its potential use in the treatment of bladder cancers.

Pharmacol Therapeut **2015**;145:1-18 doi 10.1016/j.pharmthera.2014.06.004.

137. Rivera-Rivera A, Castillo-Pichardo L, Dharmawardhane S. Regulation of Akt/AMPK/mTOR signaling by grape polyphenols in triple negative breast cancer. Faseb J **2013**;27.

138. Feng Z, Zhang H, Levine AJ, Jin S. The coordinate regulation of the p53 and mTOR pathways in cells. Proc Natl Acad Sci U S A **2005**;102(23):8204-9.

139. Feng Z, Zhang H, Levine AJ, Jin S. The coordinate regulation of the p53 and mTOR pathways in cells. Proceedings of the National Academy of Sciences of the United States of America **2005**;102(23):8204-9.

140. Alasadi A, Chen M, Swapna GVT, Tao H, Guo J, Collantes J*, et al.* Effect of mitochondrial uncouplers niclosamide ethanolamine (NEN) and oxyclozanide on hepatic metastasis of colon cancer. Cell Death & Disease **2018**;9(2):215 doi 10.1038/s41419-017-0092-6.

141. Terada H. Uncouplers of oxidative phosphorylation. Environ Health Perspect **1990**;87:213-8.

142. Tao H, Zhang Y, Zeng X, Shulman GI, Jin S. Niclosamide ethanolamine-induced mild mitochondrial uncoupling improves diabetic symptoms in mice. Nat Med **2014**;20(11):1263-9 doi nm.3699 [pii] 10.1038/nm.3699.

143. Skulachev VP. Uncoupling: new approaches to an old problem of bioenergetics. Biochim Biophys Acta **1998**;1363(2):100-24 doi S0005-2728(97)00091-1 [pii].

144. Porporato PE. Understanding cachexia as a cancer metabolism syndrome. Oncogenesis **2016**;5 doi ARTN e20010.1038/oncsis.2016.3.

145. Klingenberg M. Uncoupling protein--a useful energy dissipator. J Bioenerg Biomembr **1999**;31(5):419-30.

146. Han DH, Nolte LA, Ju JS, Coleman T, Holloszy JO, Semenkovich CF. UCP-mediated energy depletion in skeletal muscle increases glucose transport despite lipid accumulation and mitochondrial dysfunction. Am J Physiol Endocrinol Metab **2004**;286(3):E347-53 doi 10.1152/ajpendo.00434.2003 00434.2003 [pii].

147. Childress ES, Alexopoulos SJ, Hoehn KL, Santos WL. Small Molecule Mitochondrial Uncouplers and Their Therapeutic Potential. J Med Chem **2017** doi 10.1021/acs.jmedchem.7b01182.

148. Ricquier D, Bouillaud F. Mitochondrial uncoupling proteins: from mitochondria to the regulation of energy balance. J Physiol **2000**;529 Pt 1:3-10 doi PHY_1135 [pii].

149. Kozak LP, Harper ME. Mitochondrial uncoupling proteins in energy expenditure. Annu Rev Nutr **2000**;20:339-63 doi 10.1146/annurev.nutr.20.1.33920/1/339 [pii].

150. Alasadi A, Jin S. Treatment of Pancreatic Cancer Through Targeting Cancer Cell Metabolism by Mitochondrial Uncouplers. Pancreas **2017**;46(10):1387.

151. Alasadi AH, Guo JJ, Tao HL, Jin SK. Preventing and treating hepatic metastatic colon and pancreatic cancers by targeting cell metabolism. Cancer Research **2016**;76 doi 10.1158/1538-7445.Am2016-45.

152. Giatromanolaki A, Balaska K, Kalamida D, Kakouratos C, Sivridis E, Koukourakis MI. Thermogenic protein UCP1 and UCP3 expression in non-small cell lung cancer: relation with glycolysis and anaerobic metabolism. Cancer Biol Med **2017**;14(4):396-+ doi 10.20892/j.issn.2095-3941.2017.0089.

153. Nowinski SM, Solmonson A, Rundhaug JE, Rho O, Cho J, Lago CU*, et al.* Mitochondrial uncoupling links lipid catabolism to Akt inhibition and resistance to tumorigenesis. Nat Commun **2015**;6.

154. Riester M, Xu Q, Moreira A, Zheng J, Michor F, Downey RJ. The Warburg effect: persistence of stem-cell metabolism in cancers as a failure of differentiation. Ann Oncol **2018**;29(1):264-70 doi 10.1093/annonc/mdx645.

155. Warburg O. On the origin of cancer cells. Science **1956**;123(3191):309-14.

156. Hess KR, Varadhachary GR, Taylor SH, Wei W, Raber MN, Lenzi R*, et al.* Metastatic patterns in adenocarcinoma. Cancer **2006**;106(7):1624-33 doi 10.1002/cncr.21778.

157. Pestana C, Reitemeier RJ, Moertel CG, Judd ES, Dockerty MB. The Natural History of Carcinoma of the Colon and Rectum. Am J Surg **1964**;108:826-9.

158. Takahashi Y, Coppola D, Matsushita N, Cualing HD, Sun M, Sato Y*, et al.* Bif-1 interacts with Beclin 1 through UVRAG and regulates autophagy and tumorigenesis. Nature cell biology **2007**;9(10):1142-51 doi ncb1634 [pii] 10.1038/ncb1634.

159. Dawson LE, Russell AH, Tong D, Wisbeck WM. Adenocarcinoma of the sigmoid colon: sites of initial dissemination and clinical patterns of recurrence following surgery alone. J Surg Oncol **1983**;22(2):95-9.

160. Kavolius J, Fong Y, Blumgart LH. Surgical resection of metastatic liver tumors. Surg Oncol Clin N Am **1996**;5(2):337-52.

161. Sjovall A, Jarv V, Blomqvist L, Singnomklao T, Cedermark B, Glimelius B*, et al.* The potential for improved outcome in patients with hepatic metastases from colon cancer: a population-based study. Eur J Surg Oncol **2004**;30(8):834-41 doi 10.1016/j.ejso.2004.06.010S0748-7983(04)00151-9 [pii].

162. Manfredi S, Lepage C, Hatem C, Coatmeur O, Faivre J, Bouvier AM. Epidemiology and management of liver metastases from colorectal cancer. Ann Surg **2006**;244(2):254-9 doi 10.1097/01.sla.0000217629.94941.cf 00000658-200608000-00012 [pii].

163. Fong Y, Fortner J, Sun RL, Brennan MF, Blumgart LH. Clinical score for predicting recurrence after hepatic resection for metastatic colorectal cancer: analysis of 1001 consecutive cases. Ann Surg **1999**;230(3):309-18; discussion 18-21.

164. Pawlik TM, Scoggins CR, Zorzi D, Abdalla EK, Andres A, Eng C*, et al.* Effect of surgical margin status on survival and site of recurrence after hepatic resection for colorectal metastases. Ann Surg **2005**;241(5):715-22, discussion 22-4 doi 00000658-200505000-00005 [pii].

165. Marino G, Salvador-Montoliu N, Fueyo A, Knecht E, Mizushima N, Lopez-Otin C. Tissue-specific autophagy alterations and increased tumorigenesis in mice deficient in Atg4C/autophagin-3. J Biol Chem **2007**;282(25):18573-83 doi M701194200 [pii] 10.1074/jbc.M701194200.

166. Jin S, Augeri, DJ, Kimball, S.D, Liu, P.; Tao, H. Novel Mitochondrial Uncouplers for Treatment of Metabolic Diseases and Cancer. PCT/US15/61342 **2015**.

167. Sheth UK. Mechanisms of anthelmintic action. Prog Drug Res **1975**;19:147-57.

168. Weinbach EC, Garbus J. Mechanism of action of reagents that uncouple oxidative phosphorylation. Nature **1969**;221 doi 10.1038/2211016a0.

169. Londoño-Joshi AI, Arend RC, Aristizabal L, Lu W, Samant RS, Metge BJ*, et al.* Effect of niclosamide on basal-like breast cancers. Molecular cancer therapeutics **2014**;13(4):800-11.

170. Fonseca BD, Diering GH, Bidinosti MA, Dalal K, Alain T, Balgi AD*, et al.* Structure-activity analysis of niclosamide reveals potential role for cytoplasmic pH in control of mammalian target of rapamycin complex 1

(mTORC1) signaling. Journal of Biological Chemistry **2012**;287(21):17530-45.

171. Sack U, Walther W, Scudiero D, Selby M, Kobelt D, Lemm M*, et al.* Novel effect of antihelminthic Niclosamide on S100A4-mediated metastatic progression in colon cancer. J Natl Cancer Inst **2011**;103(13):1018-36 doi djr190 [pii] 10.1093/jnci/djr190.

172. Suliman MA, Zhang Z, Na H, Ribeiro AL, Zhang Y, Niang B*, et al.* Niclosamide inhibits colon cancer progression through downregulation of the Notch pathway and upregulation of the tumor suppressor miR-200 family. International Journal of Molecular Medicine **2016**;38(3):776-84.

173. Satoh K, Zhang L, Zhang Y, Chelluri R, Boufraqech M, Nilubol N*, et al.* Identification of niclosamide as a novel anticancer agent for adrenocortical carcinoma. Clinical Cancer Research **2016**;22(14):3458-66.

174. Chen B, Wei W, Ma L, Yang B, Gill RM, Chua M-S*, et al.* Computational Discovery of Niclosamide Ethanolamine, a Repurposed Drug Candidate That Reduces Growth of Hepatocellular Carcinoma Cells In Vitro and in Mice by Inhibiting Cell Division Cycle 37 Signaling. Gastroenterology **2017**.

175. Liu C, Lou W, Armstrong C, Zhu Y, Evans CP, Gao AC. Niclosamide suppresses cell migration and invasion in enzalutamide resistant prostate cancer cells via Stat3–AR axis inhibition. The Prostate **2015**;75(13):1341-53.

176. Ippolito JE, Brandenburg MW, Ge X, Crowley JR, Kirmess KM, Som A*, et al.* Extracellular pH modulates neuroendocrine prostate cancer cell metabolism and susceptibility to the mitochondrial inhibitor niclosamide. PloS one **2016**;11(7):e0159675.

177. Arend RC, Londono-Joshi AI, Samant RS, Li Y, Conner M, Hidalgo B. Inhibition of Wnt/beta-catenin pathway by niclosamide: a therapeutic target for ovarian cancer. Gynecol Oncol **2014**;134 doi 10.1016/j.ygyno.2014.04.005.

178. Arend RC, Londoño-Joshi AI, Gangrade A, Katre AA, Kurpad C, Li Y*, et al.* Niclosamide and its analogs are potent inhibitors of Wnt/β-catenin, mTOR and STAT3 signaling in ovarian cancer. Oncotarget **2016**;7(52):86803-15.

179. Wieland A, Trageser D, Gogolok S, Reinartz R, Höfer H, Keller M*, et al.* Anticancer effects of niclosamide in human glioblastoma. Clinical Cancer Research **2013**;19(15):4124-36.

180. Liao Z, Nan G, Yan Z, Zeng L, Deng Y, Ye J*, et al.* The anthelmintic drug niclosamide inhibits the proliferative activity of human osteosarcoma cells by

targeting multiple signal pathways. Current cancer drug targets **2015**;15(8):726-38.

181. Zhao J, He Q, Gong Z, Chen S, Cui L. Niclosamide suppresses renal cell carcinoma by inhibiting Wnt/β-catenin and inducing mitochondrial dysfunctions. SpringerPlus **2016**;5(1):1436 doi 10.1186/s40064-016-3153-x.

182. Chen W, Mook RA, Premont RT, Wang J. Niclosamide: Beyond an antihelminthic drug. Cellular Signalling **2017**.

183. Osada T, Chen M, Yang XY, Spasojevic I, Vandeusen JB, Hsu D*, et al.* Antihelminth compound niclosamide downregulates Wnt signaling and elicits antitumor responses in tumors with activating APC mutations. Cancer Res **2011**;71(12):4172-82 doi 0008-5472.CAN-10-3978 [pii] 10.1158/0008-5472.CAN-10-3978.

184. Ren X, Duan L, He Q, Zhang Z, Zhou Y, Wu D*, et al.* Identification of niclosamide as a new small-molecule inhibitor of the STAT3 signaling pathway. ACS medicinal chemistry letters **2010**;1(9):454-9.

185. Jin Y, Lu Z, Ding K, Li J, Du X, Chen C. Antineoplastic mechanisms of niclosamide in acute myelogenous leukemia stem cells: inactivation of the NF-kappaB pathway and generation of reactive oxygen species. Cancer Res **2010**;70 doi 10.1158/0008-5472.can-09-3950.

186. Frayha GJ, Smyth JD, Gobert JG, Savel J. The mechanisms of action of antiprotozoal and anthelmintic drugs in man. Gen Pharmacol **1997**;28(2):273-99 doi S0306362396001498 [pii].

187. Andrews P, Thyssen J, Lorke D. The Biology and Toxicology of Molluscidides, Bayluscide. Pharmc Ther **1983**;19:245-95.

188. Hecht G, Gloxhuber C. Tolerance to 2', 5-dichloro-4-nitrosalicylanilide ethanolamine salt. . Z Tropenmed Parasit **1962**;13:1-8.

189. Tanner JA, Henderson JA, Buchwald D, Howard BV, Henderson PN, Tyndale RF. Variation in CYP2A6 and nicotine metabolism among two American Indian tribal groups differing in smoking patterns and risk for tobacco-related cancer. Pharmacogenet Genom **2017**;27(5):169-78 doi 10.1097/Fpc.0000000000000271.

190. Corbett J, Goose J. A possible biochemical mode of action of the fasciolicides nitroxynil, hexachlorophene and oxyclozanide. Pesticide Science **1971**;2(3):119-21.

191. Oxyclozanide- Summary Report. Committee for Veterinary Medical Products- The European Agency for the Evaluation of Medicinal Products **1998**;WC500015368.

192. Metallo CM, Walther JL, Stephanopoulos G. Evaluation of 13C isotopic tracers for metabolic flux analysis in mammalian cells. J Biotechnol **2009**;144(3):167-74 doi S0168-1656(09)00300-9 [pii] 10.1016/j.jbiotec.2009.07.010.

193. Siegel R, Naishadham D, Jemal A. Cancer statistics, 2015. CA Cancer J Clin **2015**;65:5-29 doi 10.3322/caac.21166.

194. Rahib L, Smith BD, Aizenberg R, Rosenzweig AB, Fleshman JM, Matrisian LM. Projecting Cancer Incidence and Deaths to 2030: The Unexpected Burden of Thyroid, Liver, and Pancreas Cancers in the United States. Cancer Research **2014**;74(11):2913-21 doi 10.1158/0008-5472.can-14-0155.

195. Mimeault M, Brand RE, Sasson AA, Batra SK. Recent advances on the molecular mechanisms involved in pancreatic cancer progression and therapies. Pancreas **2005**;31(4):301-16 doi 00006676-200511000-00001 [pii].

196. Zhou W, Capello M, Fredolini C, Racanicchi L, Piemonti L, Liotta LA*, et al.* Proteomic analysis reveals Warburg effect and anomalous metabolism of glutamine in pancreatic cancer cells. J Proteome Res **2012**;11(2):554-63 doi 10.1021/pr2009274.

197. Blum R, Kloog Y. Metabolism addiction in pancreatic cancer. Cell death & disease **2014**;5(2):e1065.

198. Levine B. Cell biology: autophagy and cancer. Nature **2007**;446(7137):745-7.

199. Levine AJ, Puzio-Kuter AM. The control of the metabolic switch in cancers by oncogenes and tumor suppressor genes. Science **2010**;330(6009):1340-4 doi 330/6009/1340 [pii] 10.1126/science.1193494.

200. Livingstone LR, White A, Sprouse J, Livanos E, Jacks T, Tlsty TD. Altered cell cycle arrest and gene amplification potential accompany loss of wild-type p53. Cell **1992**;70(6):923-35.

201. Son J, Lyssiotis CA, Ying H, Wang X, Hua S, Ligorio M*, et al.* Glutamine supports pancreatic cancer growth through a KRAS-regulated metabolic pathway. Nature **2013**;496(7443):101-5.

202. Jastroch M, Divakaruni AS, Mookerjee S, Treberg JR, Brand MD. Mitochondrial proton and electron leaks. Essays Biochem **2010**;47:53-67 doi bse0470053 [pii] 10.1042/bse0470053.

203. Harper J, Dickinson K, Brand M. Mitochondrial uncoupling as a target for drug development for the treatment of obesity. Obesity Reviews **2001**;2(4):255-65.

204. Maitra A, Hruban RH. Pancreatic cancer. Annu Rev Pathol **2008**;3:157-88 doi 10.1146/annurev.pathmechdis.3.121806.154305.

205. Li D, Xie K, Wolff R, Abbruzzese JL. Pancreatic cancer. Lancet **2004**;363(9414):1049-57 doi 10.1016/S0140-6736(04)15841-8S0140-6736(04)15841-8 [pii].

206. Fryer LG, Parbu-Patel A, Carling D. The Anti-diabetic drugs rosiglitazone and metformin stimulate AMP-activated protein kinase through distinct signaling pathways. J Biol Chem **2002**;277(28):25226-32.

207. Deer EL, Gonzalez-Hernandez J, Coursen JD, Shea JE, Ngatia J, Scaife CL*, et al.* Phenotype and genotype of pancreatic cancer cell lines. Pancreas **2010**;39(4):425-35.

208. Matsubara S, Ding Q, Miyazaki Y, Kuwahata T, Tsukasa K, Takao S. mTOR plays critical roles in pancreatic cancer stem cells through specific and stemness-related functions. Scientific reports **2013**;3.

209. Sun S-Y, Yue P, Dawson MI, Shroot B, Michel S, Lamph WW*, et al.* Differential Effects of Synthetic Nuclear Retinoid Receptor-selective Retinoids on the Growth of Human Non-Small Cell Lung Carcinoma Cells. Cancer Research **1997**;57(21):4931-9.

210. Rongvaux A, Willinger T, Martinek J, Strowig T, Gearty SV, Teichmann LL*, et al.* Development and function of human innate immune cells in a humanized mouse model. Nature biotechnology **2014**;32(4):364-72.

211. Abu el Maaty MA, Alborzinia H, Khan SJ, Buttner M, Wolfl S. 1,25(OH)(2)D-3 disrupts glucose metabolism in prostate cancer cells leading to a truncation of the TCA cycle and inhibition of TXNIP expression. Bba-Mol Cell Res **2017**;1864(10):1618-30 doi 10.1016/j.bbamcr.2017.06.019.

212. DeBerardinis RJ, Mancuso A, Daikhin E, Nissim I, Yudkoff M, Wehrli S*, et al.* Beyond aerobic glycolysis: Transformed cells can engage in glutamine metabolism that exceeds the requirement for protein and nucleotide synthesis. Proceedings of the National Academy of Sciences of the United States of America **2007**;104(49):19345-50 doi 10.1073/pnas.0709747104.

213. Holness MJ, Sugden MC. Regulation of pyruvate dehydrogenase complex activity by reversible phosphorylation. Biochem Soc Trans **2003**;31(Pt 6):1143-51 doi 10.1042/.

214. Hue L, Taegtmeyer H. The Randle cycle revisited: a new head for an old hat. Am J Physiol Endocrinol Metab **2009**;297(3):E578-91 doi 00093.2009 [pii] 10.1152/ajpendo.00093.2009.

215. NCI. NCI DTP (Developmental Therapeutics Program, NCI 60 Creening Results (https://dtp.cancer.gov/services/nci60data/colordoseresponse/jpg/758440). . **2014**.